

**SYNTHESIS, CRYSTAL STRUCTURES AND MOLECULAR MODELING
OF SOME 2-OXASTEROIDS**

A Thesis
Submitted for the Degree of
Doctor of Philosophy

By
ADDLAGATTA ANTHONY



School of Chemistry
University of Hyderabad
Hyderabad 500 046
India

December 1998

to

my **PARENTS**

and **sisters**

STATEMENT

I hereby declare that the matter embodied in this thesis is the result of the investigations carried out by me in the School of Chemistry, University of Hyderabad under the supervision of Dr. Ashwini Nangia.

In keeping with the general practice of reporting scientific observations due acknowledgements have been made wherever the work described is based on the findings of other investigators.

Hyderabad

December 1998


Addlagatta Anthony

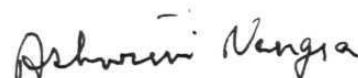
CERTIFICATE

Certified that the work entitled '**Synthesis, Crystal Structures and Molecular Modeling of Some 2-Oxasteroids**' has been carried out by **Addlagatta Anthony** under my supervision and that the same has not been submitted elsewhere for a degree.



Dean

School of Chemistry



Dr. Ashwini Nangia

Thesis Supervisor

ACKNOWLEDGEMENT

I express my deep sense of gratitude and profound thanks to Dr. Ashwini Nangia for his inspiration, guidance and constant encouragement throughout the course of this work.

I thank Professor Gautam R. Desiraju for introducing me to the field of crystallography and molecular modeling and for his help and thought provoking discussions.

I thank Dr. K.C. Kumaraswamy for the help and encouragement throughout my stay on the campus.

I thank Professor M. Nagarajan, Dean, School of Chemistry and all the faculty members of the School for their cooperation and encouragement.

I would like to acknowledge the assistance of Professor Mariusz Jaskolski, A. Mickiewicz University, Poland and Professor W.T. Robinson and Dr. K. Renu, Canterbury University, New Zealand for X-ray data collection on the compounds studied in this work.

I specially thank my primary school teacher Mrs. Nayyar Jahan for her love, affection and encouragement.

I have no words to thank Rev. Sr. Rose Linda, Rev. Sr. Angela and Rev. Fr. Y.M. Joseph without whom I would not have reached this stage.

It gives me pleasure to thank my lecturer Shree Ramesh Chaudary who inculcated my interest in chemistry.

I wish to thank former members of the group Drs. P. Bheema Rao, G. Prasuna, P.S. Chandrakala, Venkat R. Thalladi, P. Senthivel, and the present students Madhavi, Ram, Srinivasan, J.R.K. Rao, Senthil, Praveen, Sumod,

Venugopal and Vishweshwar for the pleasant atmosphere in the laboratory to make my stay a memorable one.

I wish to thank all my friends Sudha, Vijju, DRama, Saroja, Srinivas (D), Giju, Ravi, Panda, Uma, Krishna (LG), Samba (LV), Bharathi, Ramanathan, Rajesh, Ramesh, Dharma, Sreenu, Muthu, Chari, Dos (BD), Reddy, Bandaru, Ramakrishna, Muthaiah, Ramachandram, Gurubaran, Siva, Sampath, Karunakar, Jaya Kumar, Jagan, Satyen, Ashok, Reddy, Sastry, Sailaja, Mangai, Shankaran, Palas in the School of Chemistry, Ramakrishna, Jayaraju, Sreenu, Muralidhar Reddy and Vinay in the School of Life Sciences, Hari, Ramana, Sudhakar and Senthil in the School of Physics for helping me in one way or the other and in making my stay on the campus enjoyable.

I thank all the non-teaching staff of the School of Chemistry for their assistance.

I wish to thank MMG, Hema, VLN, Hotha, Sarma, Venu, Bhanu, Sowmitri, Pappu and my other M.Sc. classmates for their timely help and encouragement.

My thanks are to Gayatri, for her support and encouragement.

I am short of words to express my heartfelt thanks to my parents and sisters for their love, sacrifice, support and patience. Lastly, my nieces and nephews deserve a word of thanks for their smiles and wishes.

Addlagatta Anthony

PREFACE

The thesis entitled "Synthesis, Crystal Structures and Molecular Modeling of Some 2-Oxasteroids " is presented in three chapters. Chapter-1 describes the synthesis of 2-oxa and 2-thiasteroids. Chapter-2 deals with the X-ray crystal structure analysis of 2-oxasteroids and related androgens. Chapter-3 describes molecular modeling studies of the steroids discussed in the previous chapter. Each chapter is divided into introduction, results and discussion sections. The conclusions from the thesis are placed at the end.

Chapter 1: Synthesis of 2-Oxasteroids and 2-Thiasteroids

The beneficial properties of steroidal drugs are often accompanied by serious side effects which can, in some cases, be overcome by synthetic steroid analogues. For example, 2-oxasteroids Anavar[®] (**4**) and Nilevar[®] (**5**) are anabolic agents with minimal androgenic side effects. Many synthetic steroids have been introduced as drugs while others are undergoing clinical trials.

In this work, the synthesis of 2-oxasteroid **36** from dehydroisoandrosterone **26** was carried out according to Scheme 2. Thus, single-pot conversion of 3 β -hydroxy-5-androstene **27** to 4-ene-3,6-dione **30**, followed by 1,2-dehydrogenation with DDQ proceeded smoothly to dienedione **34**. Ozonolysis of **34** to lactol **35** and NaBH₄ reduction conveniently afforded 6 α -hydroxy-2-oxasteroid **36**. Further elaboration of hydroxy lactone **36** to B-ring functionalised heterosteroids was carried out.

Lactone **44** was prepared by Frimer's method. Attempted synthesis of thiolactone **45** from **44** is discussed. The synthesis and derivatisation of A-ring thiopyran steroid **67**, which is devoid of the crucial C3-carbonyl was completed.

Chapter 2: Crystal Structures of 2-Oxasteroids and Androgens

Out of the many 2-oxasteroids synthesised, some compounds yielded single crystals of X-ray quality and these were studied further. The importance as well as the interplay of strong (O-H...O) and weak (C-H...O) hydrogen bonding in these crystal structures was analysed. The molecular conformation of 2-oxasteroids is similar to that of the parent androgens. Interestingly, some examples of isostructurality have been found within the oxasteroid family and also in the natural steroids. The biologically important steroid **30a** and its analogues **30** and **34** are analysed to understand the role of weak interactions in crystal packing and stabilisation. The crystal structure of 5 β -androstanedione **56** is also discussed. The crystal structures of oxasteroids **41** and **60** are similar despite the replacement of strong O-H...O hydrogen bond in **41** with weak C-H...O bond in **60** along the direction of hydrogen bonded chains. The isostructurality between the two structures was confirmed by the formation of a binary solid solution, **60:41** in 3:7 ratio. Further, two steroids (**82**, **83**) were retrieved from the Cambridge Structural Database (CSD) that have a similar packing arrangement but are chemically different. The crystal structures of Anavar[®] (**4**) and steroids **34** and **43** are similar despite differences of a chemical and geometrical nature. Compound **30a** is a suicide substrate inhibitor of aromatase and its crystal structure is very similar to that of androst-4-ene-3,17-dione **55**, a natural substrate for the same enzyme. The implication of similarity in crystal packing on ligand-receptor binding leads to the next chapter.

Chapter 3: Model Receptor Surface and QSAR Evaluation of 2-Oxasteroids

This chapter describes the generation of a complementarity receptor surface model and 3D-QSAR equation for steroids. Drug Design Workbench (DDW) and related modules in the *Cerius²* program (MSI) were used in these studies. A set of 50 steroids active towards the aromatase enzyme were minimised in MOPAC 6.0 using the MNDO Hamiltonian and the overlay plots generated by the rigid-body, least-squares fitting of all the common heavy atoms. Different model receptor surfaces were generated using van der Waals or Wyvill surface criteria in combination with electrostatic or partial charge complementarity. The information on the role of 6-hydroxy functional group of 2-oxasteroids was not clear from the models generated by the set of 50 molecules since many of them contain large hydrophobic substituents at C6 position. In order to extract more information about the C6-OH functional group, another set of 27 molecules was analysed which is a subset of the 50 molecule training set and devoid of the large substituents at C6. The interaction energy of these prealigned 2-oxasteroid molecules was evaluated with the hypothetical receptor surfaces thus generated. 3D-QSAR equations were generated for the above two sets of minimised and prealigned 50 steroids using the genetic function approximation (GFA) statistical method to evaluate the activity of 2-oxasteroids.

Conclusions

A flexible and general protocol is developed for the synthesis of B-ring functionalised 2-oxasteroids. The crystal structures, conformation and packing motifs in the solid state are analysed for some selected compounds in the 2-oxasteroid family. Isostructural steroids are identified from those structures determined in this study as well from the CSD. Finally, hypothetical receptor surfaces are generated and evaluated computationally for 2-oxasteroids using

DDW in *Cerius*² platform. In summary, this thesis presents an approach to the study of biomolecules using small molecule crystallography and computational methods.

Salient crystallographic details of the crystal structures discussed in this thesis have been given at the end of the Chapter 2 and in the Appendix at the end of the thesis. A full list of atomic coordinates and structure factors can be obtained upon request.

Addlagatta Anthony

Hyderabad

December 1998

ABBREVIATIONS

Ac	acetyl
ACE	angiotensin converting enzyme
aq	aqueous
C	centigrade
DCC	N,N'-dicyclohexylcarbodiimide
CSD	Cambridge Structural Database
d	doublet
DiBAL-H	diisobutylaluminium hydride
DMF	dimethyl formamide
DMS	dimethyl sulfide
DMSO	dimethyl sulfoxide
DPC	dipyridine chromium (VI) oxide
equi	equivalents
GFA	genetic function approximation
h	hour
LAH	lithium aluminum hydride
LRMS	low resolution mass spectroscopy
m	multiplet
M	molar
<i>m</i> -CPBA	<i>meta</i> -chloroperbenzoic acid
mg	milligram
min	minutes
mL	milliliters
mmol	millimoles
mp	melting point
MRS	model receptor surface
Ms	methanesulfonyl

PCC	pyridinium chlorochromate
PDB	Protein Data Bank
PDC	pyridinium dichromate
PI	phosphatidylinositol
PLS	partial least squares
QSAR	quantitative structure-activity relationship
<i>p</i> -TsOH	<i>p</i> -toluenesulfonic acid
q	quartet
rt	room temperature
s	singlet
sat	saturated
SGC	silica gel chromatography
t	triplet
THF	tetrahydrofuran
TLC	thin layer chromatography

CONTENTS

Statement	v
Certificate	vii
Acknowledgement	ix
Preface	xi
Abbreviations	xv
CHAPTER 1	
Synthesis of 2-Oxasteroids and 2-Thiasteroids	1
1.1 Introduction	2
1.1.1 Steroids and their Importance as Biomolecules	2
1.1.2 Previous Synthetic Approaches to 2-Oxasteroids	4
1.2 Results and Discussion	9
1.2.1 Synthesis of B-Ring Functionalised 2-Oxasteroids	9
1.2.2 Synthesis of 2-Thiasteroids	16
1.3 Experimental Section	22
1.4 References	40
1.5 Spectra	41
CHAPTER 2	
Crystal Structures of 2-Oxasteroids and Androgens	55
2.1 Introduction	56
2.1.1 Small Molecule Crystallography	56
2.1.2 2-Heterosteroids in the Cambridge Structural Database	58
2.1.3 CSD Analysis of C-H...O Hydrogen Bonds in Steroids	60
2.2 Studies of 2-Oxasteroids	64
2.2.1 Crystal Structure Analysis of 2-Oxasteroids	64
2.2.2 Summary of Intermolecular Interactions	70
2.2.3 Molecular Conformation	73
2.3 Crystal Structures of Androgens	76

2.3.1	Crystal Structure Analysis of 6-Ketosteroids	76
2.3.2	Molecular Conformation	80
2.3.3	5 β -Androstane-3,17-dione	82
2.4	Isostructurality	84
2.4.1	Definition	84
2.4.2	One-dimensional Isostructurality	86
2.4.3	Two-dimensional Isostructurality	91
2.4.4	Three-dimensional Isostructurality	92
2.5	Experimental Section	94
2.6	Tables	95
2.7	References	100

CHAPTER 3

Model Receptor Surface and QSAR Evaluation of 2-Oxasteroids		105
3.1	Introduction	106
3.1.1	Aromatase Inhibitors and Drug Design Strategies	106
3.1.2	Model Receptor Surfaces	109
3.1.3	Comparative Molecular Field Analysis (CoMFA) or 3D QSAR	110
3.2	Molecular Modeling	112
3.3	Results and Discussion	116
3.3.1	Model Receptor Surfaces	116
3.3.2	3D QSAR	126
3.4	References	130

Conclusions	133
--------------------	-----

APPENDIX

Crystal Structures of Pigments from <i>Garcinia Hanburi</i>	135
About the Author	
List of Publications	

CHAPTER 1
SYNTHESIS OF 2-OXASTEROIDS AND 2-THIASTEROIDS

Contents

1.1 INTRODUCTION

1.1.1 Steroids and their Importance as Biomolecules

1.1.2 Previous Synthetic Approaches to 2-Oxasteroids

1.2 RESULTS AND DISCUSSION

1.2.1 Synthesis of B-ring Functionalised 2-Oxasteroids

1.2.2 Synthesis of 2-Thiasteroids

1.3 EXPERIMENTAL SECTION

1.4 REFERENCES

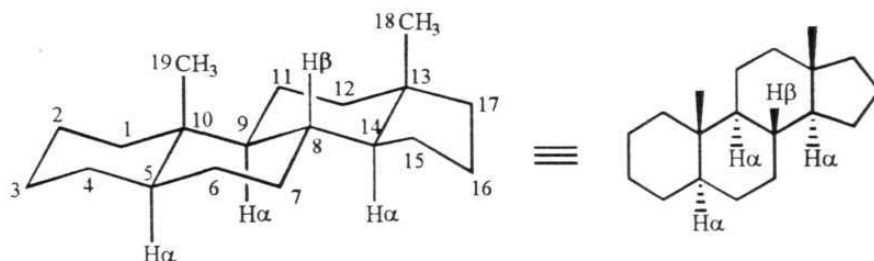
1.5 SPECTRA

1.1 INTRODUCTION

1.1.1 Steroids and their Importance as Biomolecules

Many aspects of reproduction, behaviour, differentiation and metabolism are controlled by the action of different steroid hormones. Hormones are chemical messengers that are secreted into the blood stream by specific ligands. Target cells possess receptors, usually several thousands per cell, that show specificity as well as high affinity for a particular hormone. Steroidal hormones play a vital role in a wide variety of essential physiological processes including cell growth, sexual development, maintenance of salt balance and sugar metabolism.

All steroids are named as derivatives of cholestane, androstane, pregnane or estrane. The standard system of numbering is illustrated with 5α -androstane in Scheme 1. All sp^3 carbons in the rings have one β -bond and one α -bond, with the β -bond lying closer to the 'top' or to the side of C-18 and C-19 methyl groups. The dark lines indicate β -configuration and the dashed lines α -configuration. The double bond at C4 can be represented as 4-androstene or Δ^4 -androstene.

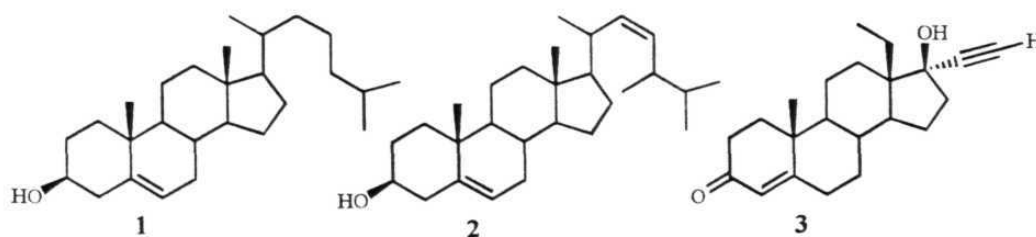


Scheme 1 Numbering and stereochemical representation of 5α -androstane.

The use of naturally occurring steroidal hormones, such as corticoids, progesterones and various anabolic agents, is well known in clinical therapy. Abnormalities in steroid hormone synthesis, metabolism and receptor interaction contribute to a variety of disease states.¹ Testosterone has been found to have primarily two kinds of activities - androgenic (or male physical characteristic promoting) and anabolic (or muscle building). Despite the immense beneficial

potential of steroid hormones, steroidal drugs are often accompanied by unwanted side effects. For example, acne, changes in the liver function, baldness, testicular atrophy and decreased sperm production have been observed in males administered with androgenic drugs. It is observed that many of the muscle building hormones are potent androgens and when used by females (particularly athletes) they produce masculine characteristics like facial hair, male pattern baldness, deepening of the voice, and menstrual irregularities.² To overcome some of these serious side effects, new analogues which possess therapeutic properties but have minimal side effects have been synthesised. For many natural steroids there are now synthetic analogues that have similar binding affinities for specific receptors.³

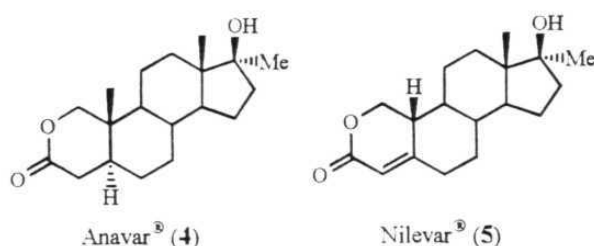
The complex carbon skeleton of steroids coupled with the multiplicity of chiral centers make these molecules challenging targets for total syntheses.⁴ The total syntheses that are reported for the steroidal hormones are too lengthy and complicated to be suitable for the preparation of bulk drug substances. Almost all the present day steroidal drugs are made by partial synthesis from one of two relatively abundant naturally occurring steroids, cholesterol (1) and stigmasterol (2).⁵ However, drugs like norgestrel (3) which have the 'unnatural' ethyl group at C13 are still produced by total synthesis (Scheme 2).^{3b}



Scheme 2. Natural products (1, 2) and synthetic steroid (3).

Since it would be very useful to have drugs which are anabolic and not androgenic, many derivatives with increased anabolic activity have been

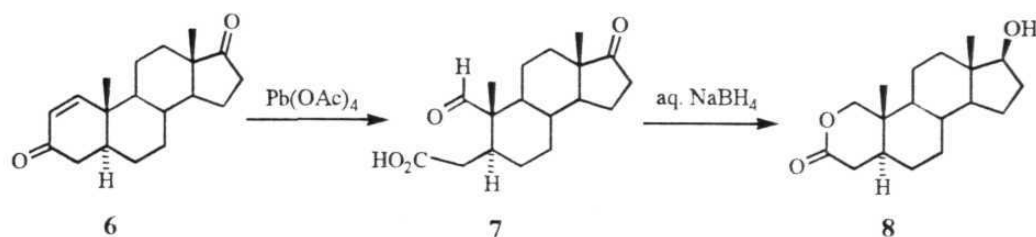
synthesised. Though the absolute separation of these properties is difficult to achieve, there has been some success in enhancing the ratio of anabolic to androgenic activity. Pappo *et al.*⁶ synthesised some 2-oxa-androgens and showed that they have increased anabolic activity with minimal androgenic side effects. In the oxasteroid group of compounds, oxaandrolone (Anavar[®]) (4) and 19-norheterosteroid (Nilevar[®]) (5) are used extensively as anabolic steroids (Scheme 3). Many different methods have been developed for the synthesis of 2-heterosteroids and these are now discussed.



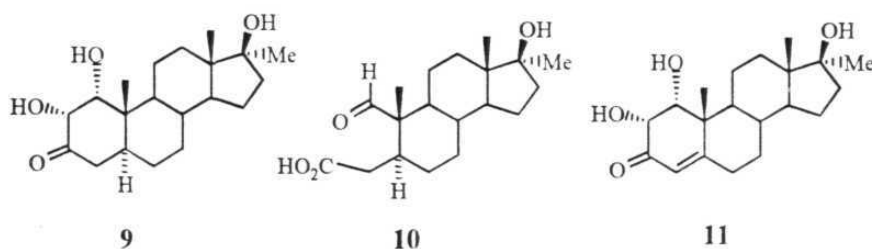
Scheme 3. Anabolic 2-oxasteroids.

1.1.2 Previous Synthetic Approaches to 2-Oxasteroids

According to Pappo's⁶ method, 1-androstene-3,17-dione 6 was treated with four equivalents of $\text{Pb}(\text{OAc})_4$ in 90 % acetic acid to obtain secoaldehyde-acid 7 in equilibrium with the lactol form. Treatment of the mixture with aqueous sodium borohydride followed by acidic work-up furnished 17β-hydroxy-2-oxaandrostane-3-one 8 in about 50-60 % yield (Scheme 4). Alternatively, acid 10 was prepared by $\text{Pb}(\text{OAc})_4$ cleavage of 1α,2α,17β-trihydroxy-17α-methylandrostande-3-one (9), which in turn was prepared by the treatment of 17β-hydroxy-17α-methyl-1-androsten-3-one with potassium chlorate in the presence of catalytic amount of OsO_4 in aqueous ^tBuOH (Scheme 5).



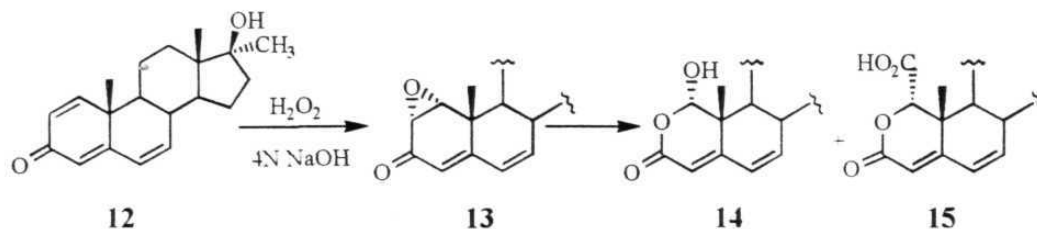
Scheme 4. Oxidative cleavage of 1-ene-3-one steroid to 2-oxa-3-one steroid.



Scheme 5. Dihydroxylation method.

Dihydroxylation reaction on androst-1,4-dien-3,17-dione resulted in a mixture of 1,2- and 3,4-dihydroxy steroids. The 1 α ,2 α -dihydroxy derivative **11** was separated by fractional crystallisation in about 10 % yield. Finally, Pb(OAc)₄ treatment afforded the corresponding lactol.⁷

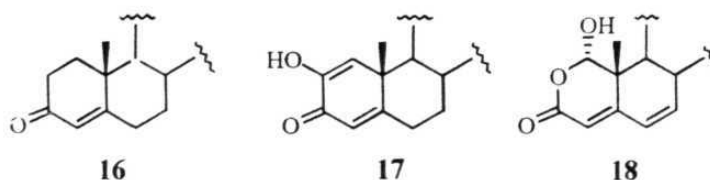
Kocor *et al.*⁸ approached the synthesis of 2-oxasteroids *via* the 1,2-epoxide route as shown in Scheme 6. The 1,2-olefin was selectively cleaved in the presence of Δ^4 - and Δ^6 -olefins. When 17 β -hydroxy-17 α -methyl-1,4,6-androstatriene-3-one (**12**) was treated with basic hydrogen peroxide, the corresponding 1 α ,2 α -epoxide **13** was obtained after 4 h and on continuing the reaction further for 72 h, lactol **14** was isolated in 12 % yield. A major side product in the reaction was 1-carboxy-2-oxa-derivative **15**, separated in 42 % yield.



Scheme 6. Epoxidation method.

Frimer *et al.*⁹ reported a very efficient and high yielding two-step methodology for the conversion of Δ^4 -3-ketosteroids to the corresponding 2-oxa- Δ^4 -3-one steroids. They treated the parent steroid **16** with ^tBuOK in the presence of 18-C-6 crown ether at -27 °C in dry toluene under an atmosphere of oxygen to generate the C2-oxygenated enol **17** in 4 h; continuation of the same reaction at room temperature for an additional day resulted in lactol **18** (Scheme 7).

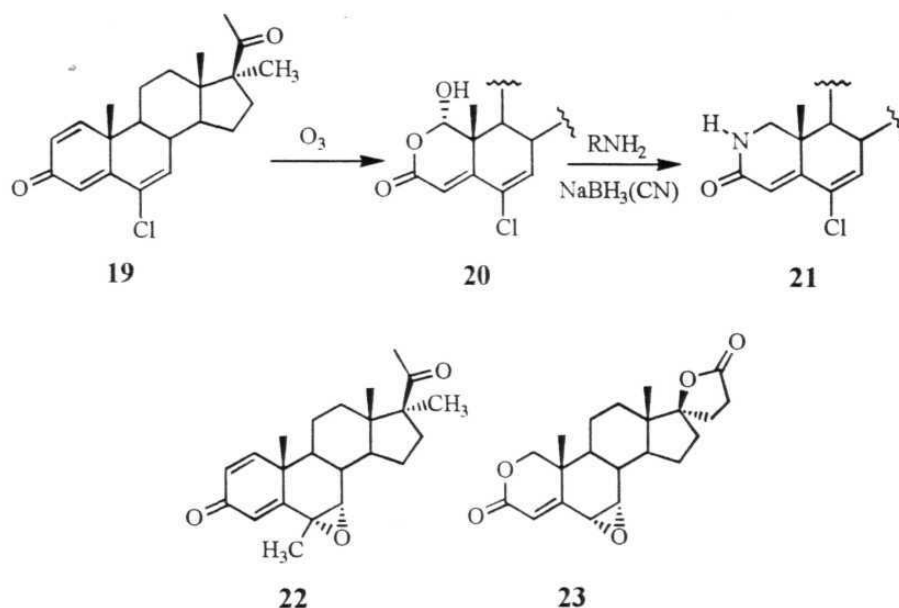
Despite the general success of the above method, the strong basic conditions give reduced yields in some substrates, particularly in the second stage when the reaction has to be carried out at room temperature for conversion to the lactol. To overcome this problem, the same group reported a modified procedure for the conversion of **17** to **18**. In this modification, the reaction is carried out by tetrabutylammonium fluoride catalysed photosensitised singlet oxygenation of steroidal α -keto enols to the corresponding lactols in the presence of polymer-based Rose Bengal.¹⁰ The yields of the lactol are generally better and it is suitable for base sensitive substrates.



Scheme 7. Base catalysed autooxidation method.

Shibata *et al.*¹¹ have reported the synthesis of B-ring functionalised 2-oxa and 2-aza steroids in moderate yields. Thus, reaction of 6-chlorotrienone **19** with OsO₄ in the presence of sodium periodate resulted in lactol **20** in 45 % yield. The lactam **21** was formed by the treatment of lactol with ammonium formate and formic acid. In another method, the lactol was prepared by ozonolysis of 6 β -methyl-6 α ,7 α -epoxy- $\Delta^{1,4}$ -3-one **22** in 1:1 pyridine-CH₂Cl₂ solution and reduced with aqueous NaBH₄ to the corresponding lactone (Scheme 8). Koizumi *et al.*¹² have recently applied this ozonolysis route to the synthesis of 17-spiro-2-oxasteroid **23**.

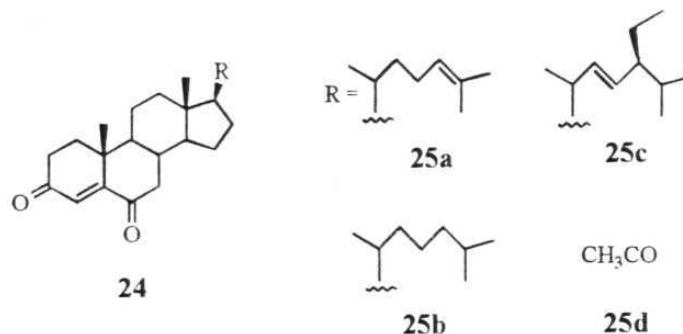
A comparison of published synthetic routes to 2-oxasteroids suggests that Frimer's⁴ method (Scheme 7) has significant advantages, but it is not adaptable to the synthesis of B-ring functionalised steroids. Similarly, Shibata's¹¹ procedure (Scheme 8) can be conveniently applied for the synthesis of B-ring functionalised analogues of 2-oxasteroids, but it has other drawbacks: mixtures of products are obtained, the number of steps is large and overall yields are modest. We reasoned that an improvement in the published protocols for the synthesis of 2-oxasteroid B-ring derivatives will greatly facilitate their synthesis for structural and biological studies. In addition to 2-oxasteroids, the synthesis of novel and as yet unsynthesised 2-thia analogues was also one of the goals in this study.



Scheme 8. B-ring functionalised 2-oxasteroids.

To prepare B-ring derivatives of steroidal lactones, our retrosynthetic analysis suggested that Δ^4 -3,6-dione **24** might be a suitable starting point. A search of the literature revealed some procedures for the synthesis of these diones. Tischler *et al.*¹³ isolated steroids **25a** and **25b** from the sponge *Anthoarcuata graceae* (Scheme 9). In the report of Piers and Worster,¹⁴ oxidation with $CrO_3 \cdot 2Py$ complex of cholesterol afforded the Δ^5 -3-one and Δ^4 -3,6-dione compounds in 9:1 ratio. Numazawa *et al.*¹⁵ applied Jones method for the oxidation of Δ^4 -3-one to Δ^4 -3,6-dione under strongly acidic conditions. Parish *et al.*¹⁶ reported that exposure of Δ^5 -3 β -tetrahydropyranyl ethers to a large excess of PCC (30 equi) in refluxing benzene for 5 h produces the corresponding Δ^4 -3,6-diones in high yields. Adapting this procedure not only meant an extra protection step, but more importantly the compatibility of the acid-sensitive protecting groups, such as ketal, to the harsh oxidation conditions was doubtful. In another report, Moreno *et al.*¹⁷ oxidised Δ^5 -3 β -ols to the corresponding Δ^4 -3,6-diones by reaction with TPAP/NMO reagent under sonochemical conditions. In this background, we explored a mild and

inexpensive method for the preparation of Δ^4 -3,6-diones which is compatible with the acid-sensitive dioxolane protecting group at C17 present in our substrates.



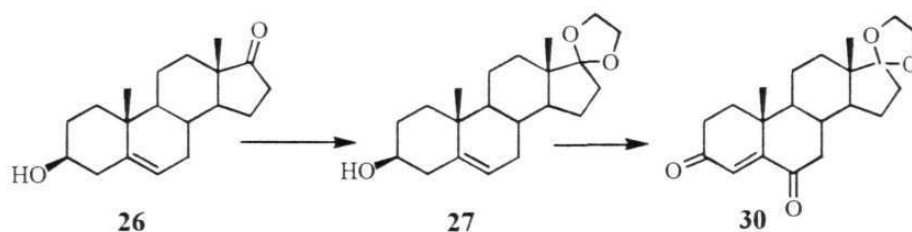
Scheme 9. Steroids with 4-ene-3,6-dione functional group.

1.2 RESULTS AND DISCUSSION

1.2.1 Synthesis of B-ring Functionalised 2-Oxasteroids

Dehydroisoandrosterone **26** was protected as its C17-dioxolane **27** in quantitative yield by treatment with a large excess of ethylene glycol (50 equi.) in the presence of catalytic amounts of *p*-TsOH in refluxing toluene. The water formed during the reaction was removed using Dean Stark apparatus. Oxidation of the homoallylic alcohol and conjugation to Δ^4 -3-one **29** with conventional reagents like PCC, PDC and DPC was attempted. These chromium-based oxidation reagents produced a mixture of products when used in about 2-fold excess. Analysis of the crude residue by ^1H NMR indicated the presence of unconjugated Δ^5 -3-one (δ 5.3, 6-H) **28**, conjugated Δ^4 -3-one (δ 5.8, 4-H) **29**, and Δ^4 -3,6-dione **30**. Notably, the ketal protecting group was intact in all cases. The conversion to these products varied depending on the reaction time - longer reaction time led to a higher proportion of the desired Δ^4 -3,6-dione **30**. The reaction was investigated further with PCC oxidant. When alcohol **27** was treated with 4 equivalents of PCC in CH_2Cl_2 at ambient temperature for 24 h, the only product isolated was the

Δ^4 -3,6-dione **30**, and significantly the acid sensitive C-17 ketal was intact (Scheme 10). The generality of this novel condition for the transformation of steroidal Δ^5 -3-ol to the biologically active Δ^4 -3,6-dione under the aegis of mild and versatile PCC oxidant was explored with a few representative substrates (**25a**, **25c** and **25d**, Table 1). The structure of Δ^4 -3,6-dione was established by single crystal X-ray analysis of ketal **30** and also of the deprotected androstenetrione **30a**.

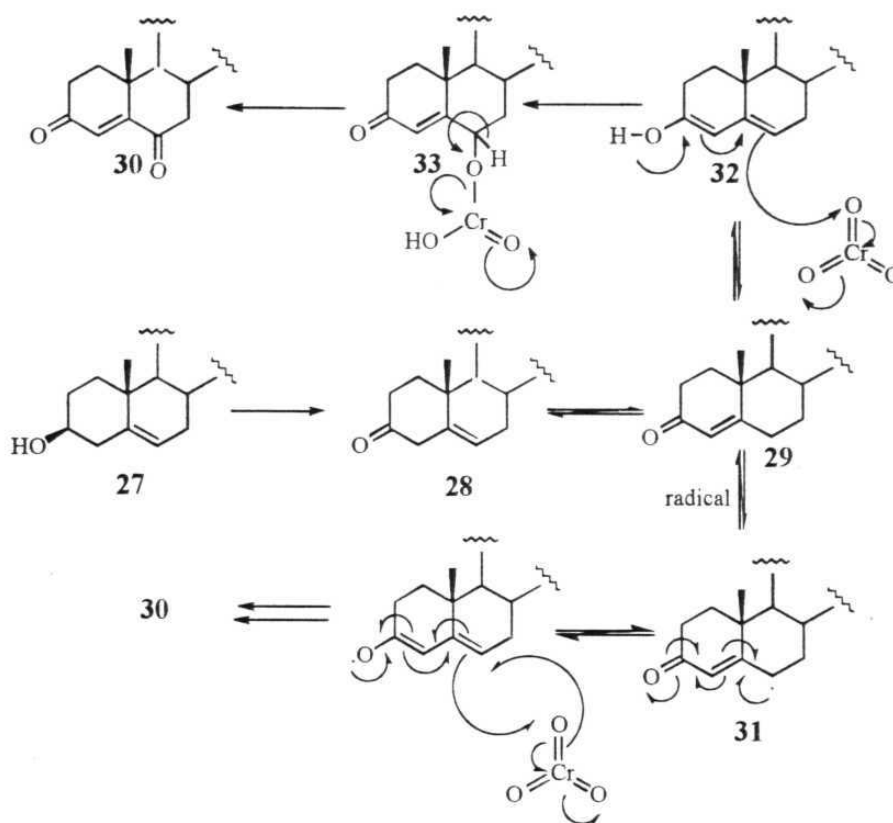


Scheme 10. PCC oxidation.

Table 1: Yields obtained for different substrates in the PCC oxidation.

Compound	25a	25c	25d	30	30a
Yield (%)	70	70	70	80	78

Based on the progressive formation of different intermediates, an ionic or a free radical pathway may be envisioned (Scheme 11). The enol form **32** is in equilibrium with Δ^5 -3-one **28** and enone **29**. Reaction of **32** at C6 with the Cr=O of PCC provides the chromate ester **33**. Subsequent oxidation of C6 alcohol smoothly provides the Δ^4 -3,6-diones **30**. The reaction could also proceed in a radical pathway via an allyl radical **31** that traps the Cr=O species (Scheme 11). Surprisingly, the C17-ketal was cleaved-off to form **30a** when the reaction was performed under sonication in order to reduce the reaction time. The deprotection could not be avoided by the addition of flame-dried powdered molecular sieves to the reaction mixture. While this work was in progress, Blaszczyk and Paryzek¹⁸ reported a similar procedure.



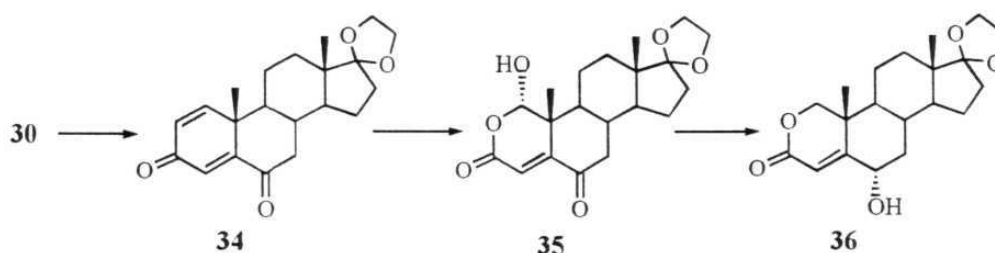
Scheme 11. Mechanism for conversion of homoallylic alcohol to enedione using PCC.

The next step was adaptation of oxygenation methodology for the elaboration of enedione **30**. Oxidation of enedione **30** ($t\text{BuOK}$, O_2) led to a mixture of products because of competing enolisation at C2 and C7. Application of DDQ-based methods¹⁹ (1-2 equiv., 1-20 h reflux, benzene or dioxane) reported in the literature for the 1,2-dehydrogenation of 4-ene-3-one substrates afforded the product in only 10-20 % yield with a significant amount of starting material being unreacted. The SeO_2 dehydrogenation method²⁰ also failed to yield the desired product. We reasoned that the presence of C6-carbonyl deactivates the enone in A-ring and diminishes its reactivity towards dehydrogenation. On the other hand, treatment of Δ^4 -3,6-dione **30** with 4 equivalents of DDQ in dioxane at reflux for 72 h afforded

a single regioisomeric product **34**, in which the C1-C2 alkene was exclusively formed; no C7-C8 isomer was detected. This was concluded from the ^1H NMR spectrum of the crude residue which displayed three coupled olefinic resonances arising from C2, C4 and C1 vinyl protons at δ 7.08, 6.34 and 6.28 for **34** and at δ 7.08, 6.40, 6.30 for **34a**. The regioselectivity in $\Delta^{1,4}$ -3,6-dione formation is a consequence of the facile enolisation at C2 and its less crowded steric environment compared to C7. A drawback of this regioselective reaction is that the C17-ketal is deprotected to a significant extent (~50 %) under the harsh conditions and long reaction time. As a result, C17-ketone **34a** was isolated along with the desired ketal after purification on column chromatography. The by-product **34a** can serve as an advanced starting material for the synthesis of functionalised steroids in which C17-protection may not be mandatory.

Reaction of C17-ketal dienedione **34** with $\text{OsO}_4/\text{NaIO}_4$, OsO_4/NMMO or $\text{RuCl}_3/\text{NaIO}_4$ produced a complex mixture of products which were not characterised further. However, application of Shibata's¹¹ ozonolysis method to **34** was fruitful. When a stream of O_3 was bubbled through a 0.03 M solution of dienone **34** in 1:1 pyridine- CH_2Cl_2 for 15-20 min. at -78°C , the only isolable product after work up was the desired lactol **35** produced essentially as a single stereoisomer. The acetal C1-H singlet appeared at δ 5.60 and the ^{13}C NMR spectrum displayed 20 carbon resonances. The configuration of C1-hydroxy was assigned to be axial based on literature precedence.¹¹ The lactol **35** was conveniently reduced to the 6 α -hydroxy lactone **36** in a heterogeneous solvent system composed of chloroform and aqueous basic solution of NaBH_4 in 70 % overall yield from dienedione **34** (Scheme 12). It has been reported earlier⁶ that the conventional NaBH_4 reduction of lactol in aqueous basic methanol produces large amounts of saturated lactonic products. However, in the heterogeneous $\text{H}_2\text{O}-\text{CHCl}_3$ system, the lactol (aldehydo-acid) is extracted into aqueous phase and

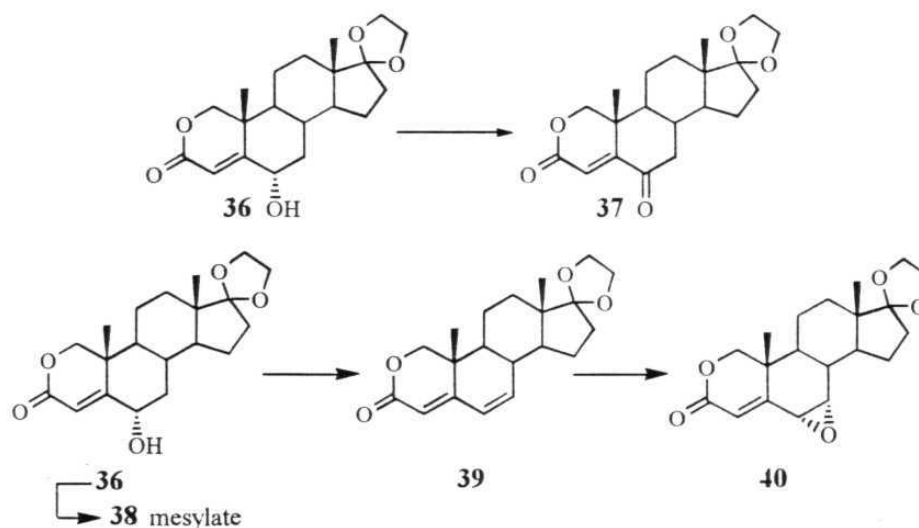
reduced to the lactone. The resulting lactone is immiscible with water and selectively extracted back into CHCl_3 , thereby protecting it from further reduction.⁹ The reduction of the C6-carbonyl takes place entirely from the exposed β -face to produce the equatorial alcohol exclusively.²¹ In lactone **36** the $AB\text{ CH}_2\text{O}$ pattern is centered at δ 4.10 ($J=12$ Hz) and the axial C6-H appears as a multiplet at δ 4.30. The weak coupling²² of C6 β -H to vinylic C4-H at δ 6.12 ($J=2$ Hz) confirms the equatorial orientation of the secondary alcoholic group. Thus, 17-ethylenedioxy-6 α -hydroxy-2-oxa-4-androsten-3-one (**36**) was produced with complete regio- and stereocontrol from the easily prepared $\Delta^{1,4}$ -3,6-dione **34**. In effect, the 17-ketal-hydroxy lactone **36** lends itself as key synthon for the synthesis of B-ring functionalised 2-heterosteroids.



Scheme 12. Enedione to hydroxy lactone.

Exposure of allylic alcohol **36** to PCC in CH_2Cl_2 for 2 h at rt produced 2-oxa-4-androsten-3,6-dione **37** with the C17-ketal still intact (Scheme 13). Many attempts to obtain single crystals of ketal **37** or its C17-ketone for single crystal X-ray crystallography were not successful. Conversion of alcohol **36** to mesylate **38** (MsCl , Et_3N) and elimination with DBU to produce the C6-C7 olefin was sluggish because of the equatorial orientation of the leaving group. Displacement of the mesylate with LiBr and *in situ* dehydrobromination proceeded smoothly with Li_2CO_3 in hot DMF to produce the conjugated lactone **39**. Attempts to isolate the intermediate axial bromide were unsuccessful since it underwent spontaneous

anti elimination. At this juncture it was clear that the axial hydroxy lactone too would be an interesting molecule to synthesise. Efforts in inverting the mesylate **38** to epimeric 6 β -alcohol with NaOAc, LiOH.H₂O or KO₂ proved to be futile. Also, Mitsunobu²³ alcohol inversion and bromination did not give the desired 6 β -derivative. Thus, under basic conditions elimination-type products were produced whereas the neutral protocol of Mitsunobu afforded the starting alcohol with no S_N2 displacement-type products being isolated.

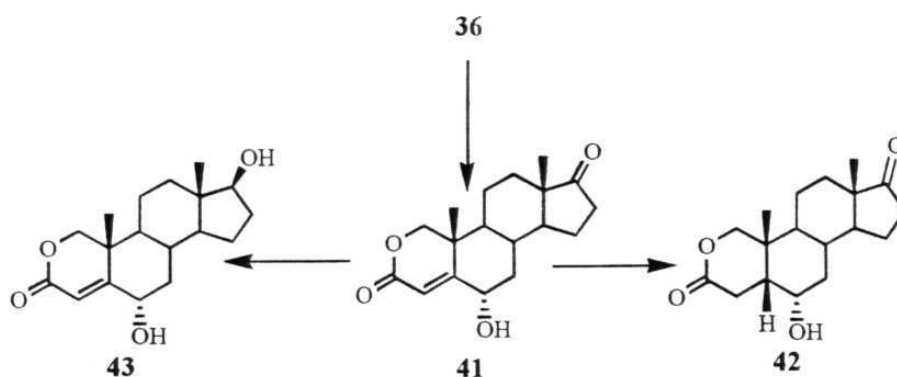


Scheme 13. B-ring functionalisation of 2-oxasteroids.

Reduction of 2-oxa-6-keto **37** with bulky reducing agent, Li(^tBuO)₃AlH once again yielded the 6 α -hydroxy lactone **36**. So the C6-C7 alkene **39** was used for further functionalisation. Reaction of alkene **39** with excess PCC or DPC under different time-temperature domain conditions was carried out to effect C8 allylic oxidation but only unreacted starting material was recovered. The idea was that the tertiary alcohol may be transformed to the C6-hydroxy via an allylic transposition. Ultimately, the conjugated lactone **39** was treated with *m*-CPBA (4 equi.) in CHCl₃ at ambient temperature for 24-36 h to furnish C6 α -C7 α -epoxide **40** (δ 3.30, 3.38) as a single stereoisomer.¹¹ The reaction was stopped at 70-80 %

conversion because longer exposure (48 h) led to bis-epoxidation products. Epoxide **40** marks another crucial synthon in the series of B-ring functionalised 2-oxasteroids.

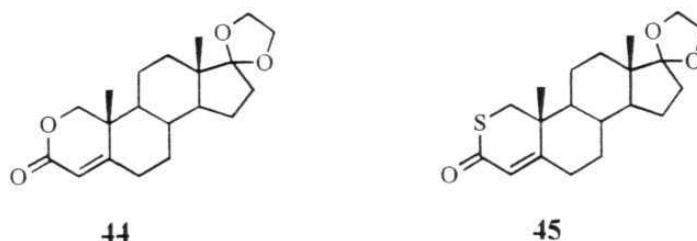
To study the single crystal X-ray structure of the B-ring functionalised 2-oxasteroids, some transformations were carried out to obtain appropriate derivative as shown in Scheme 14. The C17-ketal of lactone **36** was readily deprotected with 10 % H_2SO_4 in acetone to afford the 6α -hydroxy-2-oxaandrost-4-ene-3,17-dione (**41**) in quantitative yield. The structure of this lactone was confirmed by IR, ^1H NMR and ^{13}C NMR, mass spectroscopy and eventually by single crystal X-ray crystallography. The 6-hydroxy- Δ^4 -lactone **41** was hydrogenated under heterogenous conditions (H_2 , 10 % Pd/C) to produce saturated hydroxy lactone **42** in quantitative yield. In this reduction also only a single stereoisomer was obtained as deduced by ^1H and ^{13}C NMR. The stereochemistry was confirmed to be 5β by single crystal X-ray analysis of the saturated lactone **42**. The deprotected C-17 ketone **41** was reduced to $6\alpha,17\beta$ -dihydroxy-2-oxa-4-androsten-3-one (**43**) in 70 % yield by treatment with aqueous NaBH_4 in CHCl_3 . Only C17 β stereoisomer was obtained which was confirmed by ^1H and ^{13}C NMR and single crystal X-ray crystallography.



Scheme 14. B-ring functionalised 2-oxasteroids analysed by X-ray.

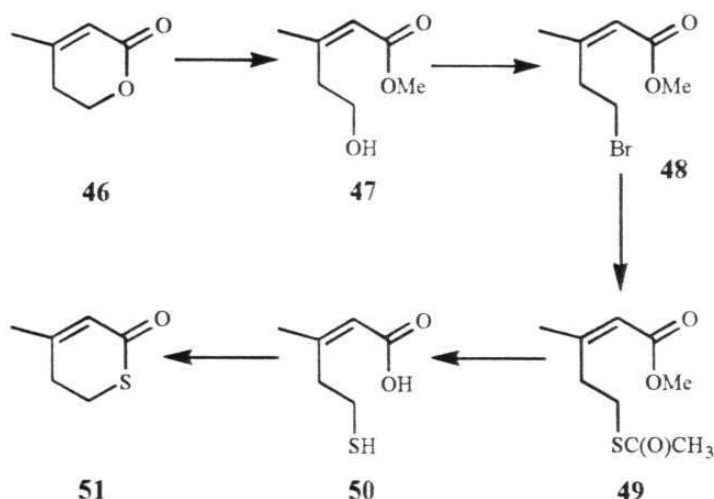
1.2.2 Synthesis of 2-Thiasteroids

To the best of our knowledge there is no report on the synthesis of 2-thiasteroids. In order to avoid complication arising out of B-ring functionality, 2-thia-4-ene-3-one **45** was first targeted. Retrosynthetic analysis suggested that lactone **44** should be a starting point (Scheme 15). Frimer's base catalysed auto-oxidation method⁹ was adopted in the preparation of these 2-oxaandrosterone derivatives.



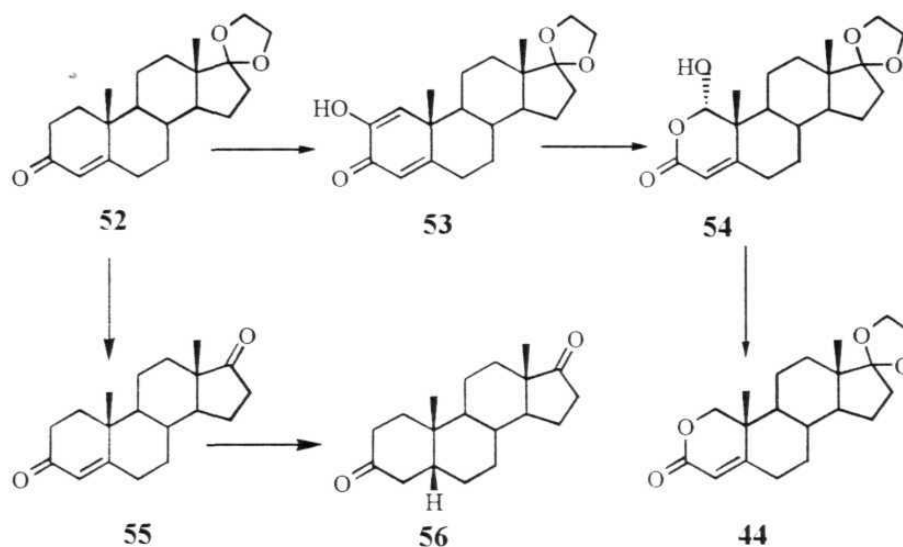
Scheme 15. *Lactone and thialactone.*

A method for the conversion of lactone to thialactone in a simple model system was first attempted (Scheme 16) for subsequently applying to the steroidal series. Anhydromevalonolactone **46** was opened to hydroxy acid by refluxing with 1 *M* NaOH and subsequent neutralization at 0 °C afforded the hydroxy acid which was treated with diazomethane to ester **47**. The hydroxy ester was converted to bromomethyl ester **48** (CBr₄, Ph₃P). Nucleophilic substitution of the bromide with sodium thioacetate readily yielded the diester **49**. Alkaline hydrolysis to thiol acid **50** which was then cyclised to thialactone **51** in an overall yield of 40 %.



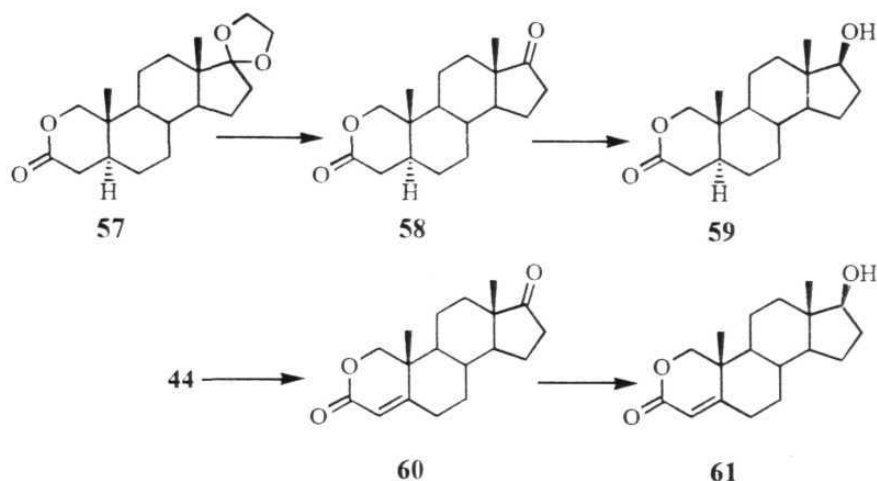
Scheme 16. Conversion of lactone to thialactone in model system.

The application of this protocol for the conversion of 2-oxasteroids to 2-thiasteroids was studied next. Thus, C17-ketal protected androsterone **27** was subjected to Oppenauer oxidation²⁴ by treatment with $\text{Al}(\text{iPrO})_3$ and cyclohexanone in refluxing toluene for 5 h to provide 17-ethylenedioxy- Δ^4 -androsten-3-one (**52**) in 50-60 % yield (Scheme 17). The same reaction was repeated by replacing cyclohexanone with acetone in toluene or benzene. The latter method produced higher yields (70-80 %) and the complication from cyclohexanone/cyclohexanol by-products in the purification step were avoided. Δ^4 -Androsten-3-one **52** was stirred with 18-crown-6 and $^t\text{BuOK}$ in dry toluene at -27°C for 5 h under dry oxygen atmosphere to produce 2-hydroxy- $\Delta^{1,4}$ -androsten-3-one **53** as an isolable intermediate. The reaction was continued for 20 h at rt to afford lactol **54** in 60 % yield as a single compound. Deprotection of the ketal in the second stage of the reaction was not observed in the oxidation step. The lactol **54** was then conveniently reduced to lactone **44** with an aqueous solution of NaBH_4 in chloroform.



Scheme 17. Synthesis of lactone from enone.

With the idea that the related 2-oxasteroids will be required for the conversion to 2-thiasteroid or for X-ray studies, **44** was functionalised to obtain different derivatives (Scheme 18). 17-Ethylenedioxy-2-oxaandrost- Δ^4 -3-one **44** was hydrogenated with 10 % Pd/C catalyst in ethyl acetate under hydrogen atmosphere at ambient temperature and pressure conditions to lactone **57** in quantitative yield as a single stereoisomer. Incidentally, Δ^4 -androstene-3,17-dione **55** produced the 5 β isomer **56** under similar hydrogenation conditions exclusively as confirmed by single crystal X-ray crystallography. Further, it should be noted that hydrogenation, of 6 α -hydroxy- Δ^4 -lactone **36** produced 5 β epimer **42**. At this stage it is not clear what is the exact role of C2 to O-atom replacement and the C6-OH group in directing attack of H₂ from different faces of the steroid skeleton. Lactone **57** was deprotected to C17 ketone **58** with 10 % H₂SO₄ in acetone, and then reduced with NaBH₄ in CHCl₃ to produce 17 β -hydroxy lactone **59**. Similarly, lactone **44** was converted to 17 β -hydroxy lactone **61**.



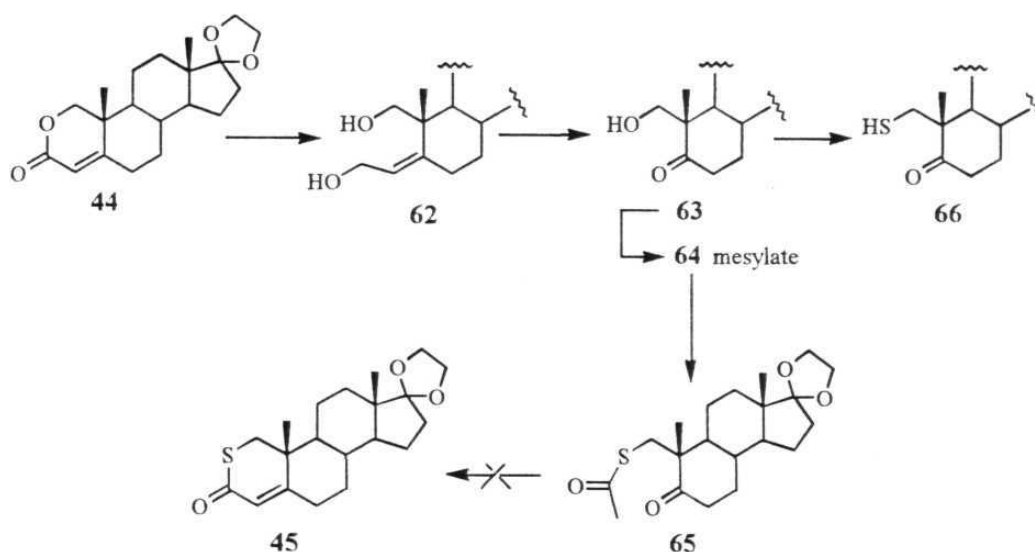
Scheme 18. Some complex 2-oxasteroids for X-ray studies.

The lactone to thialactone transform is now discussed. Lactone **44** was refluxed with sodium methoxide in methanol for 30 min., at which point TLC indicated the absence of starting material. Slow neutralisation with ice-cold 1 M HCl at -5 °C and extraction with ethyl acetate yielded starting material as confirmed by TLC and ^1H NMR. It appears that the open hydroxy-acid form cyclises spontaneously because the hydroxy and acid groups are tethered to the B/C/D carbon skeleton and the olefin has the *cis* configuration. At this juncture, the approach was to remove the substituents that constitute the A-ring and then rebuild it after the introduction of sulfur atom at C1. Thus, lactone **44** was subjected to LiAlH_4 reduction at -78 °C, which produced a complex mixture of saturated and unsaturated diols. DiBAL-H reduction at -78 °C smoothly yielded unsaturated diol **62** but it was very unstable during column chromatography and decomposed to uncharacterisable products at room temperature within a few hours. The unsaturated diol was also not amenable to mesylation (MsCl , Et_3N , CH_2Cl_2) or Mitsunobu bromination (Ph_3P , CBr_4 , THF) conditions. Thus, the diol was ozonised under buffered conditions (NaHCO_3 , DCM/MeOH) without further

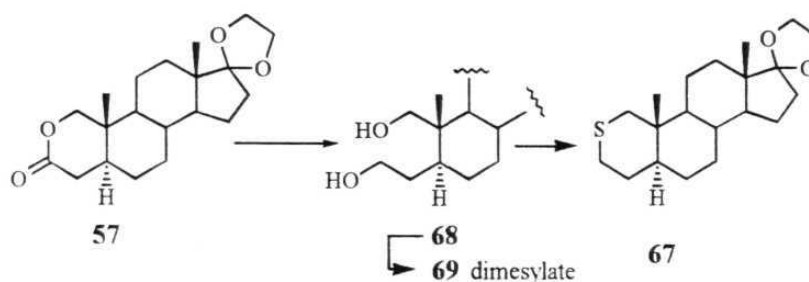
purification and characterisation, to afford keto alcohol **63** in 37 % yield from lactone **44**.

Mesylation of alcohol **63** was uneventful and mesylate **64** was treated with cesium thioacetate (Cs_2CO_3 , $\text{CH}_3\text{C}(\text{O})\text{SH}$) in hot DMF to produce thioester **65** in moderate yield (Scheme 19). Attempted aldol cyclisation of **65** with LDA, NaH or $^t\text{BuOK}$ failed to yield thiolactone **45** under a variety of temperature-solvent regime conditions. To reduce the basicity during cyclisation, the reaction was planned under the Wadsworth-Emmons conditions. Mesylate **64** was heated at 100 °C with a large excess of Na_2S for 2 h to produce ketothiol **66**. The thiol was then treated with triethyl phosphonoacetate ($(\text{EtO})_2\text{P}(\text{O})\text{CH}_2\text{CO}_2\text{Et}$) in the presence of NaH in dry THF. The reaction mixture showed only starting material and no condensation products with ketone were observed. In another attempt, ketothiol **66** was condensed with diethylphosphonoacetic acid in the presence of DCC. This reaction also did not produce the desired product; only unreacted starting material was recovered. Due to the low yields in the DiBAL-H reduction step, complex reaction mixtures and failure during the cyclisation to the target molecule **45**, this synthetic route (Scheme 19) was prematurely aborted. Instead, we planned to synthesise 2-thiaandrostane derivatives starting from saturated lactone **67**.

When saturated lactone **57** was subjected to LAH reduction in THF at 0 °C to rt, a significant amount of hemiacetal was formed. To effect complete reduction to diol **68**, the reaction mixture was refluxed for 1 h in THF under inert atmosphere. Saturated diol **68** was converted to dimesylate **69** in 90 % yield (Scheme 20). The dimesylate was heated with Na_2S in dry DMF at 100 °C to produce the desired thia steroid **67** smoothly in 60 % yield. The ketal protecting group was intact through this sequence. The structure of **67** was confirmed by the absence of carbonyl stretch in the IR and the appearance of multiple patterns centered at δ 2.57 for C1 and C3 protons.



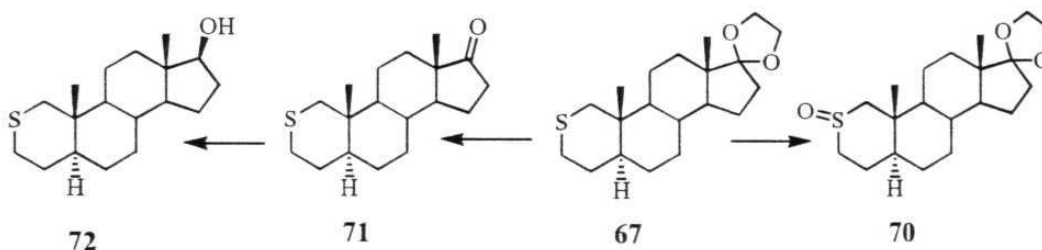
Scheme 19. Attempted synthesis of 2-thialactone.



Scheme 20. Lactone to 2-thiapyran.

NaIO_4 oxidation of thiapyran **67** in aqueous methanol at rt produced sulfoxide **70**. Attempted Pummerer rearrangement of this sulfoxide with SOCl_2 , CO_2Cl_2 failed to yield any characterisable products. The crude ^1H NMR spectrum showed the absence of C19-methyl singlet suggesting that some skeletal reorganisations had occurred. Deprotection of C17-ketal **67** with 10 % H_2SO_4 in acetone yielded 2-thiaandrostane-17-one **71** in quantitative yield (Scheme 21). Reduction of ketone **71** with LAH in dry THF proceeded smoothly to produce 17-hydroxy-3-deoxy-5 α -2-thiaandrostane **72** in 60 % yield. The thiasteroid was found to be unstable and it decomposed to unidentifiable products in a few days at ambient temperature and

even in the refrigerator. Attempted crystallisation in various solvents to obtain X-ray quality crystals was not fruitful because of the instability of the compound. At this stage, further work on the synthesis of thiasteroids was discontinued.



Scheme 21. Derivatisation of 2-thiasteroid

1.3 EXPERIMENTAL SECTION

Instrumentation:

Melting Point (mp): Melting points were determined on Superfit and Fisher-Johns melting point apparatus and are uncorrected.

Infrared Spectra (IR): Infrared spectra were recorded on Jasco 5300 spectrophotometer. All spectra were calibrated against a polystyrene absorption at 1601 cm^{-1} . Solid samples were prepared as KBr wafers and semi-solid and liquid samples were dissolved in CHCl_3 and recorded as film between NaCl plates.

Nuclear Magnetic Resonance Spectra (NMR): Proton magnetic resonance (^1H NMR) spectra and carbon-13 magnetic resonance (^{13}C NMR) spectra were recorded on Bruker ACF-200 spectrometer at 200 MHz and 50 MHz. All ^1H NMR and ^{13}C NMR samples were prepared in chloroform- D solvent unless otherwise stated. Spectral assignments for ^1H NMR are as follows: (1) chemical shift on the δ scale (tetramethylsilane $\delta = 0.00$ ppm); (2) number of hydrogens integrated for the signal; (3) multiplicity: s = singlet, d = doublet, t = triplet, q = quartet, m = multiplet, dd = doublet of doublet, dt = doublet of triplet, b = broad singlet; (3) coupling constant J in Hertz (Hz); (4) assignment of the signal (in few

cases). For ^{13}C NMR spectral data, values are calibrated against CDCl_3 ($\delta = 77.0$ ppm).

Elemental analysis: Elemental analysis was performed on a Perkin-Elmer 240C instrument.

Mass Spectra: Low resolution mass spectra (LRMS) were recorded on JOEL JMS DX-303 instrument.

Ozonolysis: Ozonolysis was carried out on Welsbach model by purging a steady stream of O_3/O_2 through the solution.

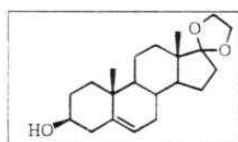
Chromatography: Analytical thin layer chromatography (TLC) was performed on glass plates (2.5x7.5 cm) coated with Acme's silica gel GF 254 containing 13 % calcium sulfate as binder. Visualisation of the spots was achieved by exposure to iodine vapor or UV light. Column chromatography (SGC) was effected using Acme's silica gel (100-200 mesh) employing appropriate solvent systems.

Cryostat: Julabo FT-901 chiller with immersion probe and temperature control (-80 to 0 °C) was used to carry out low-temperature reactions.

General:

All reactions were monitored by TLC using appropriate solvent system. Moisture sensitive reactions were carried out using standard syringe-septum techniques in inert atmosphere (nitrogen) with magnetic stirring. All anhydrous solvents were freshly distilled from appropriate drying agents.²⁵ Work-up means washing of solvent extracts with brine, drying over anhydrous magnesium sulfate and concentration on Superfit rotary evaporator at reduced pressures. All yields reported are isolated yields of material judged homogeneous by TLC and other spectroscopic techniques.

17-(Ethylenedioxy)-3 β -hydroxy- Δ^5 -androstene (27): Dehydroisoandrosterone **26** (2.8 g, 10 mmol), ethylene glycol (31.6 g, 28 mL, 500 mmol) and *p*-TsOH (190 mg, 1 mmol) were taken in dry toluene (200 mL) and refluxed for 5 h with a Dean-Stark apparatus to remove water formed during the reaction. The cooled reaction mixture was immediately washed with satd. NaHCO₃ solution and worked-up to afford pure ketal **27**.



Yield: 3.3 g, 98 %.

mp: 158-162 °C

IR: cm⁻¹ 3472, 2918, 1462.

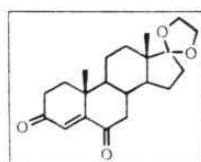
¹H NMR: δ 5.34 (1H, d, *J*=6 Hz), 3.80-3.98 (4H, m), 3.44-3.60 (1H, m), 1.01 (3H, s), 0.86 (3H, s).

¹³C NMR: δ 140.81, 121.30, 119.50, 71.49, 65.11, 64.49, 50.59, 49.98, 45.72, 42.22, 37.28, 36.53, 34.17, 32.17, 31.54, 31.23, 30.58, 22.76, 20.48, 19.39, 14.17.

General procedure for the oxidation of homoallylic alcohols to 4-en-3,6-diones:

To a suspension of PCC (15 mmol), in dry DCM (20 mL) at rt the alcohol (3 mmol) was added and stirred for 24 h. The reaction mixture was diluted with ether (50 mL) and filtered through a pad of Celite. Evaporation of the solvent and filtration through silica gel column afforded the diketone.

C17-ketal 30:



Yield: 80 %

mp: 162-164 °C

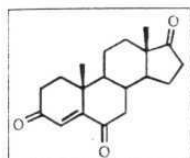
IR: cm⁻¹ 3053, 2947, 1684, 1456.

¹H NMR: δ 6.14 (1H, s), 3.80-3.98 (4H, m), 2.70 (1H, dd, *J*=12, 3 Hz), 1.15 (3H, s), 0.88 (3H, s).

^{13}C NMR: δ 201.42, 198.90, 160.56, 125.22, 118.58, 65.06, 64.35, 50.53, 50.22, 45.78, 45.67, 39.54, 35.36, 34.22, 33.77, 29.73, 22.75, 20.17, 17.32, 13.99.

Analysis: Found C, 73.20; H, 8.29. Calcd. for $\text{C}_{21}\text{H}_{28}\text{O}_4$: C, 73.23; H, 8.19 %.

C17-ketone 30a:



Yield: 78 %

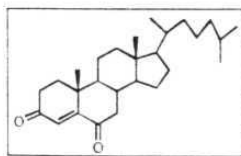
mp: 220-222 °C

IR: cm^{-1} 1736, 1672.

^1H NMR: δ 6.21 (1H, s), 1.20 (3H, s), 0.94 (3H, s).

^{13}C NMR: δ 218.92, 200.85, 198.82, 160.09, 125.38.

Cholesterol dione 25b:



Yield: 70 %

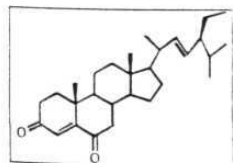
mp: 132-134 °C

IR: cm^{-1} 1687

^1H NMR: δ 6.18 (1H, s), 1.16 (3H, s), 0.70 (3H, s).

^{13}C NMR: δ 201.90, 199.21, 160.08, 125.33.

Pregnenalone dione (25c):



Yield: 70 %

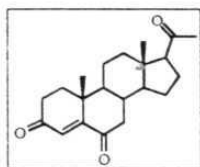
mp: 150-152 °C

IR: cm^{-1} 1691

^1H NMR: δ 6.17 (1H, s), 1.15 (3H, s), 0.75 (3H, s).

^{13}C NMR: δ 202.01, 199.24, 160.08, 125.43.

Progesterone dione 25d:

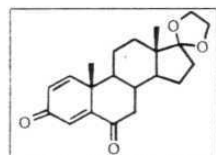


Yield: 70 %

mp: 188-190 °C

IR: cm⁻¹ 1699, 1674.¹H NMR: δ 6.19 (1H, s), 2.14 (3H, s), 1.17 (3H, s), 0.69 (3H, s).¹³C NMR: δ 208.43, 201.35, 198.93, 160.08, 125.41.

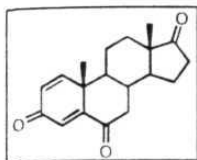
17-(Ethylenedioxy)-Δ^{1,4}-3,6-androstenedione (34): The enedione **30** (600 mg, 1.7 mmol) and DDQ (1.5 g, 6.8 mmol) were taken in dry dioxane (40 mL) and refluxed for 72 h in nitrogen atmosphere. After cooling to rt, the precipitated DDQ by-product was filtered and the filtrate concentrated under reduced pressure. The residue was dissolved in EtOAc (20 mL), and worked-up. SGC purification provided two products, the protected dienedione **34** and 17-ketal cleaved compound **34a**.

Dienone 34:

Yield: 200 mg, 45 %

mp: 208-210 °C

IR: cm⁻¹ 2943, 2881, 1699, 1657, 1620.¹H NMR: δ 7.08 (1H, d, J=9 Hz), 6.34 (1H, d, J=2 Hz), 6.28 (1H, dd, J=12, 2 Hz), 3.78-3.94 (4H, m), 2.70 (1H, dd, J=12, 2 Hz), 1.19 (3H, s), 0.90 (3H, s).¹³C NMR: δ 210.50, 185.00, 161.41, 153.51, 128.02, 124.88, 118.51, 65.25, 64.54, 50.06, 48.90, 46.18, 45.93, 44.78, 34.64, 33.83, 29.86, 22.42, 22.27, 18.98, 14.24.Analysis: Found C, 73.41; H, 7.58. Calcd for C₂₁H₂₆O₄: C, 73.66; H, 7.65 %.**Dienetrione 34a:**



Yield: 200 mg, 45 %

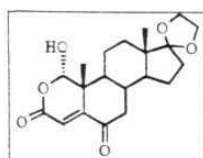
mp: 217-218 °C

IR: cm⁻¹ 2957, 1736, 1660, 1620.

¹H NMR: δ 7.08 (1H, d, J=9 Hz), 6.40 (1H, d, J=2 Hz), 6.30 (1H, dd, J=12, 2 Hz), 2.84 (1H, dd, J=12, 2 Hz), 1.26 (3H, s), 0.98 (3H, s).

¹³C NMR: δ 218.73, 200.94, 185.12, 160.96, 153.17, 128.36, 125.37, 51.12, 49.04, 47.75, 45.55, 44.67, 35.49, 35.56, 34.06, 30.94, 22.17, 21.73, 19.14, 13.88.

17-(Ethylenedioxy)-1α-hydroxy-2-oxa-Δ⁴-3,6-androstenedione (35): The dienone **34** (60 mg, 0.18 mmol) was dissolved in 1:1 mixture of DCM/pyridine (4 mL). Ozone was bubbled through the solution at -78 °C for 20 min. After flushing the excess O₃, the reaction mixture was stirred for 15 min. at rt. Diluted with 15 mL CHCl₃, washed with 1 M HCl (3x10 mL) and with sat. NaHCO₃ (2x10 mL). Work-up afforded the desired ketolactol **35**.



Yield: 50 mg, 77 %

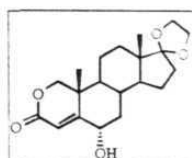
IR: cm⁻¹ 3375, 3059, 2945, 1732, 1460.

¹H NMR: δ 6.12 (1H, d, J=2 Hz), 4.25-4.36 (1H, m), 4.22 (1H, d, J=12 Hz), 4.03 (1H, d, J=12 Hz), 1.22 (3H, s), 0.88 (3H, s).

¹³C NMR: δ 198.37, 163.31, 153.61, 118.87 (2C), 100.69, 65.25, 64.53, 50.20, 45.63, 45.27, 42.86 (2C), 33.78, 33.14, 29.68, 22.48, 20.09, 18.42, 14.08.

17-(Ethylenedioxy)-2-oxa-6α-hydroxy-Δ⁴-3-androstenone (36): To lactol **35** (50 mg, 0.13 mmol) in CHCl₃ (10 mL) a solution of NaBH₄ (52 mg, 1.3 mmol) in 2 mL of water followed by 0.2 mL of 1 M NaOH were added and stirred for 4 h at

rt. Dilution with 10 mL CHCl_3 , work-up and SGC purification furnished lactone **36**.



Yield: 37 mg, 82 %

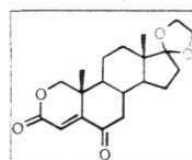
mp: 195-200 °C

IR: cm^{-1} 3489, 3057, 2939, 1709.

^1H NMR: δ 6.12 (1H, d, $J=2$ Hz), 4.25-4.36 (1H, m), 4.22 (1H, d $J=12$ Hz), 4.03 (1H, d, $J=12$ Hz), 3.78-3.98 (4H, m), 1.22 (3H, s), 0.88 (3H, s).

^{13}C NMR: δ 168.60, 164.94, 118.89, 110.89, 77.17, 67.59, 65.23, 64.53, 49.25 (2C), 45.57, 39.93, 38.39, 34.02, 33.87, 29.98, 22.66, 21.07, 17.28, 14.14.

17-(Ethylenedioxy)-2-oxa- Δ^4 -3,6-androstenedione (37): 6-Hydroxy lactone **36** (20 mg, 0.056 mmol) was added to a suspension of PCC (80 mg, 0.336 mmol) in 4 mL dry DCM and the mixture was stirred for 2 h at rt. Dilution with 20 mL ether, filtration through a pad of Celite and SGC purification yielded the pure compound **37**.



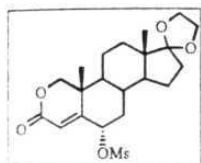
Yield: 16 mg, 80 %

IR: cm^{-1} 3059, 2949, 1728, 1705.

^1H NMR: δ 6.37 (1H, s), 4.37 (1H, d, $J=10$ Hz), 4.15 (1H, d, $J=10$ Hz), 3.78-3.98 (4H, m), 2.75 (1H, dd, $J=12, 2$ Hz), 1.24 (3H, s), 0.89 (3H, s).

17-(Ethylenedioxy)-2-oxa-6 α -mesyloxy- Δ^4 -3-androstenone (38): To the hydroxy lactone **36** (15 mg, 0.043 mmol) in 1 mL dry DCM, Et_3N (65.3 mg, 90 μL , 0.6 mmol) and MsCl (50 mg, 34 μL , 0.43 mmol) were added at -5 °C and the mixture stirred for 30 min. The solvent was evaporated and the residue dissolved

in 5 mL EtOAc. The organic layer was washed with ice-cold 1 M HCl (2x5 mL), satd. NaHCO₃ (2x5 mL) and worked-up to afford mesylate **38**.

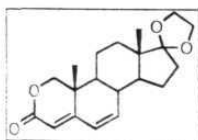


Yield: 15 mg, 87 %

IR: cm⁻¹ 2947, 2891, 1761.

¹H NMR: δ 6.04 (1H, d, J=12 Hz), 5.18-5.30 (1H, m), 4.27 (1H, d, J=12 Hz), 4.04 (1H, d, J=12 Hz), 3.80-3.98 (4H, m), 3.12 (3H, s), 2.48 (3H, s), 2.44-2.30 (1H, m), 1.26 (3H, s), 0.88 (3H, s).

17-(Ethylenedioxy)-2-oxa-Δ^{4,6}-androst-3-one (39): To a solution of dimesylate **38** (13 mg, 0.03 mmol) in dry DMF (1 mL), LiBr (26 mg, 0.3 mmol), Li₂CO₃ (22 mg, 0.3 mmol) were added, and heated at 100 °C for 1.5 h. The cooled reaction mixture was diluted with 10 mL water and extracted with EtOAc (3x10 mL). Work-up and SGC purification gave the desired doubly conjugated lactone **39**.

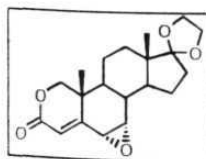


Yield: 8 mg, 80 %

IR: cm⁻¹ 2928, 2878, 1722, 1624.

¹H NMR: δ 6.16 (2H, s), 5.63 (1H, s), 4.27 (1H, d, J=12 Hz), 4.05 (1H, d, J=12 Hz), 3.80-4.00 (4H, m), 1.18 (3H, s), 0.93 (3H, s).

17-(Ethylenedioxy)-2-oxa-6,7α-epoxy-Δ⁴-androst-3-one (40): To the diene **39** (5 mg, 0.015 mmol) in dry CHCl₃ (1 mL), *m*-chloroperbenzoic acid (10 mg, 0.06 mmol) was added and the mixture was stirred for 24 h at rt. The reaction mixture was diluted with 10 mL of CHCl₃. Work-up and SGC purification provided epoxide **40**.



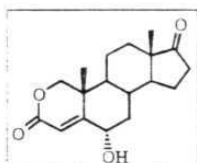
Yield: 4 mg, 80 %

IR: cm⁻¹ 2926, 2826, 1734.

¹H NMR: δ 6.06 (1H, s), 4.02 (1H, d, J=12 Hz), 3.98 (1H,

d, $J=12$ Hz), 3.74-3.90 (4H, m), 3.38 (1H, d, $J=4$ Hz), 3.30 (1H, d, $J=4$ Hz), 1.09 (3H, s), 0.84 (3H, s).

2-Oxa-6 α -hydroxy- Δ^4 -androstene-3,17-dione (41): To a solution of 17-Ethylenedioxy-6-hydroxy lactone **36** (30 mg, 0.086 mmol) in acetone (2 mL), 0.5 mL of 10 % H_2SO_4 was added and stirred for 1 h. The solvent was removed and the residue was dissolved in EtOAc (10 mL) and washed with satd. NaHCO_3 solution. Work-up and SGC purification afforded hydroxy dione **41**.



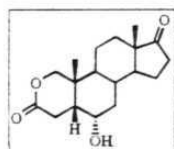
Yield: 25 mg, 95 %

mp: 244-246 °C

IR: cm^{-1} 3445, 2957, 1725, 1701.

^1H NMR: δ 6.12 (1H, d, $J=2$ Hz), 4.44-4.30 (1H, m), 4.22 (1H, d, $J=6$ Hz), 4.04 (1H, d, $J=6$ Hz), 1.02 (3H, s), 0.88 (3H, s).

2-Oxa-6 α -hydroxy-5 β -androstane-3,17-dione (42): To 6 α -Hydroxy lactone **41** (25 mg, 0.082 mmol) in EtOAc (5 mL), 25 mg of 10 % Pd/C was added and stirred for 1 h under hydrogen atmosphere. After confirming that all the starting material is consumed, the reaction mixture was filtered through a pad of Celite. Solvent evaporation has provided pure 5 β lactone **42**.



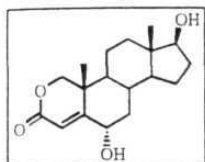
Yield: 23 mg, 92 %

IR: cm^{-1} 3447, 2934, 1734.

^1H NMR: δ 4.20-4.00 (2H, m), 3.80 (1H, d, $J=6$ Hz), 0.96 (3H, s), 0.84 (3H, s).

2-Oxa-6 α ,17 β -dihydroxy- Δ^4 -androstene-3-one (43): The 17-keto lactone **41** (20 mg, 0.082 mmol) was dissolved in CHCl_3 and an aq. solution of NaBH_4 (16 mg,

0.4 mmol) taken in 1 mL water and 0.1 mL 1 M NaOH solution were added and stirred at rt for 4 h. The reaction was worked-up to afford **43**.



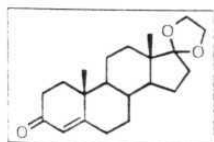
Yield: 18 mg, 90 %

IR: cm^{-1} 3447, 3314, 2932, 1699, 1456.

^1H NMR (10 % DMSO-d_6 in CDCl_3): δ 5.42 (1H, s), 4.14-3.98 (2H, m), 3.88 (1H, d, $J=6$ Hz), 3.40 (1H, t, $J=4$ Hz), 1.04 (3H, s), 0.45 (3H, s).

MS: 306 (M^+)

17-(Ethylenedioxy)- Δ^4 -androstene-3-one (52**):** Homoallylic alcohol **27** (1 g, 3 mmol), $\text{Al}(\text{iPrO})_3$ (2.448 g, 12 mmol) and acetone (3.5 mL, 60 mmol) were taken in 25 mL dry toluene and stirred at reflux for 7 h. The reaction mixture was diluted after cooling to rt with EtOAc (50 mL), washed with ice-cold 1M HCl (3x10 mL) and satd. NaHCO_3 solution. Work-up and SGC purification has afforded the required enone **52**.



Yield: 800 mg, 80 %

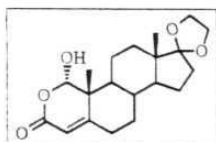
IR: cm^{-1} 2924, 1672, 1620.

^1H NMR: δ 5.73 (1H, s), 4.00-3.80 (4H, m), 1.20 (3H, s), 0.89 (3H, s).

^{13}C NMR: δ 199.23, 171.14, 123.80, 119.02, 65.17, 64.50, 53.59, 49.68, 45.65, 38.57, 35.81, 35.69, 34.05, 33.91, 32.76, 31.28, 30.31, 22.57, 20.43, 17.38, 14.25.

17-(Ethylenedioxy)-1 α -hydroxy-2-oxa- Δ^4 -androsten-3-one (54**):** Enone **52** (420 mg, 1.26 mmol), 18-crown-6 (500 mg, 1.90 mmol) were taken in 110 mL dry toluene and cooled to -27°C . $^t\text{BuOK}$ (420 mg, 1.78 mmol) was added and the reaction flask was connected to oxygen balloon. Stirred at -27°C for 5 h and

continued at rt for 20 h. Dilution with 35 mL EtOAc, work-up followed by SGC purification has yielded lactol **54**.

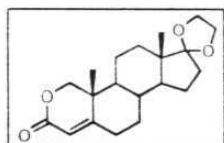


Yield: 270 mg, 70 %

IR: cm^{-1} 3368 (b), 2949, 1728, 1622.

^1H NMR: δ 5.72 (1H, s), 5.46 (1H, s), 3.98-3.80 (4H, m), 2.48-2.32 (2H, m), 1.21 (3H, s), 0.88 (3H, s).

17-(Ethylenedioxy)-2-oxa- Δ^4 -androst-3-one (44): To the lactol **54** (120 mg, 0.33 mmol) in 20 mL CHCl_3 an aq. solution of NaBH_4 (185 mg, 4.62 mmol) in 3 mL water and 0.5 mL 1M NaOH solution were added and stirred for 5 h. Work-up and SGC purification provided the desired lactone **44**.



Yield: 90 mg, 82 %

mp: 153-155 $^\circ\text{C}$

IR: cm^{-1} 2841, 1726, 1683, 1460.

^1H NMR: δ 5.60 (1H, s), 4.17 (1H, d, $J=12$ Hz), 3.94 (1H, d, $J=12$ Hz), 3.90-3.75 (4H, m), 2.38-2.26 (2H, m), 1.18 (3H, s), 0.82 (3H, s).

^{13}C NMR: δ 167.67, 164.57, 118.96, 113.51, 78.00, 65.19, 64.50, 49.43, 49.05, 45.52, 37.87, 35.18, 33.88, 30.48, 30.40, 22.64, 21.06, 15.41, 14.16.

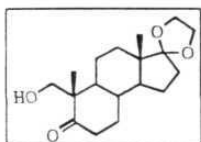
Analysis: Found C, 72.48; H, 8.88. Calcd. for $\text{C}_{20}\text{H}_{28}\text{O}_4$: C, 72.31; H, 8.42 %.

MS: 332 (M^+)

Hydroxy ketone 63: To the lactone **44** (140 mg, 0.4 mmol) in dry THF (10 mL) at -78 $^\circ\text{C}$ 20 % DiBAL-H in hexane (1.5 mL, 2 mmol) was added and stirred for 1 h. The reaction mixture was quenched by slow addition of 1 mL EtOAc. Diluted with 30 mL sat. NH_4Cl solution and extracted with EtOAc (3x10 mL). The solvent was evaporated at low temperature under vacuum and the unstable diol **62**

was immediately processed for ozonolysis without further purification or characterisation.

To the diol **62** taken in a mixture of MeOH/CH₂Cl₂, 40 mg of NaHCO₃ was added and ozone was passed through the solution for 15-20 min. at -78 °C until the reaction turned light blue. Excess ozone was flushed off by passing O₂ for 5 min., 0.2 mL of DMS was added and stirred for 30 min at 0 °C. The solvent was evaporated and the crude was processed by SGC purification to provide pure keto alcohol **63**.



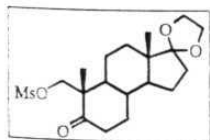
Yield: 46 mg, 37 %

IR: cm⁻¹ 3450 (b), 2841, 2882, 1697.

¹H NMR: δ 4.00-3.80 (4H, m), 3.75 (1H, d, J=12 Hz), 3.45 (1H, d, J=12 Hz), 2.58 (2H, dt, J=6, 10 Hz), 2.36-2.20 (2H, m), 1.06 (3H, s), 0.94 (3H, s).

¹³C NMR: δ 218.15, 119.00, 63.62, 65.24, 64.58, 52.66, 49.40, 46.34, 45.87, 38.27, 35.06, 33.98, 31.05, 29.98, 22.67, 20.81, 15.66, 14.27.

Keto mesylate 64: To the ketoalcohol **63** (30 mg, 0.1 mmol) in dry DCM at 0 °C, Et₃N (275 μL, 1 mmol) and MsCl (40 μL, 0.5 mmol) were added and the reaction was stirred for 1 h. Solvent was evaporated and the crude was subjected to filter column purification.

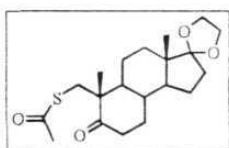


Yield: 30 mg, 85 %

IR: cm⁻¹ 3398, 2941, 1709.

¹H NMR: δ 4.50 (1H, d, J=11 Hz), 4.38 (1H, d, J=11 Hz), 3.92-3.80 (4H, m), 3.08 (3H, s), 1.07 (3H, s), 0.90 (3H, s).

Keto thioester 65: The keto mesylate **64** (16 mg, 0.044 mmol), Cs_2CO_3 (186 mg, 0.57 mmol) and thiolacetic acid (40 μL , 0.57 mmol) taken in dry DMF (2 mL), were heated at 100 °C for 3 h. The reaction mixture was diluted with sat. NH_4Cl solution (15 mL) and extracted with EtOAc (3x5 mL). Work-up and SGC purification yielded thioester **65**.

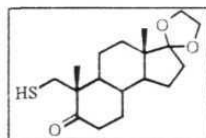


Yield: 12 mg, 74 %

IR: cm^{-1} 2935, 1707, 1698.

^1H NMR: δ 4.00-3.82 (4H, m), 3.12 (1H, d, $J=10$ Hz), 3.05 (1H, d, $J=12$ Hz), 1.18 (3H, s), 0.90 (3H, s).

Keto thiol 66: To the mesylate **64** (20 mg, 0.057 mmol) in dry DMF (2 mL) Na_2S (45 mg, 0.57 mmol) was added and stirred at 100 °C for 4 h. Diluted with satd. NH_4Cl solution (15 mL) and extracted with EtOAc (3x5 mL). Work-up and SGC purification yielded ketothiol **66**.

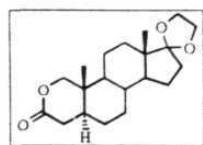


Yield: 15 mg, 81 %

IR: cm^{-1} 3398, 2941, 2874, 1765, 1707.

^1H NMR: δ 4.00-3.78 (4H, m), 3.10 (1H, d, $J=10$ Hz), 3.05 (1H, d, $J=10$ Hz), 2.58-2.18 (4H, m), 1.12 (3H, s), 0.90 (3H, s).

17-(Ethylenedioxy)-2-oxa-5 α -androstan-3-one (57): To the lactone **44** (108 mg, 0.33 mmol) in EtOAc (5 mL), 100 mg 10 % Pd/C was added and stirred under H_2 atmosphere for 1 h at ambient temperature and pressure. Filtration through a pad of Celite yielded pure saturated lactone **57**.



Yield: 105 mg, 98 %

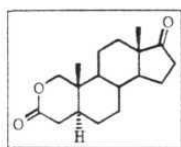
IR: cm^{-1} 2932 (b), 1738, 1448.

^1H NMR: δ 4.5 (1H, d, $J=13$ Hz), 3.90-3.75 (4H, m), 3.68

(1H, d, J=13 Hz), 2.48 (2H, dd, J=10, 2 Hz), 0.89 (3H, s), 0.78 (3H, s).

¹³C NMR: δ 172.04, 119.39, 119.07, 75.19, 65.17, 49.84, 45.83, 39.45, 38.19, 35.11, 34.41, 34.03, 31.06, 30.24, 25.19, 24.51, 22.50, 20.51, 17.24, 14.25.

2-Oxa-5α-androstan-3,17-dione (58): To the saturated ketal **57** (130 mg, 0.4 mmol) in acetone (5 mL), 10 % H₂SO₄ (1 mL) solution was added and stirred for 1 h. Solvent was evaporated and the residue was dissolved in 10 mL EtOAc and worked-up to afford pure 3,17-dione **58**.



Yield: 81 mg, 62 %

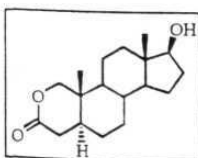
mp: 160-162 °C

IR: cm⁻¹ 2939, 1736.

¹H NMR: δ 4.20 (1H, d, J=6 Hz), 3.75 (1H, d, J=6 Hz), 1.00 (3H, s), 0.92 (3H, s).

MS: 290 (M⁺).

17β-Hydroxy-2-oxa-5α-androstan-3-one 59: To the 17-keto saturated lactone **58** (60 mg, 0.21 mmol) in CHCl₃ (5 mL) a solution of NaBH₄ (41 mg, 1.03 mmol) in 1 mL water was added followed by 0.1 mL NaOH and stirred for 4 h. Work-up and SGC purification provided 17-hydroxy saturated lactone **59**.



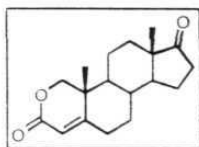
Yield: 30 mg, 73 %

IR: cm⁻¹ 3418, 2920, 1725.

¹H NMR: δ 4.22 (1H, d, J=6 Hz), 3.76 (1H, d, J=6 Hz), 3.62 (1H, t, J=4 Hz), 0.92 (3H, s), 0.76 (3H, s).

¹³C NMR: δ 172.43, 81.62, 75.34, 39.87, 38.28, 36.34, 35.08, 34.82, 31.17, 30.58, 25.33, 24.85, 23.3, 20.70, 17.32, 11.07.

2-Oxa- Δ^4 -androst-3,17-dione 60: The 17-ketal of lactone **44** was deketalised using 10 % H_2SO_4 in acetone to **60**.



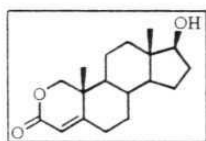
Yield: 80 %

mp: 185-186 °C.

IR: cm^{-1} 2940, 1736 (b), 1626.

^1H NMR: δ 5.70 (1H, s), 4.25 (1H, d, $J=6$ Hz), 4.02 (1H, d, $J=6$ Hz), 1.25 (3H, s), 0.92 (3H, s).

17 β -Hydroxy-2-oxa- Δ^4 -androst-3-one (61): The NaBH_4 reduction conditions were used to convert **60** to **61**.



Yield: 68 %

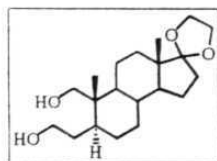
mp: 200-202 °C

IR: cm^{-1} 3418, 1712, 1640.

^1H NMR: δ 5.72 (1H, s), 4.28 (1H, d, $J=4$ Hz), 4.00 (1H, d, $J=4$ Hz), 3.68 (1H, t, $J=4$ Hz), 1.23 (3H, s), 0.79 (3H, s).

^{13}C NMR: δ 157.63, 118.78, 113.62, 81.48, 50.32, 49.41, 42.76, 37.88, 36.21, 35.05, 30.70, 30.54, 30.31, 23.37, 21.26, 16.40, 10.87.

5 α -Diol 68: To the saturated lactone **57** (60 mg, 0.18 mmol) at -5 °C in dry THF (3 mL) under inert atmosphere LAH (136 mg, 3.6 mmol) was added and refluxed for 1 h. After cooling to 0 °C the reaction was quenched with EtOAc (1 mL) and diluted with 20 mL sat. NH_4Cl solution. Extraction with EtOAc (3x10 mL) and work-up followed by SGC purification provided pure diol **68**.



Yield: 50 mg, 82 %

IR: cm^{-1} 3381 (b), 2930, 1454.

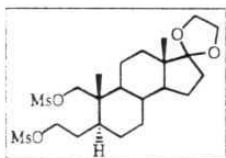
^1H NMR: δ 4.00-3.82 (4H, m), 3.80-3.90 (1H, m), 3.62-

3.48 (1H, m), 3.58 (1H, d, J=13 Hz), 3.44 (1H, d, J=13 Hz), 1.07 (3H, s), 0.83 (3H, s).

^{13}C NMR: δ 119.50, 69.43, 65.16, 64.49, 62.09, 50.10, 45.66, 43.85, 39.65, 36.53, 35.23, 32.01, 30.71, 29.69, 25.31, 22.92, 22.66, 20.63, 17.91, 12.42.

MS: 338 (M^+).

5 α -Dimesylate 69: To the diol **68** (30 mg, 0.10 mmol) in dry DCM, Et_3N (0.4 mL, 3 mmol) and MsCl (0.10 mL, 1.5 mmol) were added at -5°C under N_2 atmosphere. After stirring for 1 h, the solvent was evaporated under vacuum and crude was subjected to SGC purification to provide the pure dimesylate **69**.

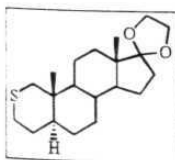


Yield: 50 mg, 82 %

IR: cm^{-1} 2934, 1467.

^1H NMR: δ 4.32-3.87 (8H, m), 3.05 (3H, s), 3.02 (3H, s), 1.44 (3H, s), 0.83 (3H, s).

17-(Ethylenedioxy)-2-thia-5 α -androstane (67): To the dimesylate **69** (30 mg, 0.06 mmol) in dry DMF (1 mL) powdered Na_2S (190 mg, 2.4 mmol) was added and heated at 100°C for 2 h. Diluted with 15 mL brine and extracted with EtOAc (3x10 mL). Work-up and SGC purification yielded the pure thiopyran **67**.



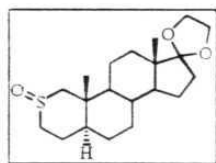
Yield: 12 mg, 60 %

IR: cm^{-1} 2938, 1452, 1333.

^1H NMR: δ 4.20-3.98 (4H, m), 2.68-2.53 (4H, m), 1.04 (3H, s), 0.85 (3H, s).

^{13}C NMR: δ 119.52, 65.22, 64.57, 50.23, 46.14, 43.46, 39.90, 39.64, 36.13, 35.62, 34.25, 30.73, 29.98, 28.46, 28.04, 25.69, 23.35, 22.86, 19.92, 14.36.

17-(Ethylenedioxy)-2-sulfoxy-5 α -androstande (70): To the thiopyran **67** (10 mg, 0.030 mmol) in MeOH (2 mL), a 0.5 mL solution of NaIO₄ (32 mg, 0.15 mmol) was added and stirred for 10 h. Solvent was removed in vacuum and the residue was dissolved in EtOAc. Work-up and SGC purification provided the pure sulfoxide **70**.

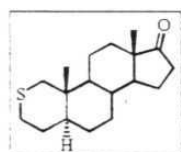


Yield: 8 mg, 60 %

IR: cm⁻¹ 2935, 1448.

¹H NMR: δ 3.98-3.80 (4H, m), 3.54 (2H, m), 2.66-2.48 (1H, m), 2.28 (1H, d, J=14 Hz), 1.11 (3H, s), 0.84 (3H, s).

2-Thia-5 α -androstan-17-one (71): Thiopyran **67** (12 mg, 0.03 mmol) was dissolved in 1 mL acetone and 0.1 mL 10 % H₂SO₄ was added and stirred for 1 h. Work-up and SGC purification has provided the pure thiaketone **71**.



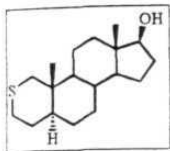
Yield: 8 mg, 76 %

IR: cm⁻¹ 2934, 1740, 1452.

¹H NMR: δ 2.74-2.32 (4H, m), 1.05 (3H, s), 0.90 (3H, s).

MS: 292 (M⁺).

17-Hydroxy-2-thia-5 α -androstande (72): To the thiaketone **71** (8 mg, 0.03 mmol) in 2 mL dry THF at rt LAH (8 mg, 0.25 mmol) was added under nitrogen atmosphere and stirred for 5 h. The reaction mixture was quenched by adding 1 mL EtOAc, diluted with 10 mL sat. NH₄Cl solution and extracted with EtOAc (3x5 mL). Work-up and SGC purification has afforded pure 17-hydroxy thiopyran **66**.



Yield: 5 mg, 62 %

IR: cm^{-1} 3474, 2918, 2881, 1462.

^1H NMR: δ 3.68 (1H, t, $J=8$ Hz), 2.65-2.52 (3H, m), 2.36 (1H, d, 14 Hz), 1.02 (3H, s), 0.75 (3H, s).

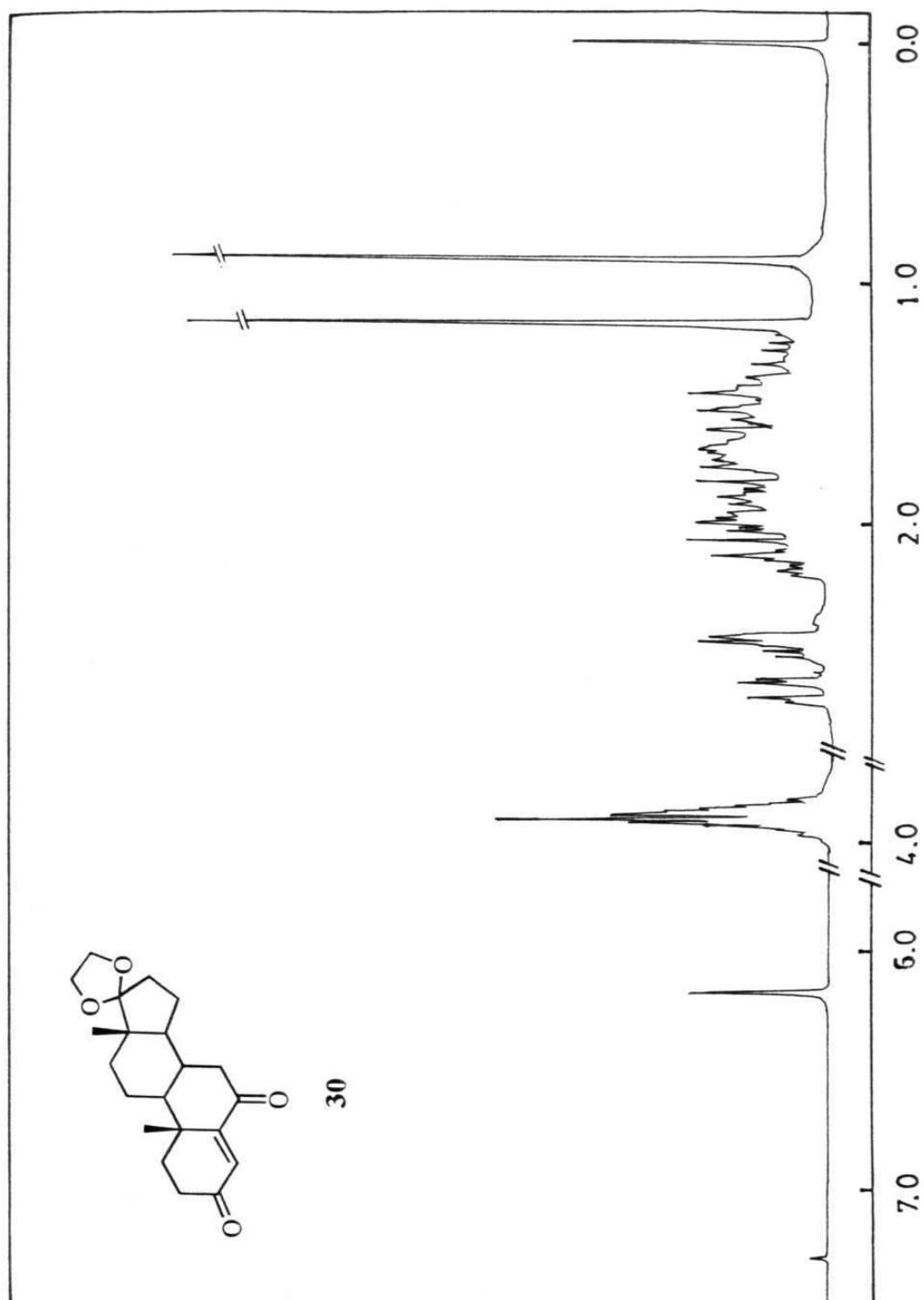
1.4 REFERENCES

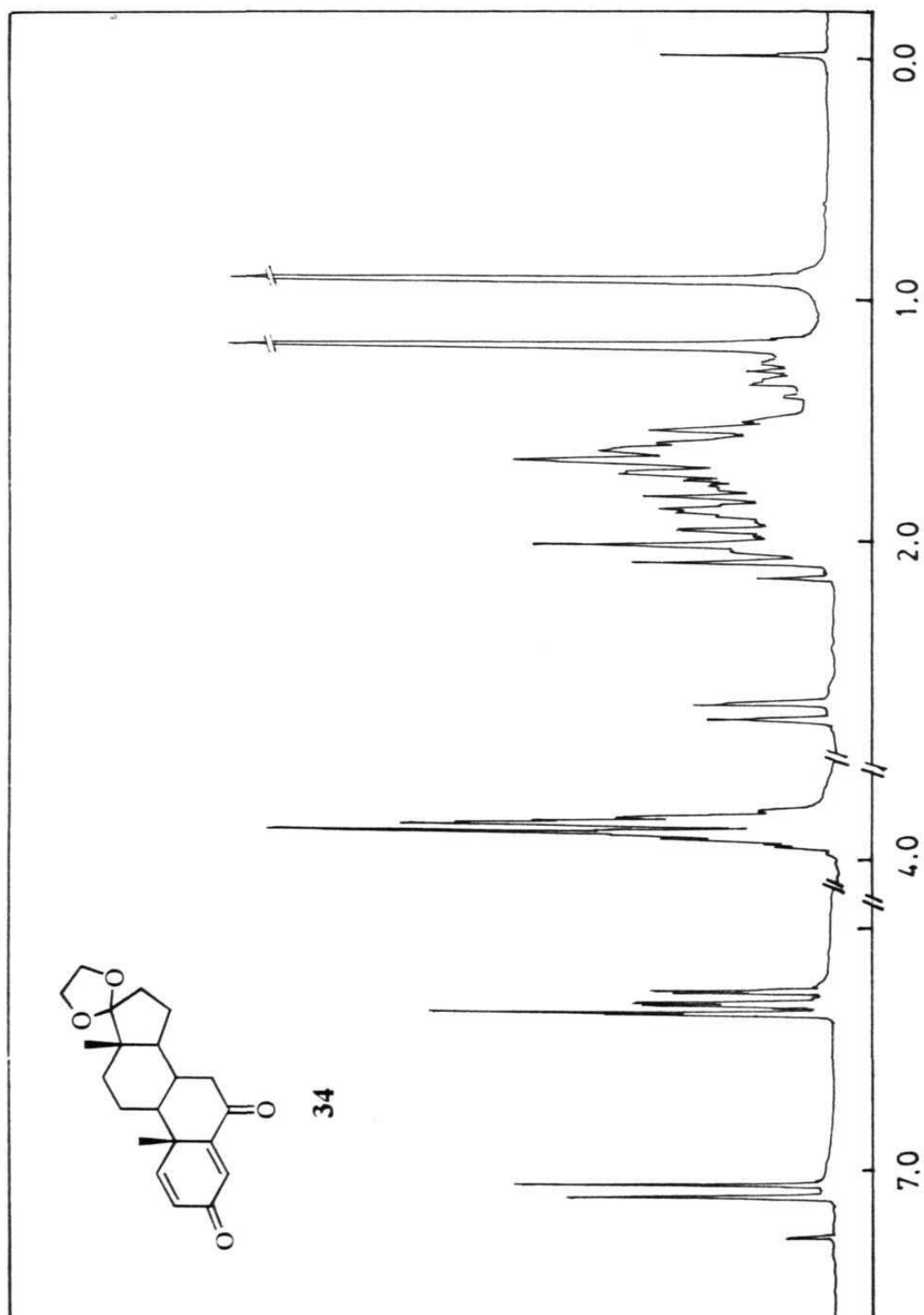
1. Duax, W.L., Griffin, J.F., Ghosh, D. In *Structure Correlation*, 1994, Volume 2, Bürgi, H.-B., Dunitz, J.D., (Eds.), VCH, New York, pp 605-633.
2. Zurer, P.S. *Chem. Eng. News*, 1984, April 30, 69.
3. (a) Wilson, C.O., Gisvold, O., Delgado, J.N., Remers, W.A. *Wilson and Gisvold's Textbook of Organic and Pharmaceutical Chemistry*, 1991, Lippincott, Philadelphia. (b) Robert, T.B. In *Encyclopedia of Molecular Biology and Molecular Medicine*, 1996, Volume 5, 485.
4. (a) Akhrem, A.A., Titov, Y.A. *Total Steroid Synthesis*, 1970, Plenum, New York. (b) Bilkenstaff, R.T., Ghosh, A.C., Wolf, G.C. *Total Synthesis of Steroids*, 1974, Academic, New York.
5. Lednicer, D., Mitscher, L.A. *Organic Chemistry of Drug Synthesis*, Vol. 4, 1990.
6. Pappo, R., Allen, Jr., D.D., Lemieux, R.V., Johnson, W.S. *J. Org. Chem.*, 1956, 21, 478.
7. Pappo, R., Jung, J.J. *Tetrahedron Lett.*, 1962, 365.
8. Kocor, M., Kerek, A., Dabrowski, J. *Tetrahedron*, 1969, 25, 4257.
9. Frimer, A.A., Hameiri-Buch, J., Ripshtos, S., Gilinsky-Sharon, P. *Tetrahedron*, 1986, 42, 5692.
10. Frimer, A.A., Ripshtos, S., Marks, V., Aljadeff, G., Hameiri-Buch, J., Gilinsky-Sharon, P. *Tetrahedron*, 1991, 47, 8361.
11. Shibata, K., Takegawa, S., Koizumi, N., Yamakoshi, N., Shimazawa, E. *Chem. Pharm. Bull.*, 1992, 40, 935.
12. Koizumi, N., Takegawa, S., Mieda, M., Shibata, K. *Chem. Pharm. Bull.*, 1996, 44, 2162.
13. Tischler, M., Ayer, S.W., Andersen, R.J. *Can. J. Chem.*, 1988, 66, 1173.

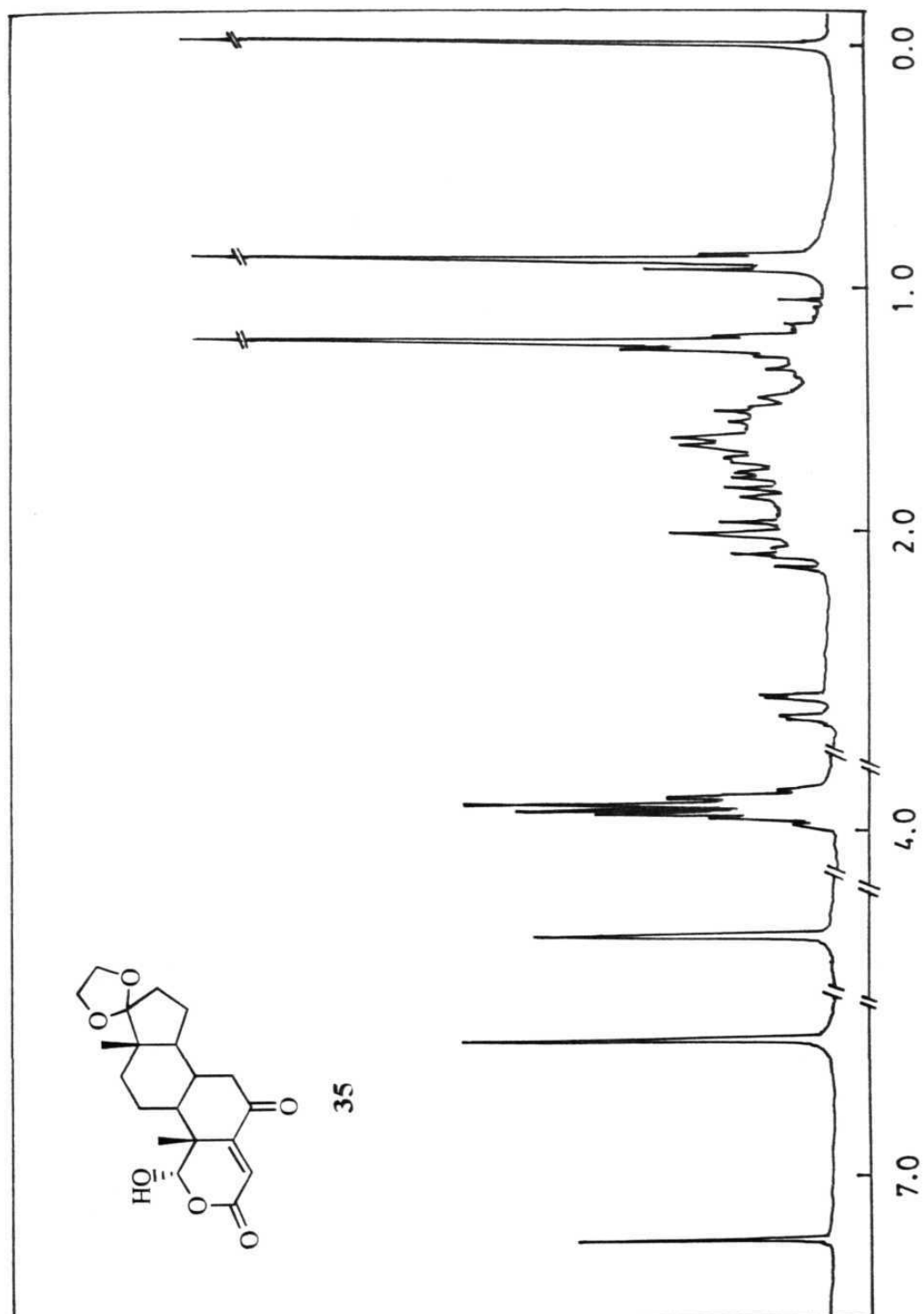
14. Piers, E., Worster, P.M. *Can. J. Chem.*, **1977**, 55, 733.
15. Numazawa, M., Mutsumi, A., Tachibana, M., Hoshi, K. *J. Med. Chem.*, **1994**, 37, 2198.
16. Parish, E.J., Kizito, S.A., Hiedepriem, R.W. *Synth. Commun.*, **1993**, 23, 223.
17. Moreno, M.M.J.S., Sa e Melo, M.L., Campos Neves, A.S. *Tetrahedron Lett.*, **1991**, 32, 3201.
18. Blaszczyk, K., Paryzek, Z. *Synth. Commun.*, **1994**, 24, 3255.
19. Chai, K. B., Sampson, P. *J. Org. Chem.*, **1993**, 58, 6807.
20. Edwards, J. A., Ringold, H. J., Djerassi, C. *J. Am. Chem. Soc.*, **1960**, 82, 2318.
21. You, Z., Koreeda, M. *Tetrahedron Lett.*, **1993**, 34, 2745.
22. Jackman, L.M., Sternhell, S. *Applications of Nuclear Magnetic Resonance Spectroscopy in Organic Chemistry*, **1972**, Edition 2, Pergamon, Oxford, p. 322.
23. Mitsunobu, O. *Synthesis*, **1981**, 1.
24. Childers, W.E., Furth, S.P., Shih, M.-J., Robinson, C.H. *J. Org. Chem.*, **1988**, 53, 5947.
25. Perrin, D.D., Amarego, W.L.F., Perrin, D.D. *Purification of Laboratory Chemicals*, **1986**, Edition 2, Pergamon, Oxford.

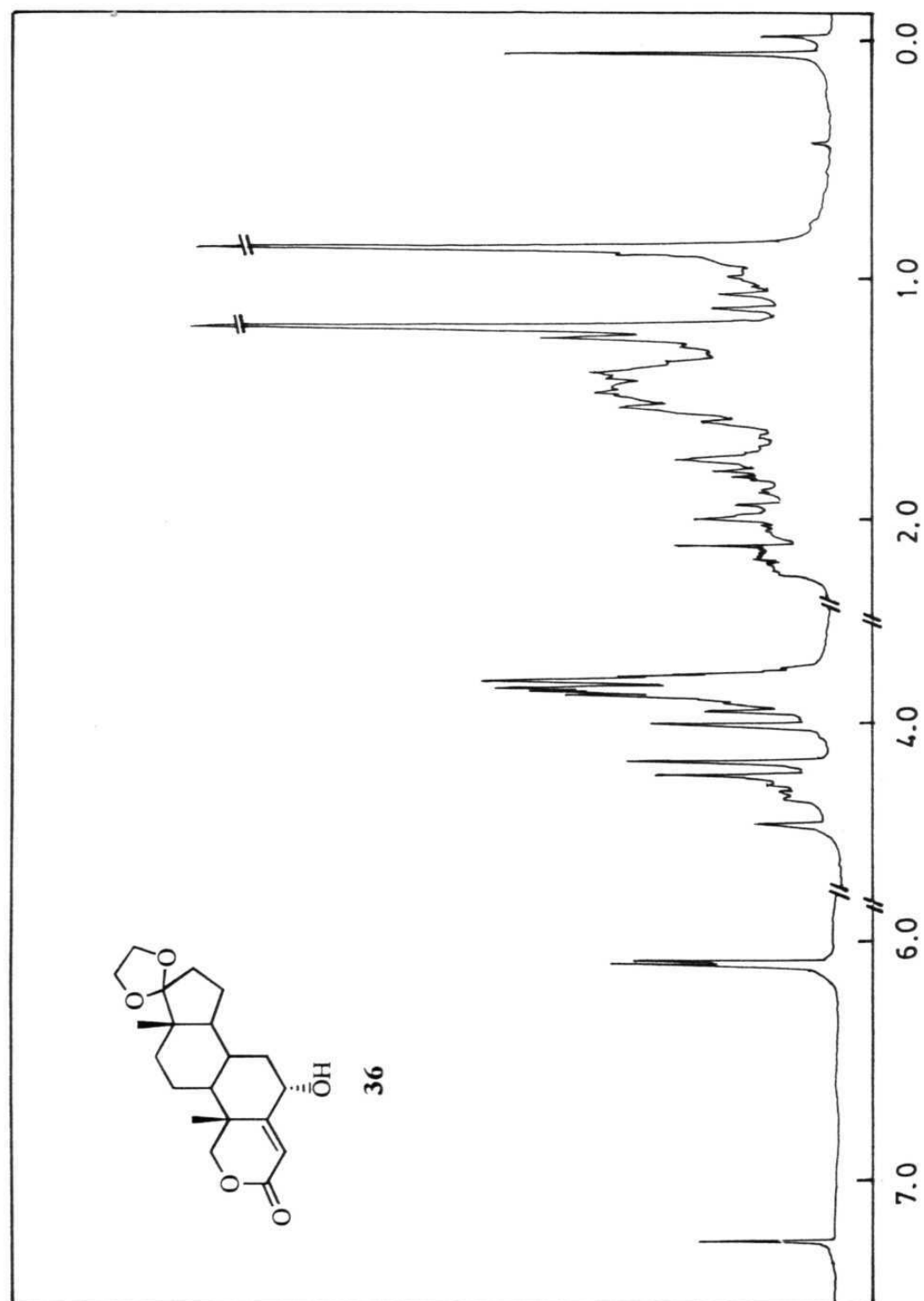
1.5 SPECTRA

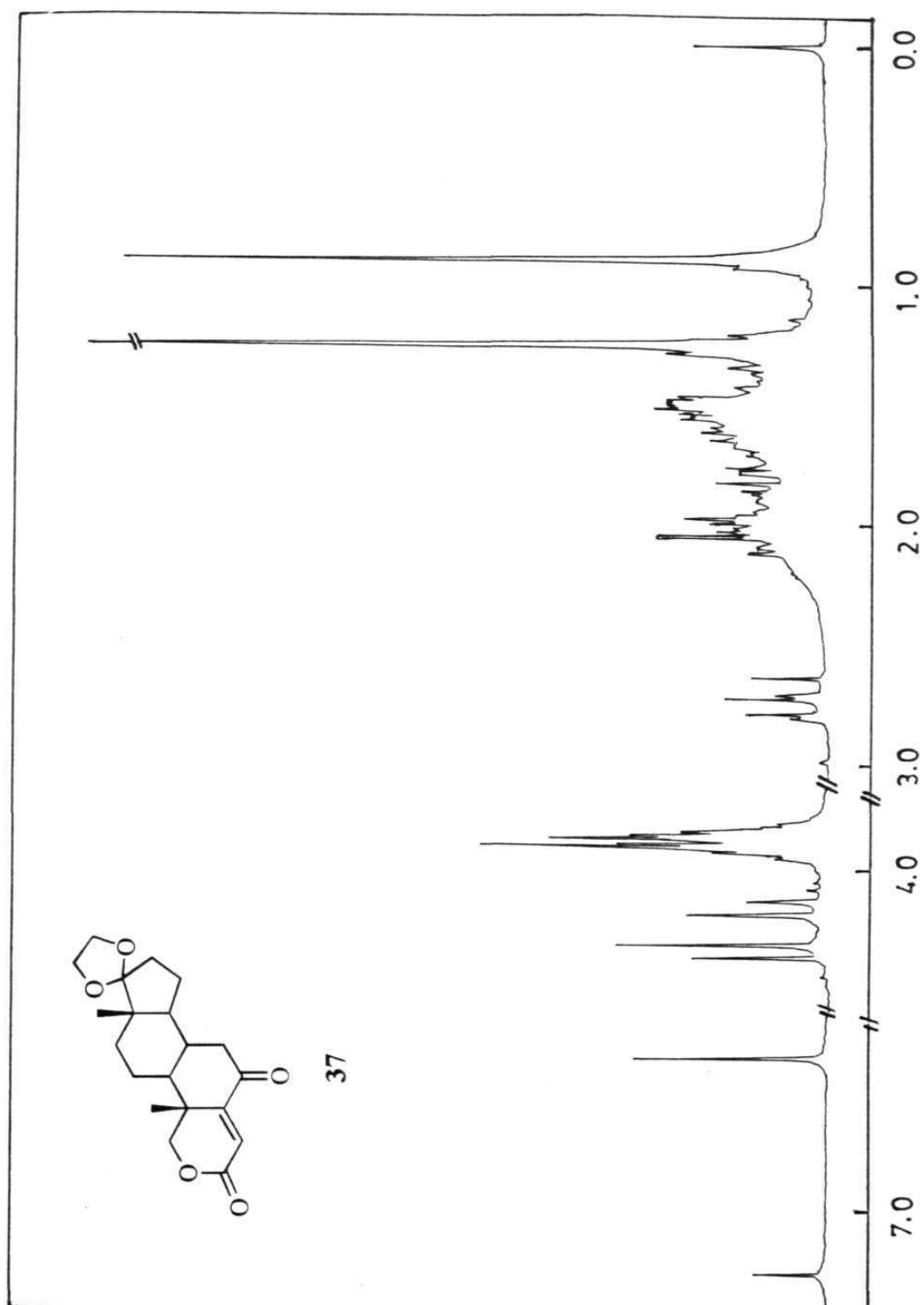
¹H NMR spectra of some selected steroids are shown in the following pages.

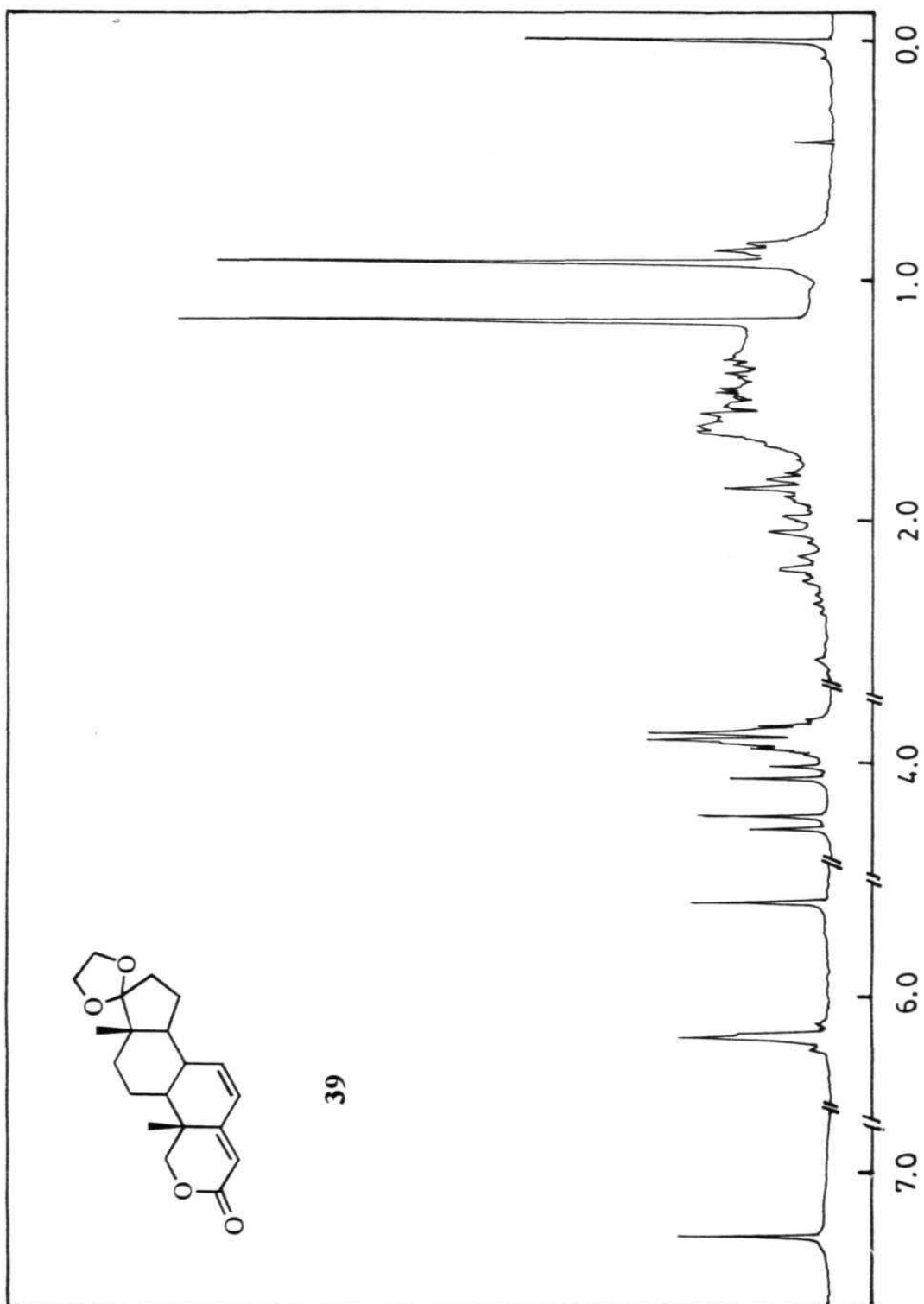


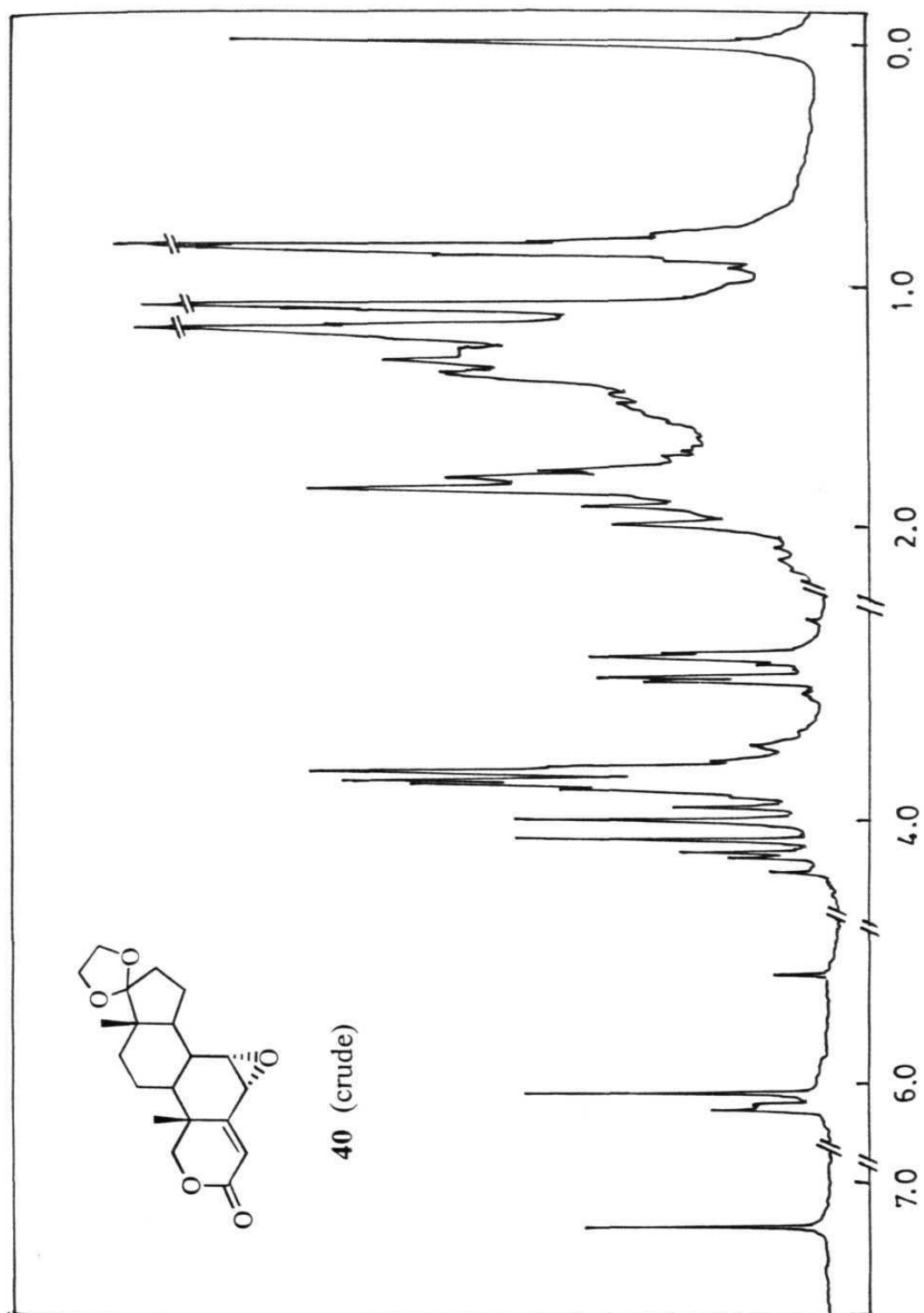


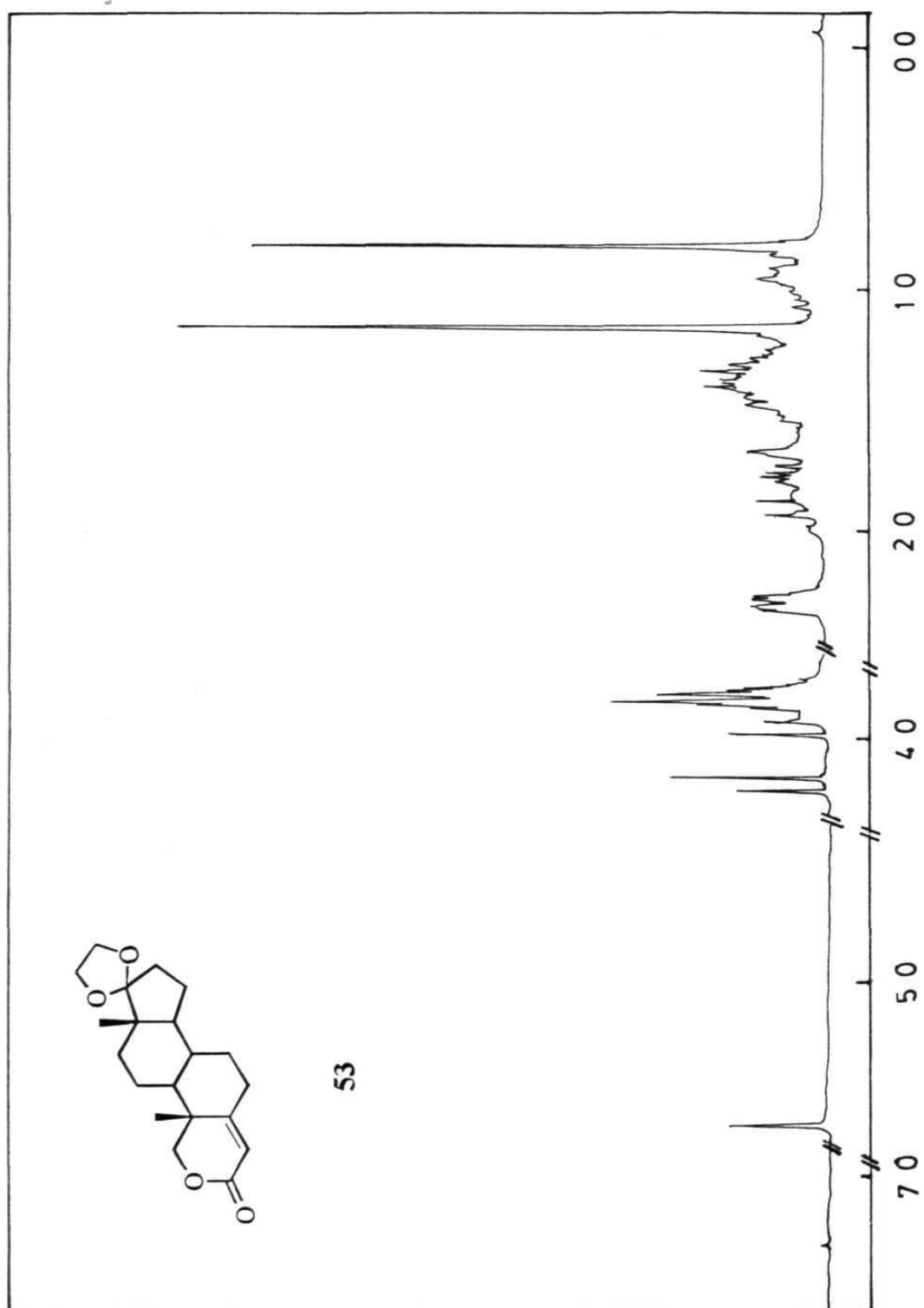


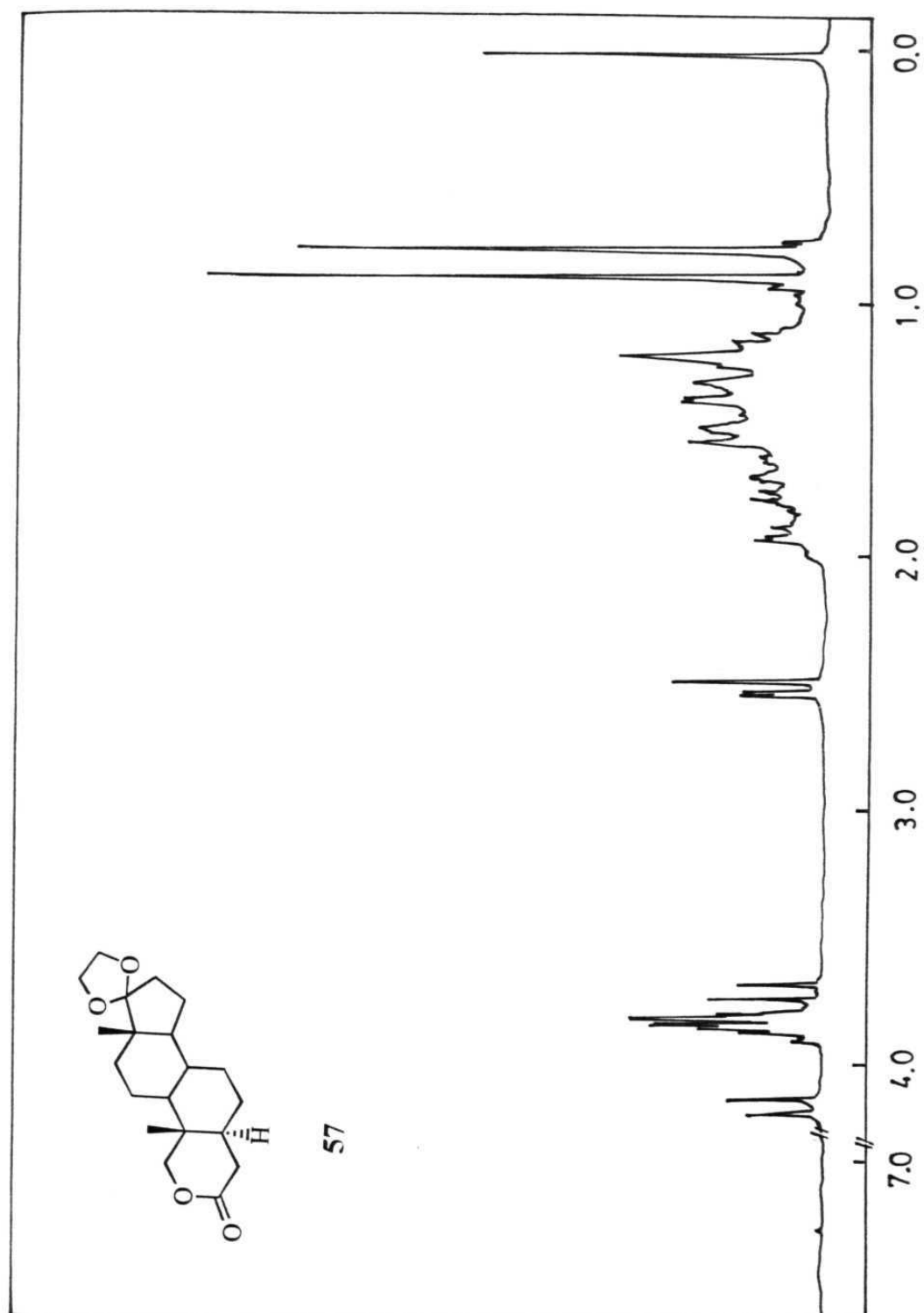


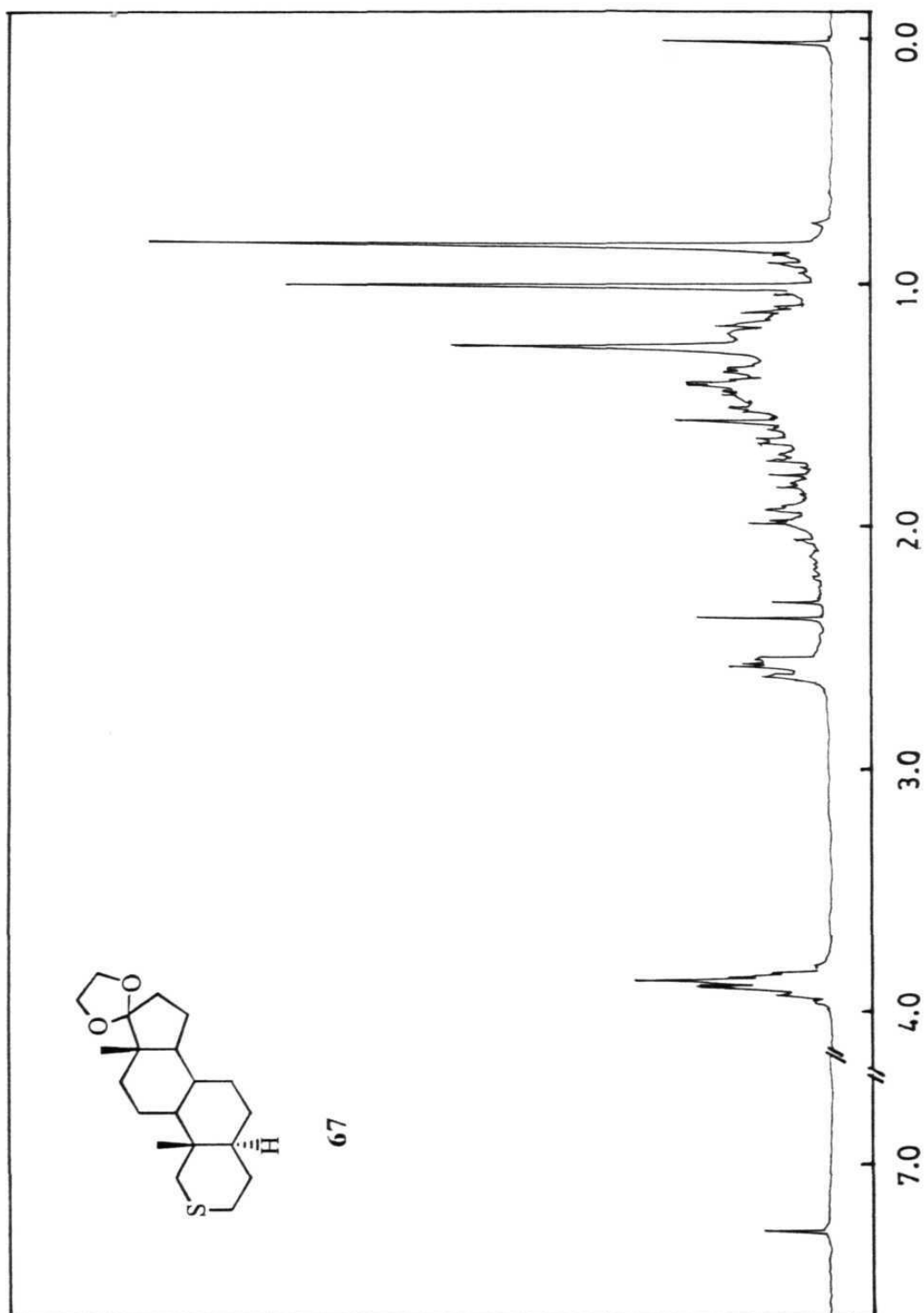


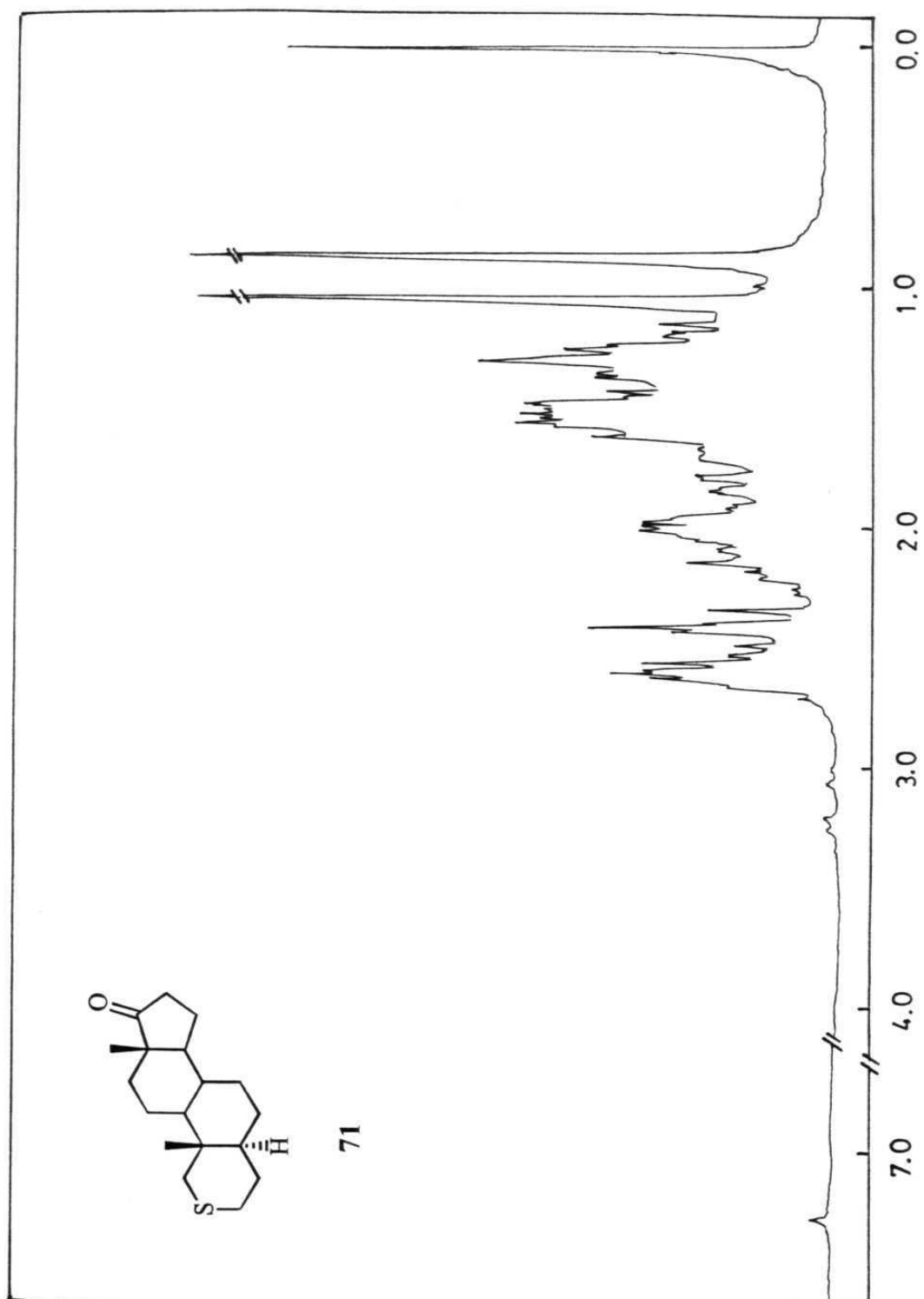


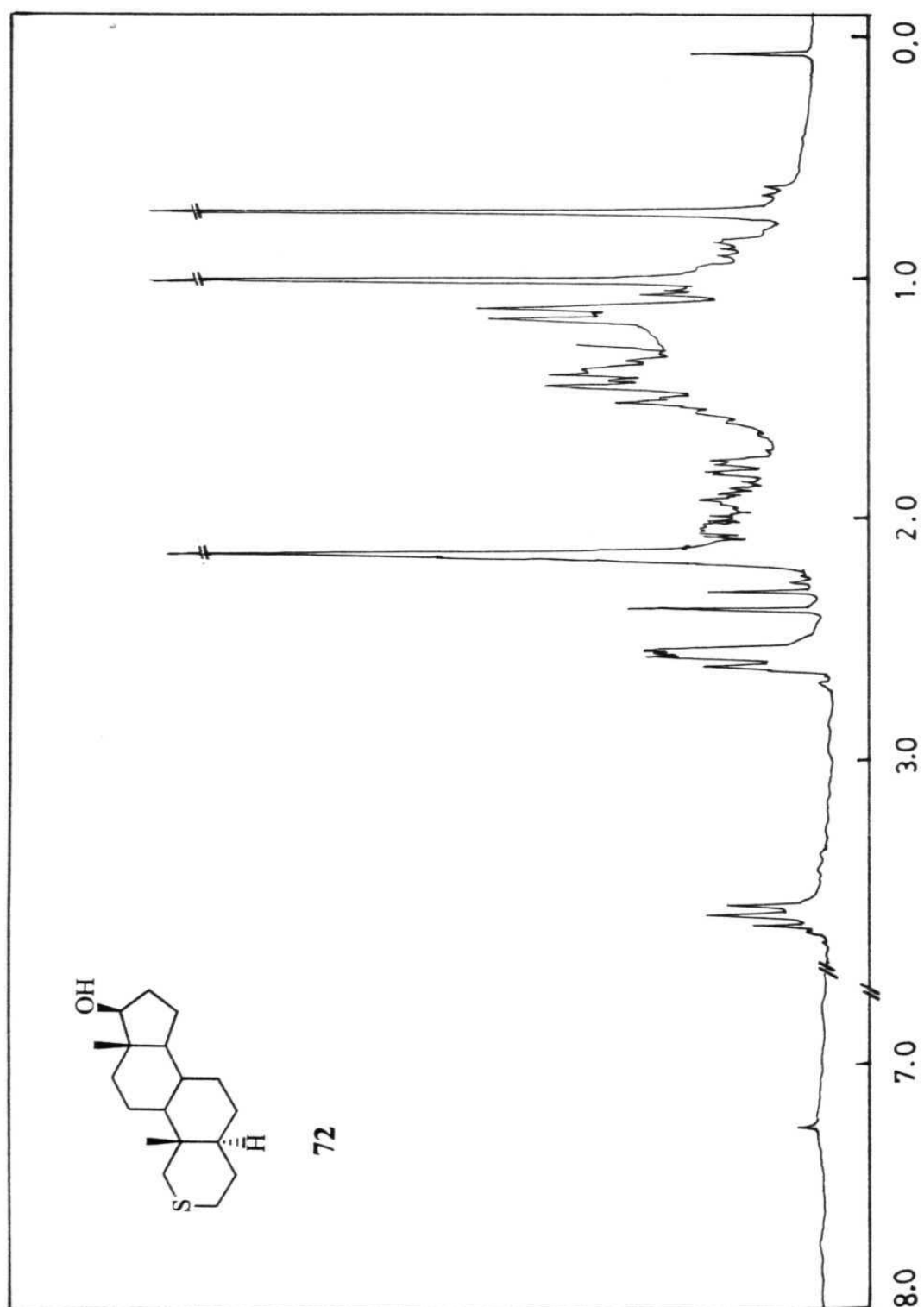












CHAPTER 2
CRYSTAL STRUCTURES OF 2-OXASTEROIDS AND ANDROGENS

Contents

2.1 INTRODUCTION

- 2.1.1 Small Molecule Crystallography
- 2.1.2 2-Hetero Steroids in the Cambridge Structural Database
- 2.1.3 CSD analysis of C-H...O Hydrogen Bonds in Steroids

2.2 STUDIES ON 2-OXASTEROIDS

- 2.2.1 Crystal Structure Analysis of 2-Oxasteroids
- 2.2.2 Summary of Intermolecular Interactions
- 2.2.3 Molecular Conformation

2.3 CRYSTAL STRUCTURES OF ANDROGENS

- 2.3.1 Crystal Structure Analysis of 6-Ketosteroids
- 2.3.2 Molecular Conformation
- 2.3.3 5 β -Androstane-3,17-dione

2.4 ISOSTRUCTURALITY

- 2.4.1 Definition
- 2.4.2 One-dimensional Isostructurality
- 2.4.3 Two-dimensional Isostructurality
- 2.4.4 Three-Dimensional Isostructurality

2.5 EXPERIMENTAL

2.6 TABLES

- 2.6.1 Intermolecular Interactions
- 2.6.2 Crystallographic Details

2.7 REFERENCES

2.1 INTRODUCTION

2.1.1 Small Molecule Crystallography

For a long time, the crystal structure of small molecules were regarded as useful only for establishing the stereochemical formulae of the crystallised compound.¹ The importance of structural information on the binding characteristics of chemical groups has recently been realised by systematic studies of different classes of compounds in which the environment of a molecule in the crystal is correlated with that of the same molecule in the ligand-receptor complex. Such an approach assumes greater significance in cases where the three-dimensional structure of the active site of the macromolecule is not known. The indirect approach consists of deriving the stereochemical requirements of the binding site of the macromolecule by its complementarity to the pharmacophore common to a family of active ligands. In our group, such an approach has been employed to develop a pharmacophore model for β -lactam antibiotics by identifying the important functional groups and their approach geometries as retrieved from the CSD.² In the overlay plot of the biologically active β -lactam antibiotics, the hydrogen bonding functional groups (lactam carbonyl and carboxylic acid) are bunched in a narrow region while in the inactive compounds they are scattered. A study of angiotensin converting enzyme (ACE) inhibitors was reported by Pascard *et al.*³ Rosenfeld *et al.*⁴ have analysed 69 crystal structures which revealed specific directions of approach to a divalent sulfur by electrophiles and nucleophiles. In a statistical study⁵, the directionality of hydrogen bonding to sp^2 and sp^3 hybridised oxygen atoms in small molecules has been correlated with those found in ligand-receptor complexes. Further, Klebe⁶ has convincingly shown that the crystal field environment for the approach of donor hydrogen atoms to various acceptor groups retrieved from the CSD is similar in that found in ligand-

receptor complex crystal structures reported in the PDB. Thus, an analysis of small molecule crystal structures of biomolecules, such as steroids, should provide a better understanding of their binding characteristics to the receptor protein even as one is aware that there may be slight differences between the small and macromolecular structures.

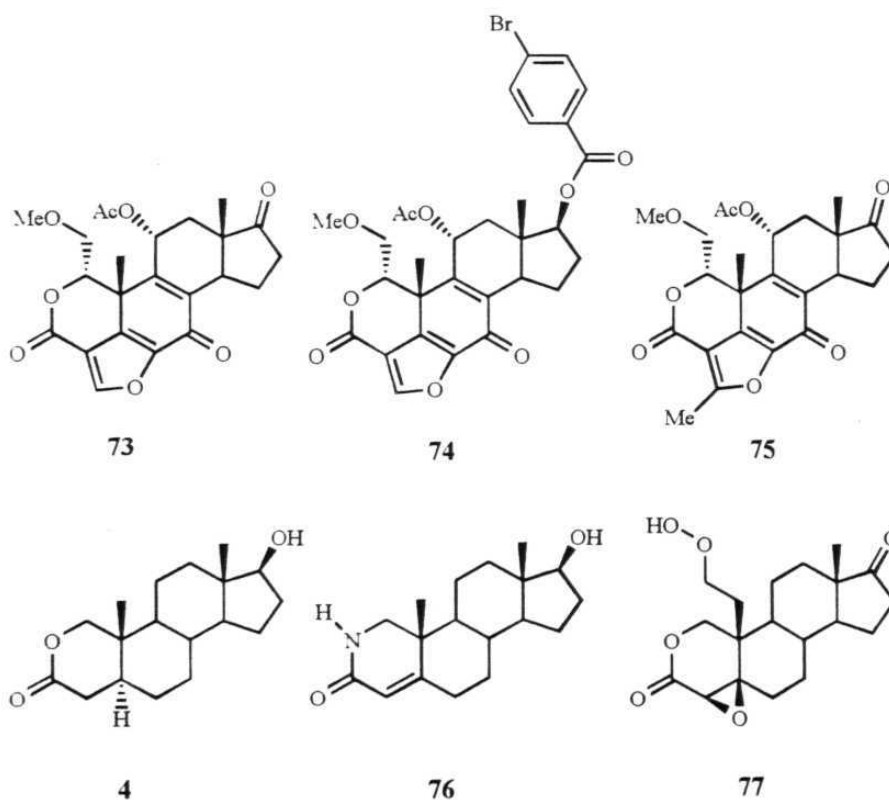
The role and importance of O-H...O hydrogen bonding in biomolecules has been well-known for quite some time.⁷ It is only recently that the significance of the weaker C-H...O and C-H...N hydrogen bonding is beginning to be appreciated.⁸ Sutor was first to report C-H...O hydrogen bonds in nucleotides.⁹ The statistical study of Derewanda *et al.*¹⁰ emphasises the existence of weak hydrogen bonds in proteins. The neutron crystal structures of carbohydrates, a class of biomolecules rich in O-H groups, exhibit numerous C-H...O hydrogen bonds.¹¹ Wahl and Sundaralingam have concluded in a recent review that C-H...O hydrogen bonds play a significant role in determining the structure as well as the function of biological macromolecules.¹²

Steroids are an important class of biomolecules and they bind to receptors in specific conformations utilising unique hydrogen bonding motifs. Duax *et al.*¹³ have noted that about 85 % of the steroids pack in either $P2_12_12_1$ or $P2_1$ space groups. They pack in chains, layers or coils connected in a head-to-tail fashion. From an analysis of 234 steroid crystal structures available in 1974, they concluded that structures which have the potential to form one or two-dimensional networks, such as chains and layers, pack in monoclinic space group while those which form three-dimensional hydrogen bonded architectures pack in orthorhombic $P2_12_12_1$ space group. Steroids are rich in C-H donors and have basic acceptor O-atoms, suggesting that they could form weak hydrogen bonds in their crystal structures. However, C-H...O hydrogen bonding in steroids has not been

studied systematically, though some recent reports have examined weak interactions in ethynyl steroids.¹⁴ Since 2-oxasteroids are analogues with a medicinal relevance, we decided to examine the packing motifs, intermolecular interactions and conformational preferences of this family of compounds.

2.1.2 2-Heterosteroids in the Cambridge Structural Database

The synthesis and biological activity of 2-hetero steroids has been extensively studied. The crystal structures of a few heterosteroids are reported in the Cambridge Structural Database (CSD) (Scheme 1).¹⁵

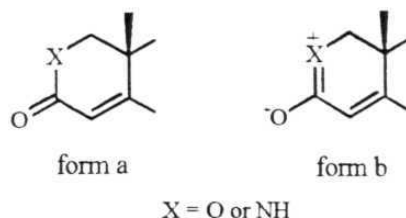


Scheme 1. Heterosteroids reported in the CSD.

Wortmannin **73** was isolated by Brian *et al.*¹⁶ from *Penicillium Wortmanni*. It was identified as a potent and selective inhibitor of PI 3-kinase.¹⁷ The absolute

configuration of the native compound was established by chemical¹⁸ and single crystal X-ray diffraction of **73**¹⁹ as well as of its *p*-bromobenzoate ester **74**. While studying the mechanism of inhibition of PI 3-kinase with wortmannin, Norman *et al.*²⁰ determined the crystal structure of another derivative, 21-methylwortmannin **75**.

Anavar[®] (**4**) is a commercially available anabolic steroid which has been extensively used in combination with growth hormone to treat Turner's syndrome.²¹ Rendle and Trotter²² analysed the crystal structure and noted that the δ -lactone group imposes a greater distortion on the A-ring due to planarity of the canonical form 'b' (X = O in Scheme 2). The normal chair conformation of B- and C-rings is not changed. The crystal packing was analysed in terms of the strong hydrogen bonding interactions (O-H...O). The contribution from C-H...O hydrogen bonds was ruled out on the basis of a cut-off distance criteria of 2.6 Å, the sum of the van der Waals radii of oxygen and hydrogen.²³

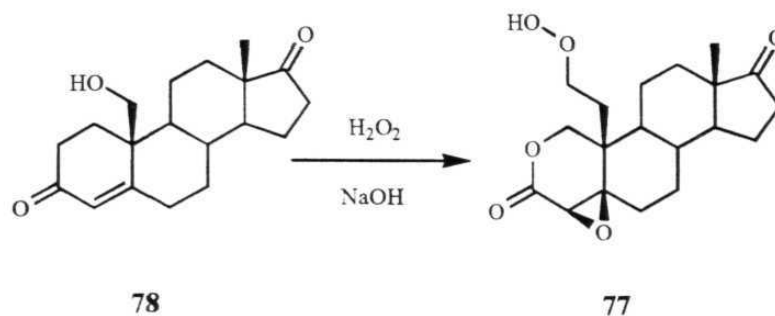


Scheme 2. Two canonical forms of lactones and lactams.

In the context of photochemical reactions on steroidal lactones and lactams, it was observed that 17 β -hydroxy-2-aza-4-androsten-3-one (**76**) shows specific reactivity ascribed to canonical form 'b' (X = NH). To confirm this hypothesis, Brianso *et al.*²⁴ determined the crystal structure of the aza-steroid **76**.

Treatment of 19-hydroxyandrost-4-ene-3,17-dione (**78**) under epoxidation conditions afforded a rearranged product, the epoxy lactone **77** (Scheme 3).²⁵ The

chemical structure of the rearrangement product was unambiguously established by X-ray analysis.



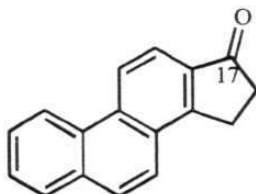
Scheme 3. Epoxidation of 19-hydroxy-4-ene-3-one steroid to 2-oxasteroid.

It may be noted that the motivation to carry out the X-ray determination in the above-mentioned examples was largely to confirm the molecular structure or to study the conformation of the steroid. There is very little emphasis in these papers on the intermolecular interactions, hydrogen bonds and molecular recognition motifs. The absence of a systematic crystallographic study of 2-oxasteroids has, in part, prompted the present study of this family of compounds. The packing motifs in the crystal structures are analysed in terms of the strong (O-H \cdots O) as well as weak (C-H \cdots O) hydrogen bonding interactions.⁸

2.1.3 CSD Analysis of C-H \cdots O Hydrogen Bonds in Steroids

The overall shape of the steroid and the hydroxy functional group play an important role in the packing and stabilisation of crystal structures, and in turn influence recognition and binding to the receptor.¹³ Steroids have donor and acceptor atoms on the molecular periphery that can form O-H \cdots O and C-H \cdots O hydrogen bonds. In this respect, there is some similarity between these compounds and the cyclopenta[*a*]phenanthrenes **79** (Scheme 4).²⁶ The cyclopentaphenanthrenes have one acceptor O-atom at C17 and C-H donor

hydrogen atoms on the molecular periphery. In **79**, almost all the C-H groups are aromatic and readily participate in C-H...O hydrogen bonds. However, in steroids the carbon atoms are sp^3 hybridised and as such are unactivated, though some methylene groups are acidic because of an adjacent carbonyl group or olefin. Further, in the tetracyclic steroid skeleton the hydrogen bond forming ability of the sp^3 methylene hydrogens will be different depending on whether they are on the convex (β) or the concave (α) face. The methyl groups are unactivated, but are readily accessible because they extend out on the β face. As a result, it may be expected that different C-H groups on the steroid skeleton should exhibit varying tendencies to form C-H...O hydrogen bonds.

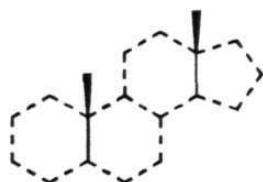


79

Scheme 4. Cyclopentaphenanthrene skeleton.

In order to study the role of above-mentioned factors in androgenic steroids, a CSD survey for C-H...O contacts formed by sub-structure **80** (Scheme 5) was carried out. Ordered and error free (screens 33 and 35) steroid crystal structures (class 6) with $R \leq 0.075$ were retrieved and stored as a sub-database (975 hits). This sub-database was searched for C-H donors on C1, C2, C4, C6, C7, C11, C12, C15, C16, C18 and C19 in separate files with H...O distance (d) of 2.0-2.8 Å and C-H...O angle (θ) of 110-180°. The C-H distance was normalised to 1.083 Å. No constraints were imposed on the hybridisation of the O-acceptor atom, that is sp^2 (carbonyl) and sp^3 (ether, hydroxyl) were considered together. The C-H...O hydrogen bond is electrostatic in nature ($C^{\delta-}-H^{\delta+}\cdots O^{\delta-}$) and the positive H-atom

acts as a screen between the negatively charged carbon and oxygen atoms. Therefore, C-H...O bonds that are short also tend to be linear whereas the longer interactions can be bent, and this behavior is exhibited in the form of a linear and inverse correlation between the distance (d) and angle (θ).^{8a} The distance-angle scatter plot of the C-H...O bonds at C1, C2, C4, C6 and C16 shows an inverse d - θ relationship, indicating that these contacts have the characteristics of hydrogen bonds (Figure 1). This data may be examined in conjunction with the observation of Duax *et al.*¹³ that steroids prefer to pack from head-to-tail with donors and acceptors in A- and D-rings participating in the intermolecular interactions. Steroids contain hetero atom substituents like carbonyl and hydroxy groups in the A- and D-rings making the C-H atoms in their vicinity more acidic than those in B- and C-rings. In compounds with Δ^4 -alkenes, the C6-H atoms are allylic in nature and hence are sufficiently acidic to participate in C-H...O bonds. Further, the C-H atoms in these rings are sterically exposed to participate in intermolecular interactions. On the other hand, the C-H...O contacts formed by H-atoms at C12, C18 and C19 show more of a random distribution in the d - θ scatterplot indicating that the short contacts observed for these H-atoms are probably a result of other intermolecular interactions. It may be noted that in any crystal structure there are always a few short contacts which can be repulsive in nature.¹



80

Scheme 5. Structure 80 used to search for C-H...O hydrogen bonds. Dotted lines indicate any bond between carbon atoms.

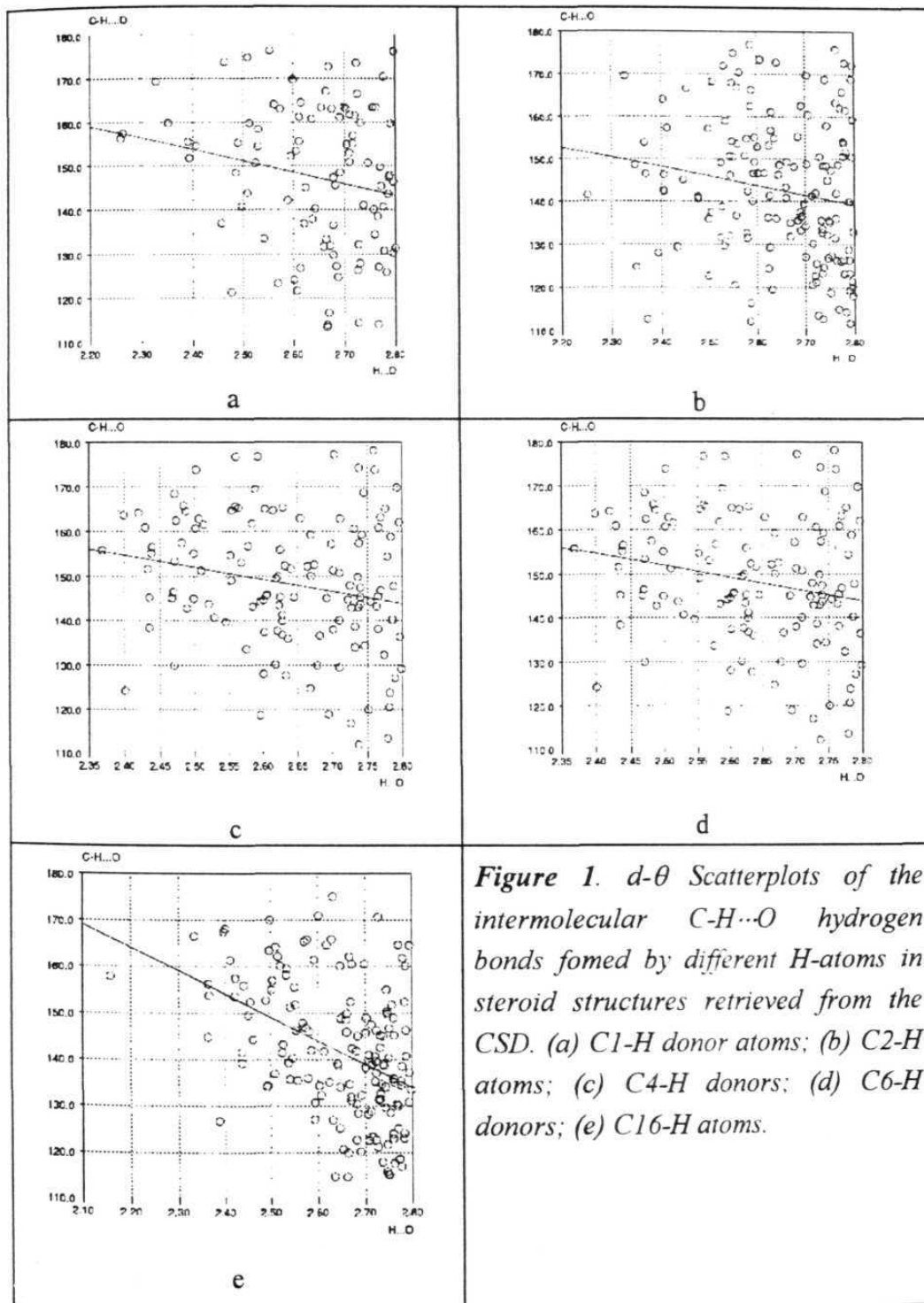


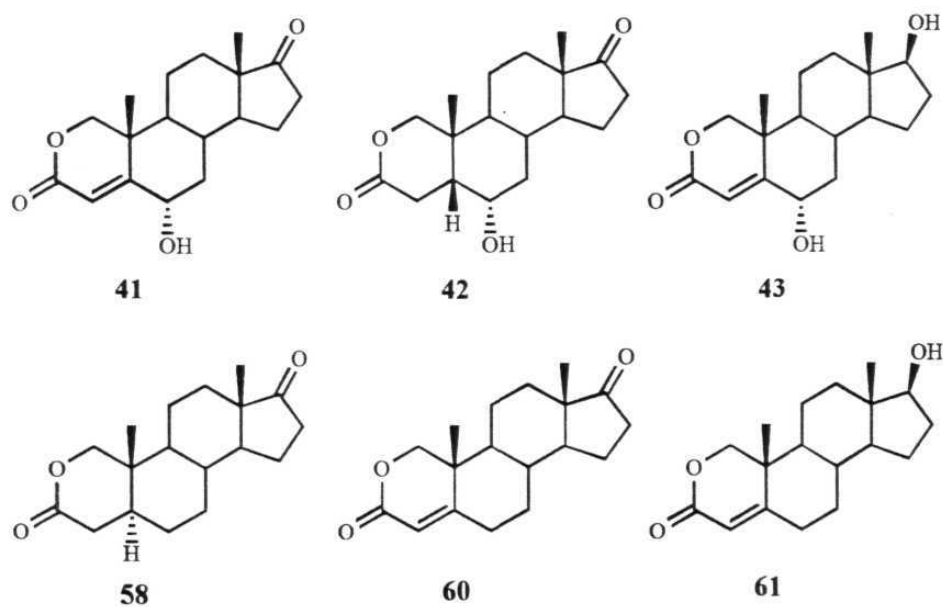
Figure 1. *d-θ* Scatterplots of the intermolecular C-H...O hydrogen bonds fomed by different H-atoms in steroid structures retrieved from the CSD. (a) C1-H donor atoms; (b) C2-H atoms; (c) C4-H donors; (d) C6-H donors; (e) C16-H atoms.

When the C2 methylene is replaced by an oxygen atom, two C-H *donors* are replaced by an *acceptor* and the C3 ketone carbonyl becomes a lactone carbonyl group. Due to this chemical change, the acidity of H-atoms at C1 is enhanced while the geometry of A-ring should resemble that found in Anavar[®] (**4**) or 2-azasteroid **76** because of the contribution from canonical form 'b' (Scheme 2). Thus, the conformation, shape and hydrogen bonding motifs of oxa-steroids should be different, and yet related, to the androgenic steroids.

2.2 STUDIES ON 2-OXASTEROIDS

2.2.1 Crystal Structure Analysis of 2-Oxasteroids.

The crystal structures of six 2-oxasteroids are discussed in this section. Supramolecular packing arrays supported by O-H...O and C-H...O hydrogen bonds and the molecular conformation are analysed. The 2-oxasteroids described here are: 6 α -hydroxy-2-oxaandrost-4-ene-3,17-dione (**41**), 6 α -hydroxy-2-oxa-5 β -androstane-3,17-dione (**42**), 6 α ,17 β -dihydroxy-2-oxaandrost-4-ene-3-one (**43**), 2-oxa-5 α -androstan-3,17-dione (**58**), 2-oxaandrost-4-ene-3,17-dione (**60**) and 17 β -hydroxy-2-oxaandrost-4-ene-3-one (**61**) (Scheme 6). A sequential progression in the molecular structure from saturated lactone **58** to unsaturated lactone **60**, and then to 6-hydroxy lactone **41**, the saturated 6-hydroxy lactone **42**, the 17-hydroxy lactone **61** and finally the 6,17-dihydroxy lactone **43** is taken up. This should provide information about the influence of functional groups on the overall shape and intermolecular packing motifs in these structures. An analysis of structures in the oxasteroid family will provide an understanding of the role of strong O-H...O and weak C-H...O hydrogen bonded motifs¹¹ in crystal packing as well as an appreciation of the contribution of steric and electronic factors in hydrogen bond formation.²⁷



Scheme 6. 2-Oxasteroids studied in this work.

In the crystal structure of **58**, space group $P2_12_12_1$, four distinct screw-related molecules pack in a head-to-head and tail-to-tail fashion along [001]. At the head end, O3 is bonded to the C1-H atoms of distinct screw-related molecules forming a chain of C-H...O hydrogen bonds along [010] (2.39, 2.70 Å; 138, 156°). The two hydrogen bond donor molecules involved in such chains are in turn related by translation (Figure 2). At the tail end, translation related molecules are connected by a chain of C-H...O hydrogen bonds along [100] involving C15-H atom and C17 carbonyl oxygen (2.62 Å, 153°).

In lactone **60** ($P2_1$), both C3 and C17 carbonyl oxygen atoms form bifurcated C-H...O hydrogen bonds. The C6 methylene hydrogens are bonded to the O3 of a screw-related molecule and form a C-H...O hydrogen bonded chain along [100] (Figure 3). The C1-H α and C11-H β atoms from two translation related molecules are hydrogen bonded to the O17 of a screw-related molecule.

In 6-hydroxylactone **41** ($P2_1$), the C3 and C17 carbonyl oxygen atoms are bifurcated and form intermolecular interactions similar to those found in the structure of lactone **60** (Table 4). The C6-OH and C6-H atoms from two translation related molecules are hydrogen bonded to the O3 of a screw-related molecule to form a chain of alternating O-H...O and C-H...O hydrogen bonds along [100]. Similarly, O17 forms a chain of C-H...O bonds along [100] as shown in Figure 4.

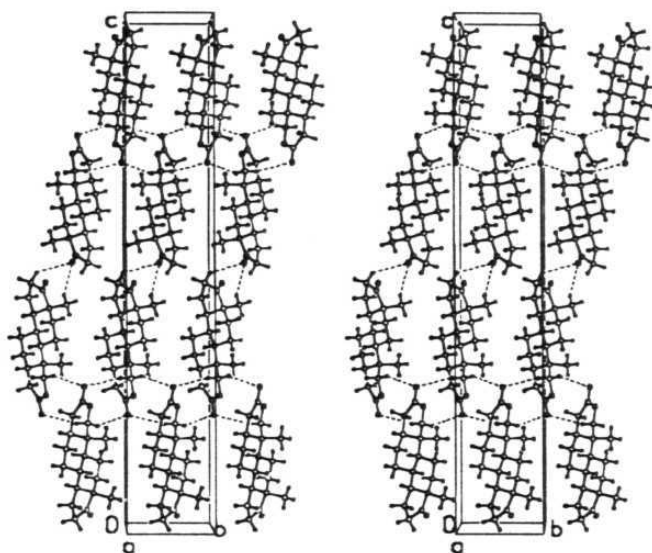


Figure 2. Stereo diagram of the packing pattern for **58** down $[100]$. A tape of C-H...O hydrogen bonds along $[010]$ connects C1-H atoms from distinct 2_1 related molecules to O3.

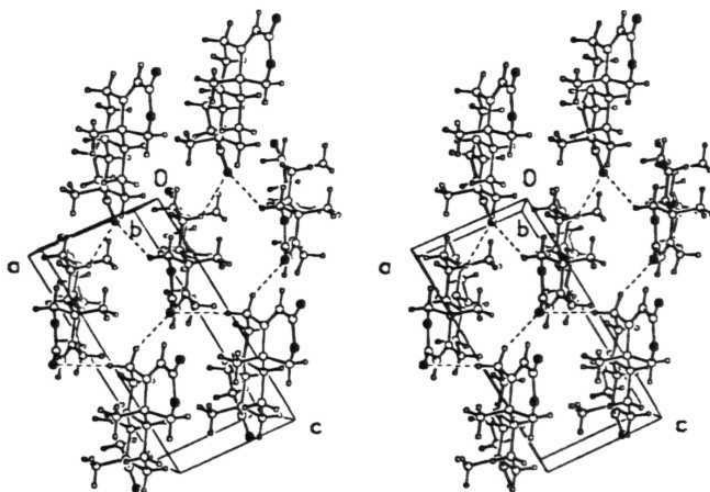


Figure 3. Stereoview of the crystal structure of **60** showing the two C-H...O hydrogen bonded chains along $[100]$ involving bifurcated O3 and O17 acceptor atoms.

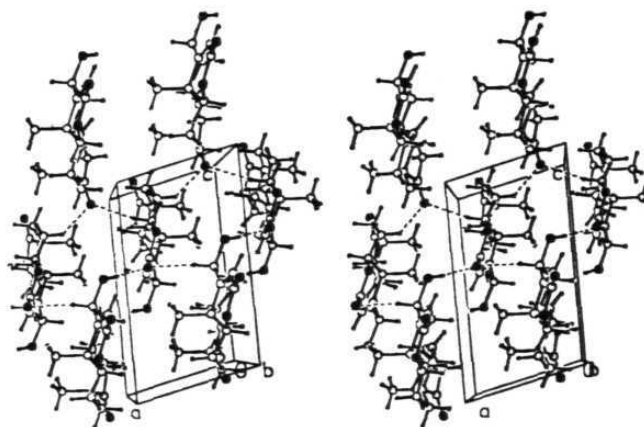


Figure 4. Stereoview of the crystal structure of **41** with two intermolecular hydrogen bonded chains along $[100]$.

In 6 α -hydroxy-5 β -lactone **42**, space group $P2_12_12_1$, translation related molecules along $[001]$ pack in columns connected by C6-OH and O3 atoms. Adjacent screw-related columns are interconnected by a right-handed (*P*) C-H \cdots O hydrogen bonded spiral²⁸ along $[001]$ (Figure 5). It may be noted that the A-ring is bent with respect to the rest of the steroid skeleton (B-, C- and D-rings) because the A/B ring junction is *cis*. The observed arrangement optimises the intermolecular interactions in the crystal.

In 17-hydroxy lactone **61** ($P2_12_12_1$), the molecules form a twisted chain and are connected by a head-to-tail chain of O-H \cdots O hydrogen bonds along $[100]$ (C17-OH \cdots O3: 1.97 (3) Å, 171 (3)°). Such translation related chains are interconnected by C-H \cdots O hydrogen bonds (C6-H \cdots O17 and C12-H \cdots O3) and form a corrugated sheet in (110) (Figure 6). Further, a weak contact connects O2 with C15-H atom (2.77 Å, 121°). Adjacent screw-related layers stacked along $[001]$ are interconnected by C-H \cdots O hydrogen bonds utilising the H-atoms on C7 and C19 (Table 4).

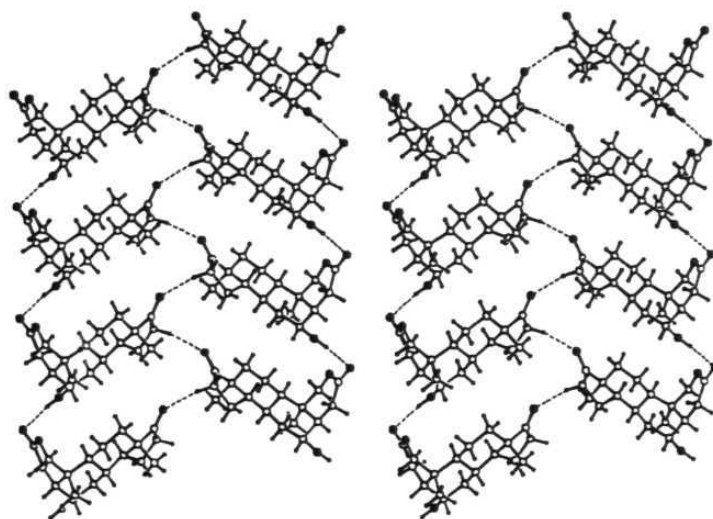


Figure 5. Stereoview of the structure **42**. Screw-related O-H...O hydrogen bonded columns are interconnected by a C-H...O hydrogen bonded spiral chain.

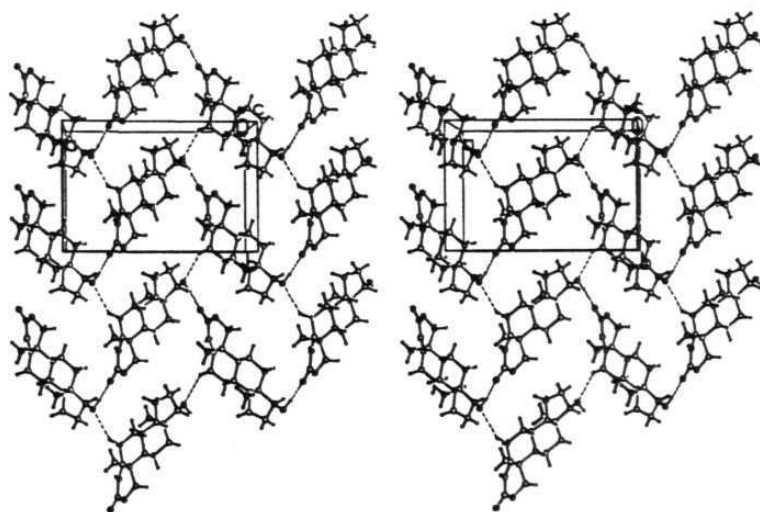


Figure 6. Stereoview of the structure **61** showing O-H...O hydrogen bonded chains of molecules along [100] interconnected by C-H...O hydrogen bonds along [010].

In dihydroxylactone **43**, ($P2_12_12_1$), translation related molecules pack in a head-to-tail fashion connected by O-H...O hydrogen bonds involving O17-H and C3 carbonyl oxygen. Translation related chains in (110) are connected by O6-H...O17 hydrogen bonds while the inter-layer region is connected through weak C-H...O hydrogen bonds (Table 4). There are four such screw-related layers stacked in one unit length along [001] (Figure 7).

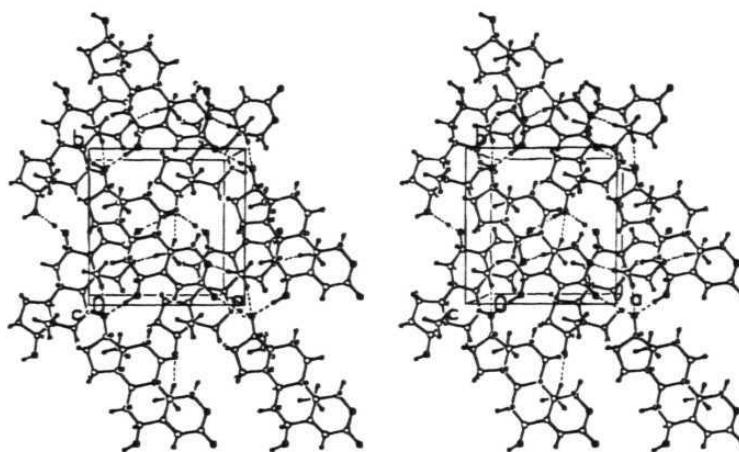


Figure 7. Stereoview of the layered structure of **43** interconnected by C-H...O hydrogen bonds.

2.2.2 Summary of Intermolecular Interactions

In these lactonic steroids, the hydroxy group is present at C6, C17 and the carbonyl group at C3, C17. When only O17 hydroxy group is present, a head-to-tail O-H...O hydrogen bonded chain with O3 is formed similar to that observed for the natural steroids. In cases where both O6 and O17 are hydroxy groups, O17 prefers to form O-H...O hydrogen bond with O3. This is because O17 and O3 are on the edges of the tetracyclic skeleton and form the commonly observed head-to-tail packing motif. In such cases, the C6-hydroxy is used to connect the chains

formed by O17 and O3. On the other hand, when O6 is a hydroxy group and O3 and O17 are carbonyl groups the hydrogen bonding is formed with O3 carbonyl rather than O17, perhaps because the former is more basic being lactonic in nature.

The preferences observed for different C-H donors in forming C-H...O hydrogen bonds in 2-oxasteroids are similar to those observed in the parent steroids. In almost all the structures, the H-atoms on C1 and C6 are involved in short C-H...O hydrogen bonds (Table 4). In the saturated structure **58**, both the hydrogens participate in C-H...O hydrogen bond due to their enhanced acidity³⁰ and planar shape of the A-ring.²² Similarly, the C6 allylic hydrogen atoms in **60** are involved in intermolecular interactions with two different acceptors. The hydrogen atoms at C15 are geometrically accessible while those at C16 are acidic, and this could explain their participation in C-H...O hydrogen bonds. However, the C4 hydrogens are relatively acidic (sp^2) but rarely participate in hydrogen bonding. The C-H...O hydrogen bonding ability of sp^3 C11, C12, C18 and C19 hydrogen atoms can be ascribed more to their geometric accessibility than to acidity effects. The d- θ scatterplot of C-H...O interactions in these six lactones are depicted in Figure 8. It may be noted that in some cases the contacts are at the limit or beyond the van der Waals radii sum ($H\cdots O = 2.7 \text{ \AA}$). The distance criterion is so chosen because C-H...O contacts exhibit the characteristics of hydrogen bonds and could play a structure-determining role even at long distances.²⁹

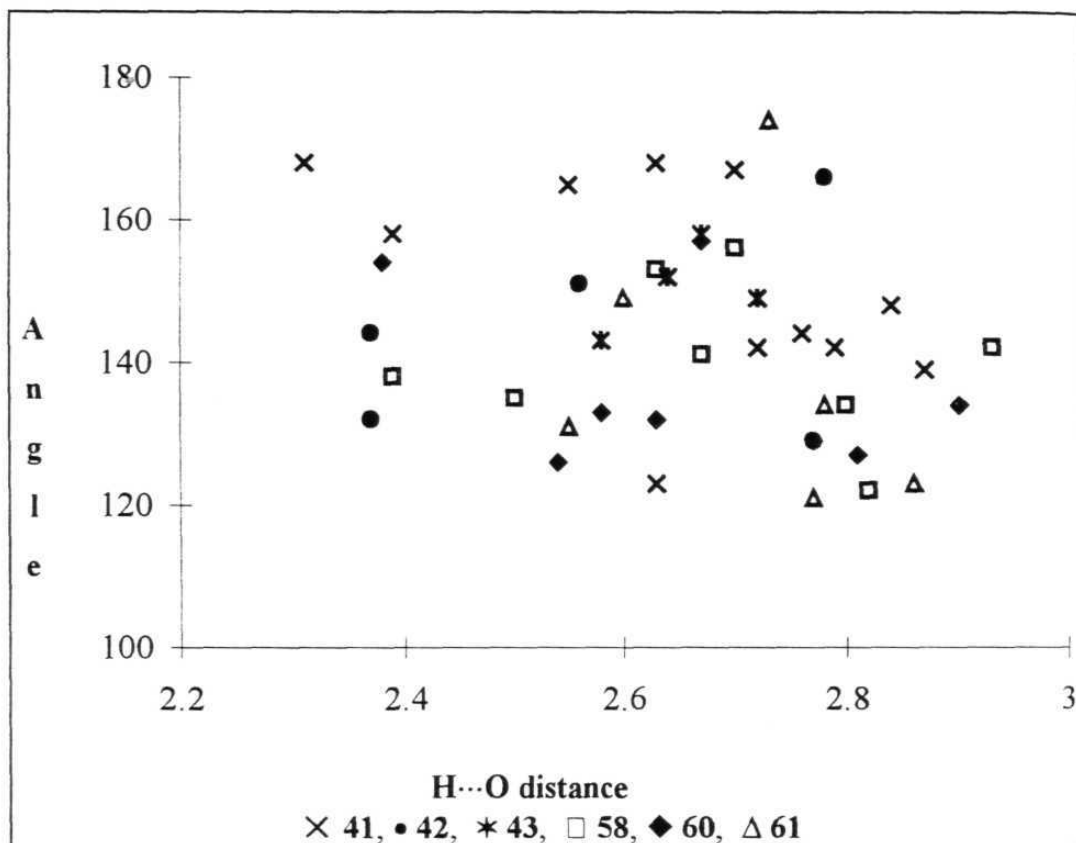


Figure 8. Scatter plot ($d-\theta$) for the C-H...O hydrogen bonds observed in 2-oxasteroids.

In the lactone structures studied here, five chemically distinct types of O-atoms are present: 2-oxa-, 3-carbonyl, 6-hydroxy, 17-carbonyl and 17-hydroxy (Scheme 6). An analysis of the intermolecular interactions formed by distinct oxygen atoms could reveal the dependence of these interactions on their basicity³¹ and geometric accessibility. Of the C3 and C17 carbonyl oxygen acceptors, O3 forms short C-H...O contacts involving acidic C-H donor atoms. The difference in acceptor strengths of C3 and C17 carbonyl groups in lactonic steroids could be because O3 is more basic due to resonance contribution from O2 (Scheme 2). Of the two hydroxy oxygen atoms, O17 forms better C-H...O hydrogen bonds than O6 and

this could be because the former is sterically more accessible. The lactonic O2 atom is a poor acceptor and rarely participates in intermolecular interactions. The histogram (Figure 9) shows the number of C-H...O hydrogen bonds formed by different acceptor O-atoms in each of the six oxasteroids.

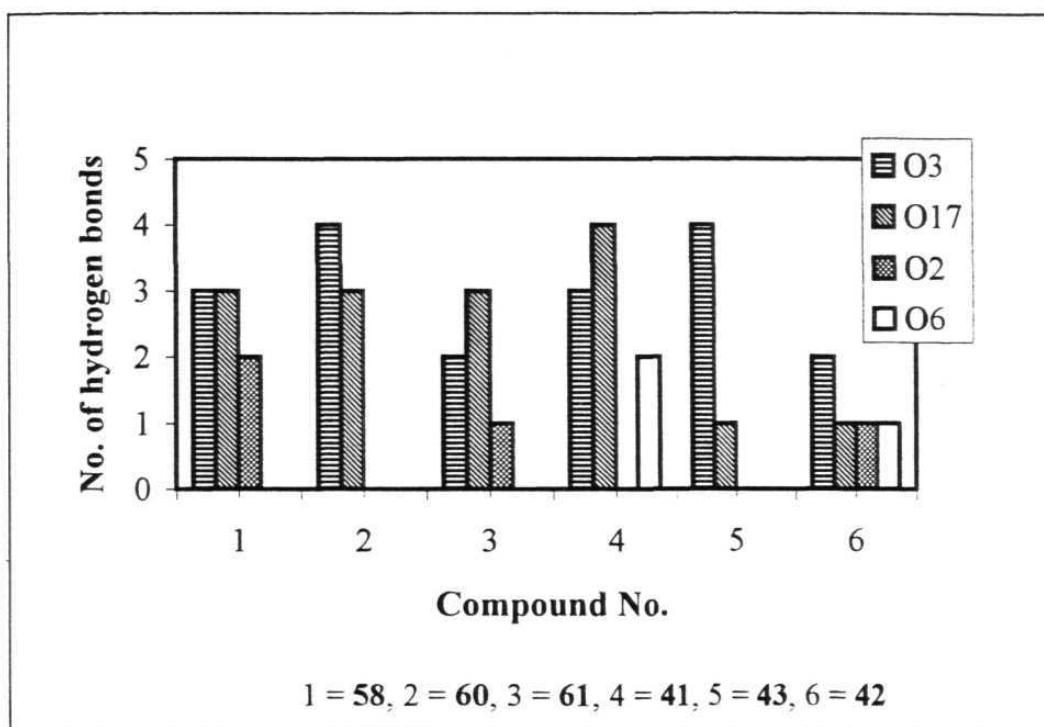


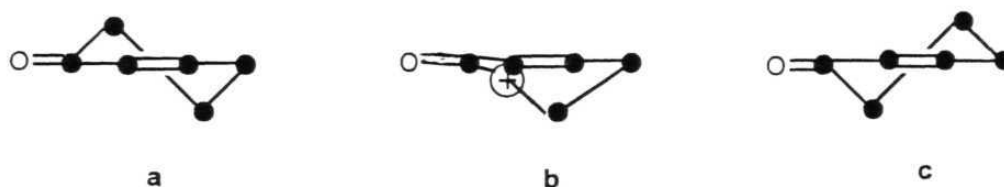
Figure 9. Histogram of C-H...O hydrogen bonds to different acceptor atoms in 2-oxasteroids.

2.2.3 Molecular Conformation.

The understanding of molecular shape of steroids is important because of its role in the recognition of these biomolecules by the receptor protein. Small changes in the number and position of functional groups on the steroid skeleton results in large differences in physiological activity, hormonal and drug action.³² An examination of the molecular structure and three dimensional shape of the

steroids should provide information on features that influence their biological activity.³¹

The conformation of the A-ring is important in determining steroid-receptor interactions. Duax *et al.* have studied the conformational flexibility of A-ring in 191 4-ene-3-one steroids.³² Three conformations are adopted: $1\alpha,2\beta$ -half chair (commonly observed) an ideal 1α -sofa conformation and inverted $1\beta,2\alpha$ -half chair conformation (Scheme 7).



Scheme 7. Three most common conformations of the A-ring for 4-en-3-one steroids: **a.** $1\alpha,2\beta$ -half chair; **b.** 1α -sofa; **c.** $1\beta,2\alpha$ -half-chair conformation.

An analysis of the A-ring in 2-oxa-4-ene-3-one steroids shows that they adopt the normal $1\alpha,2\beta$ -half chair conformation while the saturated 2-oxa- 5α -steroid **58** has 1α -sofa conformation. In the 5β -steroid, **42** the A-ring has a bowing angle of 81.7° with respect to the mean plane of B-, C- and D-tricyclic ring system, a value that is comparable to other 5β -steroids reported recently [81.53° , 81.97° and 58.91°].³⁴ Figure 10 shows the overlay plot of the 5β -oxasteroid **42** along with the other 4-ene-3-one oxasteroids discussed earlier.

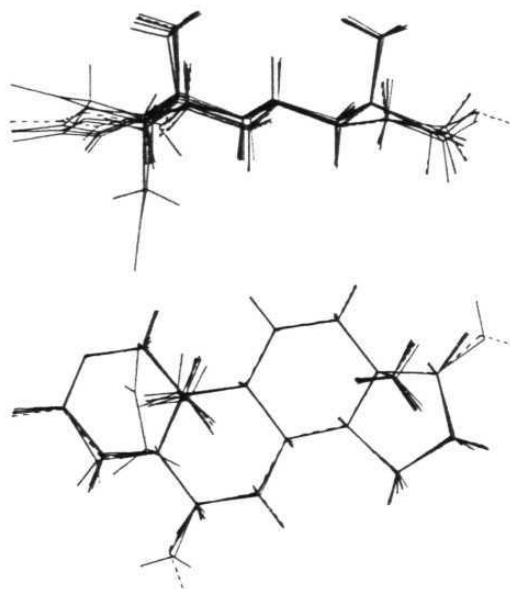


Figure 10. Overlay diagram of six 2-oxasteroids. Lateral view (above) of the overlay plot and top view (below). Notice that the 5 β -oxasteroid is not part of the tightly bunched population of 4-ene-3-one oxasteroids.

The conformational flexibility of the A-ring is more compared to the D-, B- and C-rings. In all these oxasteroids, the B- and C-rings have slightly flattened chair conformation with weighted average torsion angles (τ_{av}) of 53 (2) $^\circ$ and 55 (2) $^\circ$ respectively, values that are comparable to the natural steroids.³³ The D-ring has an envelope conformation with τ_{av} in the range 27 (3) $^\circ$ to 30 (2) $^\circ$ for the C17-carbonyl and C17-hydroxy compounds.

A comparison of the molecular shape of the oxasteroid skeleton with the natural substrates will reveal the conformational changes brought about by the conversion of ketone to a lactone group in the A- ring. An overlay plot of the 2-oxaandrost-4-ene-3,17-dione (**60**) with androst-4-ene-3,17-dione **55**³⁵ has an overall r.m.s deviation of 0.1003 Å for the common tetracyclic ring system while it is 0.0485 Å for the overlay of B-, C- and D-rings, indicating the extent of change

in the geometry of A-ring between the oxa- and natural steroids (Figure 11). Although, the molecular conformation of **60** and **55** is similar, no similarity is observed either in their space group or packing motifs. This is because the C2-H atoms are involved in short C-H...O hydrogen bonds with O17 (2.51 Å, 171°) in the crystal structure of **55** which is not possible in the 2-oxa analogue **60**.

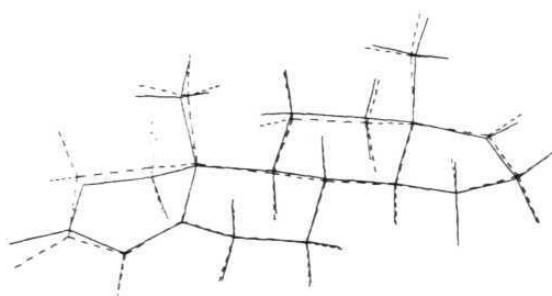
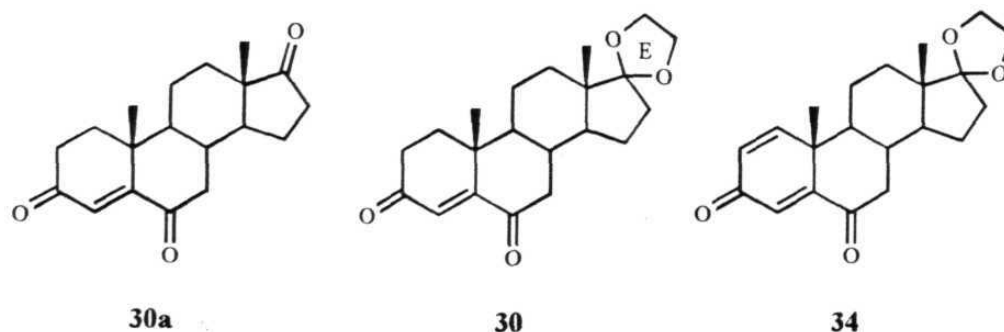


Figure 11. Overlay diagram of **55** and **60** for all rings (**55** is shown in dashed lines).

2.3 CRYSTAL STRUCTURES OF ANDROGENS

2.3.1 Crystal Structure Analysis of 6-Ketosteroids

In this section the crystal structures of androst-4-ene-3,6,17-trione (**30a**), 17-ethylenedioxyandrost-4-ene-3,6-dione (**30**) and 17-ethylenedioxyandrost-1,4-diene-3,6-dione (**34**) are discussed (Scheme 8).



Scheme 8. 6-Ketosteroids discussed in this section.

Steroids with Δ^4 -3,6-dione functional group occur in nature and are isolated from *Anthoarcuate graceae*.³⁴ These are known to be potent inhibitors of aromatase. Androst-4-ene-3,6,17-trione (**30a**) is one of the earliest synthetic suicide substrate inhibitor of aromatase with an apparent K_i of 0.43 μM .³⁶ Subsequently, many potent derivatives of **30a** have been synthesised and tested against aromatase.³⁷ Though steroids with this functional group were studied synthetically and biochemically, only one crystal structure is reported with the androgen basic skeleton for which no 3D-coordinates are published.³⁸ The scarce crystallographic data on Δ^4 -3,6-dione steroids has prompted the studies on these structures.

Trione **30a** crystallises in space group $P2_12_12_1$. The acceptor O-atoms participate in multiple hydrogen bonds: O17 tetrafurcated, O6 trifurcated and O3 bifurcated (Figure 12 and Table 5). The C2-H is involved in short C-H...O contact with O17 (2.39 Å, 172°) and C16-H with O3 (2.52 Å, 153°). Numerical parameters of these interactions are detailed in Table 5. The C4=C5 double bond is in stronger conjugation with O3 than with O6 as inferred from the bond distances [C3=O3 1.217 (3), C3-C4 1.452 (4), C4=C5 1.334 (3), C5-C6 1.502 (3) C6=O6 1.215 (3) Å].

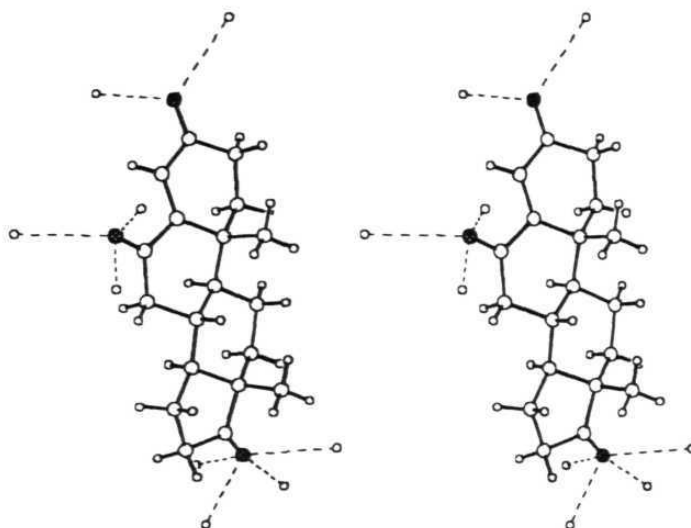


Figure 12. Stereoview of the structure **30a** showing different C-H atoms approaching the three carbonyl groups.

In the crystal structure of enone-ketal **30**, screw-related molecules pack along [001]. A right-handed (P)²⁸ spiral chain of C-H \cdots O hydrogen bonds between C2-H and O3 runs along [010] (2.64 Å, 161°) (Figure 13a). Molecules related by screw-axis pack as coils connected by C-H \cdots O hydrogen bonds involving C4-H with O20 (2.41 Å, 167°) and C1-H and O6 atoms (2.64 Å, 121°) along [100] (Scheme 13b).

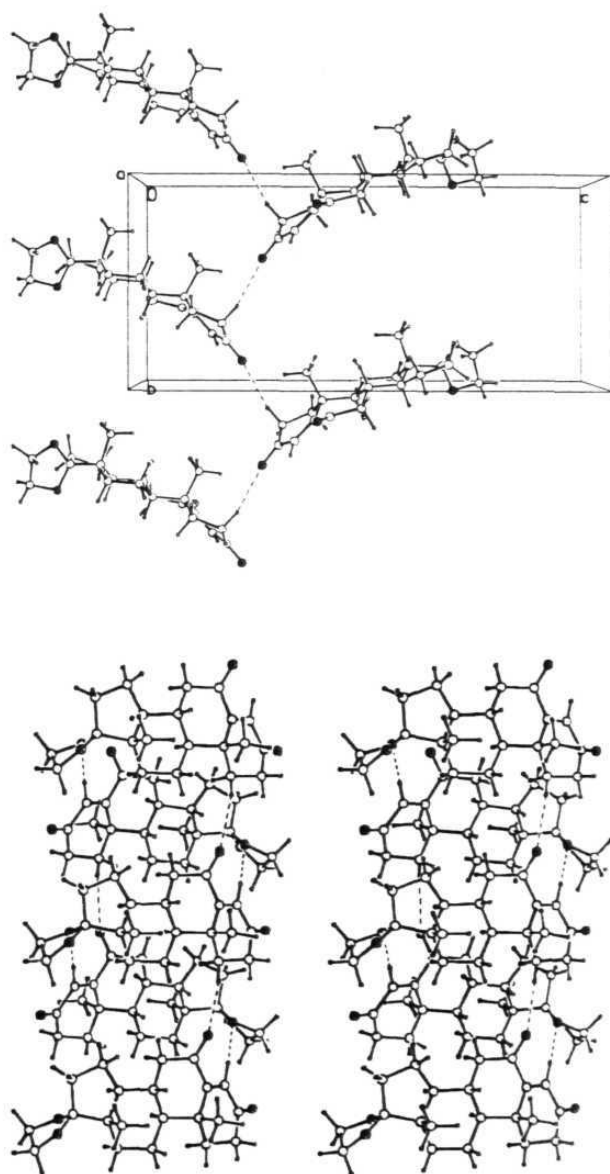


Figure 13. *a.* A spiral C-H...O hydrogen bonded chain in **30** along [010] connecting C2-H and O3 atoms of two distinct screw related molecules. *b.* Stereoview of molecules of **30** packed in coils along [100] connected by C-H...O hydrogen bonds.

In dienedione-ketal **34** ($P2_12_12_1$), hydrogen bonds along [010] (C22-H...O 2.92 Å, 121°) connect molecules from head-to-tail to form chains. These chains are interconnected by C-H...O hydrogen bonds involving C12-H and O6 (2.60 Å, 143°) forming layers in (110). Molecules in one layer utilise the bent shape of the skeleton in such a way that the head and tail portions of one molecule fit into the concave cavities of molecules in the adjacent layer, connected by C-H...O hydrogen bonds as shown in Figure 14 (Table 5).

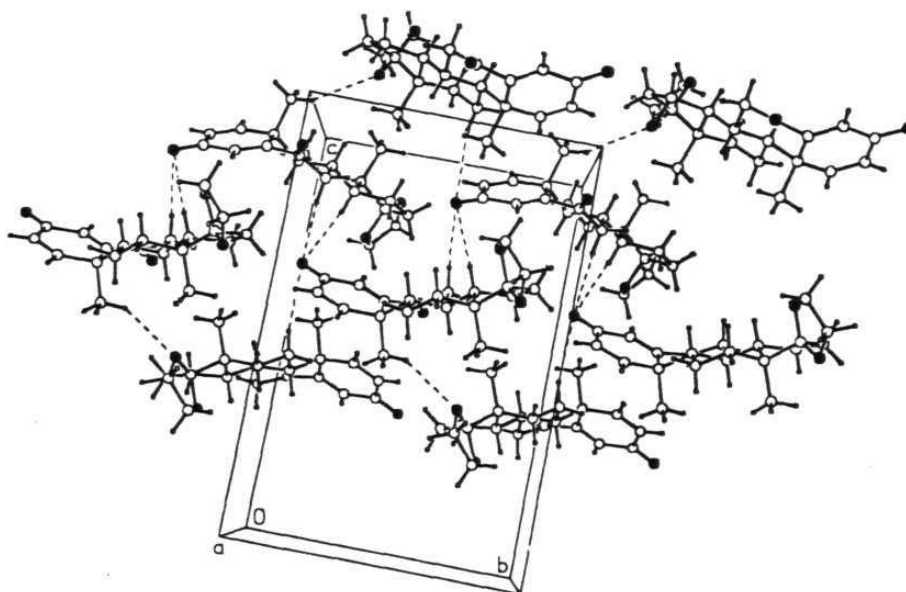


Figure 14. Packing diagram of **34** down [100] showing head-to-tail orientation of the bow-shaped molecules in a close packed arrangement.

2.3.2 Molecular Conformation

The conformation of the A-ring in **30** and **30a** is the normal $1\alpha,2\beta$ -half chair with the weighted average torsional angle (τ_{av}) being 25.24 (3)° and 24.33 (3)°. The τ_{av} values of the other three rings in **30** and **30a** are: B-ring (47.00 (3)°, 43.61 (4)°); C-ring (55.09 (4)°, 54.76 (3)°); D-ring (26.24 (3)°, 27.03 (4)°). Though the

two molecules are similar in the A-, B- and C-rings, an overlay plot of the common atoms of the tetracyclic skeleton of **30** and **30a** shows that the conformation of the A- and B-rings is slightly different.

The τ_{av} in **34** for A-, B-, C-, D- and E-rings is 1.75 (6)°, 52.32 (5)°, 55.72 (5)°, 32.41 (5)° and 9.22 (4)°, respectively. The A-ring is almost planar and bent to the α -face of the skeleton with a bowing angle 34.8°. The τ_{av} of the E-ring in **34** is low compared to the value in **30**. This is inferred from the extent of deviation of C21 atom from the mean plane of the other four atoms (0.5505 Å in **30** and 0.2140 Å in **34**). The E-ring is flexible and can adopt numerous low energy conformations in the crystal. This was evaluated by a 'Systematic Search' in *Cerius*² for possible conformations.⁴⁰ The search was performed by minimisation of the molecules with MOPAC 6.0 program (MNDO Hamiltonian) followed by breakage and recombination of one bond chosen arbitrarily (C(1)-C(2), C(6)-C(7), C(11)-C(12), C(15)-C(16) and C(21)-C(22)) to search for the numerous possible conformations in each ring with a maximum limit of 100. The overlay plot (100 conformations, $\Delta E < 13 \text{ KJ mol}^{-1}$ Figure 15) confirms that the dioxolane E-ring has large conformational flexibility. Further, the A-ring in enone **30** is conformationally more flexible compared to the A-ring in dienone **34**. In both structures, the B- and C-rings are largely inflexible.

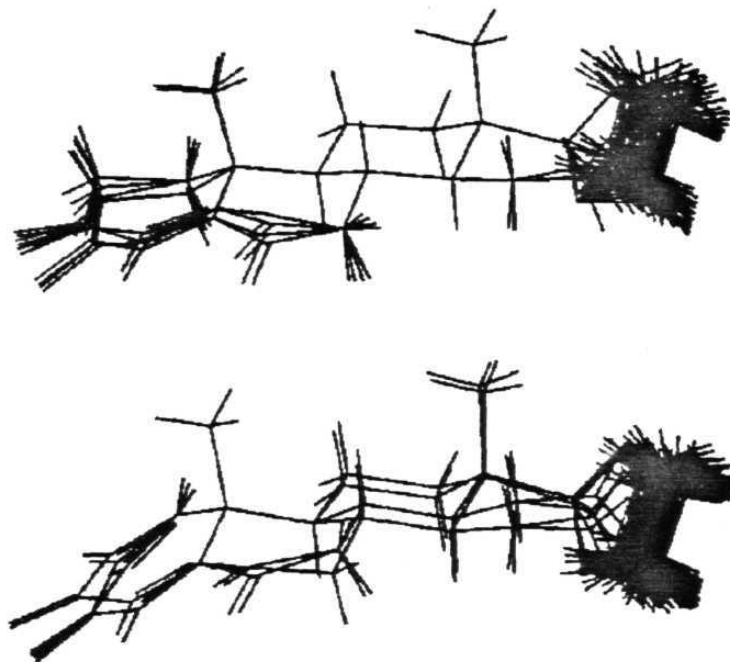
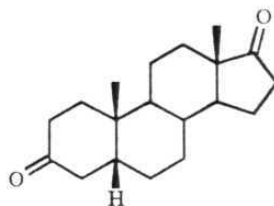


Figure 15. 100 conformations of 30 (top) and 34 (bottom) generated through the 'Systematic Search' module in Cerius². A large number of dioxalane ring conformations are possible in both the structures.

2.3.3 5 β -Androstane-3,17-dione

Lawrence *et al.* have studied structure-activity relationship of sex steroid analogues as inhibitors of Ca²⁺-ATPase.⁴¹ 5 β -Androsterones were found to be active compared to testosterone in assays using female-source membranes, while 5 α -androsterones were less active. The discrepancy in activity was attributed to the bent shape of the molecule in 5 β -steroids. A comparison of the crystal structures of 5 α - and 5 β -androstanes should shed light on the binding characteristics of the two molecules. Two crystal structures of 5 α -androstane-3,17-dione are reported in the CSD, one of them being the bromophenol solvate with two molecules in the asymmetric unit.⁴² In the case of the 5 β -analogue 56, only cell axis were determined and no 3D-coordinates are reported to compare its

geometry with that of 5α -androstanedione.⁴³ Since, this compound was synthesised as an intermediate in the synthesis of 2-oxasteroids (Chapter 1), we have explored the crystal structure of **56**.



56

Scheme 9. 5β-Androstane-3,17-dione.

In the crystal structure of **56** ($P2_12_12_1$), both the acceptor atoms are multiply C-H...O hydrogen bonded (Figure 16, Table 6). A hydrogen bonded chain along [010] connects C7-H and O3 atoms of translation-related molecules. These chains are interconnected with C-H...O hydrogen bonds from C5β-H and C19-H atoms to O3 carbonyl of screw-related molecules. In the D-ring, O17 acts as an acceptor to C4-H and C9-H atoms.

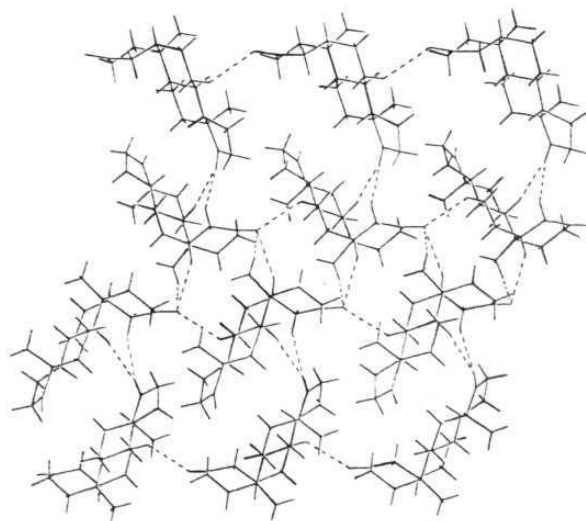


*Figure 16. The bent shape of **56**. C-H...O hydrogen bonds stabilise the structure.*

In **56**, the A-ring is in the half chair conformation while the B- and C-rings are in the normal chair conformation and D-ring adopts the 14α -conformation. The bowing angle between the mean plane of the A-ring and the mean plane of B-, C- and D-rings is 70.83° , a value comparable to other 5β -steroids reported recently (81.53° , 81.97° and 58.91°).³³ An overlay plot of B-, C- and D-rings of the three different conformers reported for 5α -androstande with the 5β -analogue **56** showed low r.m.s deviations (0.0824 \AA , 0.0586 \AA and 0.0664 \AA ; Figure 17).

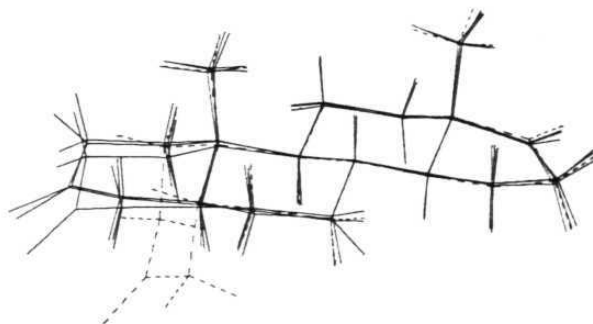


Figure 17. Overlay plot of 5β -androstande **56** (dashed lines) with the three conformers reported for 5α -androstande.

2.4 ISOSTRUCTURALITY

2.4.1 Definition

The phenomenon of isomorphism is known for more than two centuries when Rome de 'Ile noticed the growth of potassium alum crystals in a saturated solution of ammonium alum. Since then many reports have appeared on isomorphism in inorganic salts. Kitaigorodskii was the first to summarise isostructurality behavior in organic compounds.⁴⁴ Duax *et al.*¹³ have reported ten isomorphous pairs in 164 crystal structures of steroids. In six of these, there is no simple correspondence between the cell parameters, the packing of molecules in the crystal lattice, and the

hydrogen bonding motifs. Recently, under the banner of 'Main Part Isostructuralism' Kalman *et al.* have reported pairs of isostructural cardenolides and bufadienolides.⁴⁵ Some of the isostructural pairs form co-crystals and it was observed that greater the isostructurality index, the more easily the components form a binary solid solution. In the isostructural pairs of steroids discussed by Kalman, a 3-hydroxy group is always present that forms a head-to-tail hydrogen bonded chain with the C17 carbonyl oxygen atom. This strong O-H...O hydrogen bonded chain is insensitive to minor perturbations in molecular shape and substitution, and is the basis for isostructurality in related pairs of molecules. The presence or absence of an extra oxygen atom in B- or C-rings is found to have a nominal effect on the overall packing and interaction motifs in the crystal.

Some cases have been reported of isomorphous crystal structures in which an O-H...O or N-H...O hydrogen bond in one structure is structurally and functionally replaced by a C-H...O or C-H...N bond. The well-known examples in this category are the complexes of urea-barbital and acetamide-barbital,⁴⁶ and the complexes of β -cyclodextrin with diethanolamine and pentane-1,5-diol.⁴⁷

Kalman has suggested two parameters which estimate the extent of isostructurality, or likeness, between two similar structures, *the unit cell similarity index* (Π) and *the isostructurality index* ($I_i(n)$). In the equation for unit cell similarity index (Π), a , b , c , and a' , b' , c' are the orthogonalised lattice parameters of the related crystals. Ideally, for a pair of completely isostructural crystals Π should be close to zero.

$$\Pi = \left| \frac{a+b+c}{a'+b'+c'} \right| - 1 \cong 0$$

The isostructurality index, $I_i(n)$ is a measure of the degree of internal isostructuralism, where n is the number of distance differences (ΔR_i) between the absolute coordinates of identical non-hydrogen atoms within the same section of asymmetric units of related (A and B) structures. Ideally, $I_i(n)$ should be close to 100 %, for isostructural crystals.

$$I_i(n) = \left[1 - \left(\frac{\sum \Delta R_i^2}{n} \right)^{1/2} \right] \times 100$$

2.4.2 One-dimensional Isostructurality

The unit cell similarity index (Π) for the pair of **41** and **60** is 0.002 but the isostructurality index, $I_i(17)$ is only 75 % which indicates that the difference in their molecular shape is significant. Despite the low $I_i(17)$ value, **41** and **60** are found to have similar crystal structures.

The crystal structures **60** and **41** adopt the same space group, $P2_1$ and the length of the a -axes are strikingly similar (6.2321 and 6.2214 Å). This is the direction of the hydrogen bond interactions. In **60**, the bifurcated O3 forms a C-H...O hydrogen bonded chain along [100] with both the H-atoms of C6 (Figure 18). The C6-H α atom in **60** is replaced by a hydroxy group in **41**, that is the C-H...O...H-C-H...O chain in **60** is replaced by C-H...O...H-O-C-H...O chain in **41** (Scheme 10). In effect, one of the C-H...O hydrogen bonds in **60** behaves as a surrogate of the C-O-H...O bond in **41**. Such an equivalence in one direction may be termed as 'one dimensional isostructuralism'.

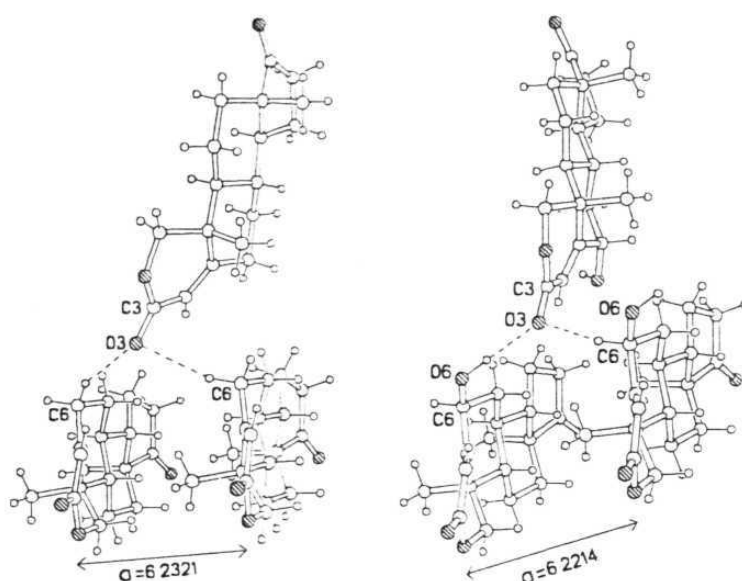
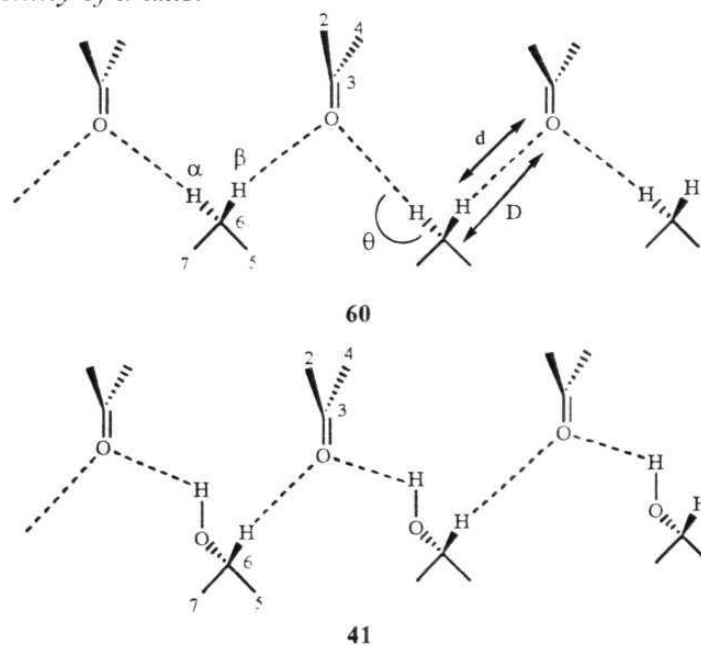


Figure 18. Structural similarity between lactones **60** and **41**. In **60**, the C6-methylene H-atoms are hydrogen bonded to the carbonyl O3 atom of different 2_1 -related molecules, and **41** the C6-hydroxy and C6-H are bonded to O3 atom. Notice the identity of *a*-axis.



Scheme 10. Supramolecular synthons in **60** and **41**.

When a 1:1 mixture of **41** and **60** was recrystallised from EtOAc-MeOH, crystals^a were obtained in the space group $P2_1$ and with cell dimensions very similar to those of pure **41**. Structure solution and refinement with partial positional occupancy for O6 yielded a converged model with occupancies of 0.720(6) and 0.28 for **41** and **60** respectively showing that crystal is a binary solid solution. The presence of components **41** and **60** in a single crystal of binary solid solution, **81** was confirmed by IR, and their ratio found to be in the range 3:7 to 4:6 by ^1H NMR integration on individual crystals. Further, the formation of solid solution was inferred by two sets of ORTEP plots of **41** and **81** (Figure 19). The probability level of the ellipsoids was examined at 35 % and 50 %. The size of the O6 atom in **81** with s.o.f of 1.00 is larger than that in **41** but the size of the ellipsoid of O6 in **81** with s.o.f of 0.72 exactly matches with that of pure **41**. This also indicates that the final s.o.f of O6 is 0.72 and hence **81** is a binary solid solution. We feel that the ORTEP plots in Figure 19 convincingly show the formation of binary solid solution.

Two structures (HMEPRG **82**, HPRGDP **83**; both $P2_12_12_1$)^{48,49} (Scheme 11) of the pregnane family were retrieved from the CSD that have similar hydrogen bonding motifs (Scheme 10) as observed in **60** and **41** despite having a different chemical structure. This packing motif appears to be insensitive to perturbations in the molecular structure. The acetyl group at C17 compared to the carbonyl group in **41** and **60** or the hydroxy group at C17 in **82** adapts to the robust C-H...O packing motif and does not cause a significant change in the crystal structure.

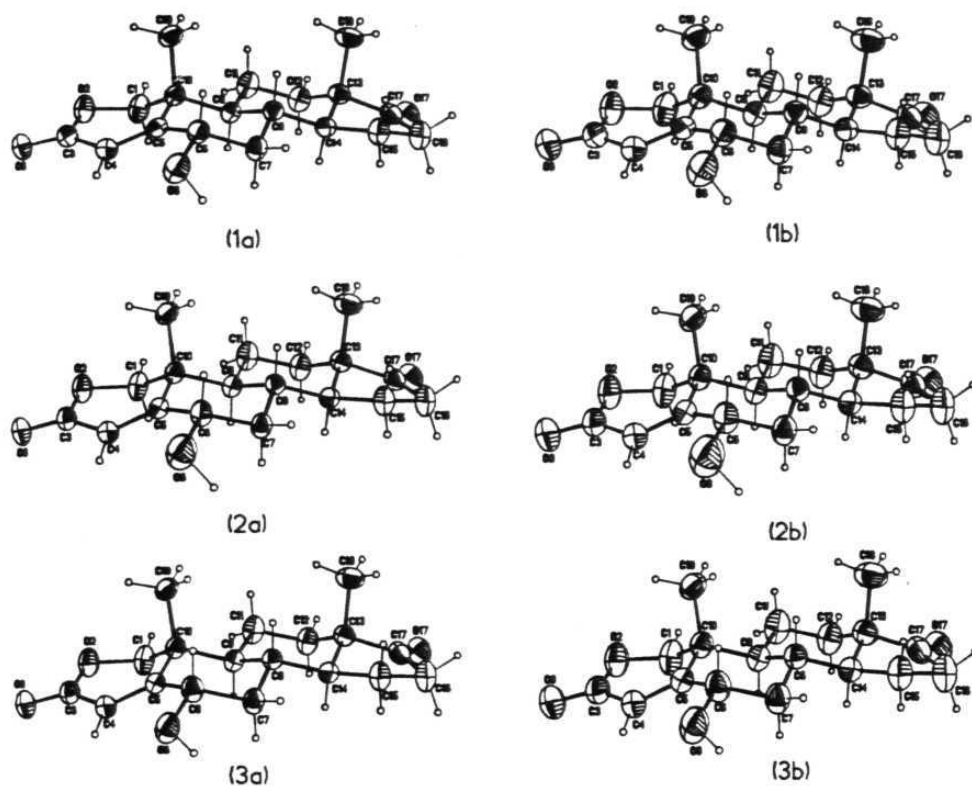
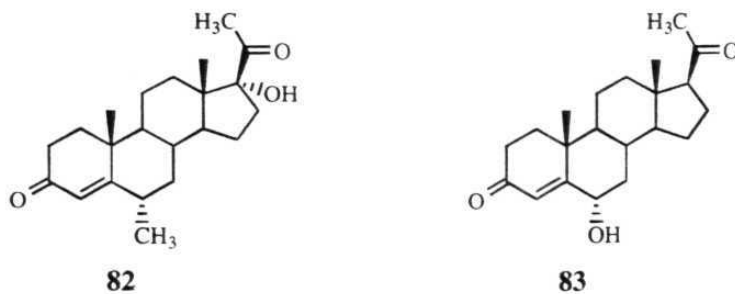


Figure 19. ORTEP plots of hydroxy steroid **41** and solid solution **81** at 35 % (left) and 50 % (right) probability level. Plots 1a/b are of pure **41**. Plots 2a/b are of solid solution **81** with s.o.f. of 1.00 for O6. Plots 3a/b are of **81** with s.o.f of O6 fixed 0.72. Notice the similar size of the O6 ellipsoid in 3a/b compared to that in 1a/b.



Scheme 11. Isostructural pregnanes that are similar in 'one-dimension' to the pair of lactones **41** and **60**.

The cell axis parallel to the hydrogen bonded motif in **82** and **83** (in this case the *c*-axis) is very similar to the *a*-axis in **41** and **60**. In the orthorhombic crystal structures **82** and **83**, the *a*- and *b*-axes are also similar (Table 1) making them another isomorphous set. Although the functional group at C6 which participates in hydrogen bonding is very different in the two compounds, OH in **83** and CH₃ in **82**, the packing motif is conserved showing the mimicry of CH₃ and OH groups in their interaction patterns and overall steric contribution (Figure 20).

Table 1. Lattice parameters of pregnanes in $P2_12_12_1$ space group.

	<i>a</i> -axis (Å)	<i>b</i> -axis (Å)	<i>c</i> -axis (Å)
HMEPRG 82	12.8535	22.8640	6.4504
HPRGDP 83	12.5220	23.0880	6.1620

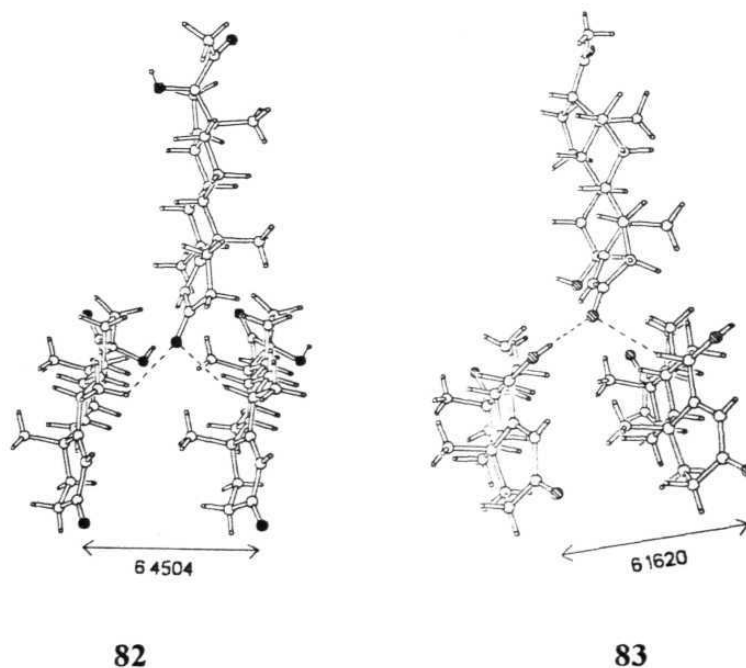


Figure 20. Similarity of HMEPRG **82** and HPRGDP **83**. In the former, the C6-methyl (H...O 2.68 Å and 119°) and C6-H (2.47 Å and 155°) atoms are C-H...O hydrogen bonded to bifurcated O3-atom. In the latter case, C6-OH and C6-H (H...O 2.61 Å and 151°) atoms are bonded to O3. Note the similarity of interactions with those observed in **41** and **60**.

The fact that this set of four compounds with different molecular structures exhibit 'one-dimensional isostructurality' highlights the importance of structure-determining supramolecular synthons in crystal structures. This phenomenon could be of relevance in the comparison of crystal structures.

2.4.3 Two-dimensional Isostructurality

The crystal structure of **43** is in space group $P2_12_12_1$ and that of Anavar[®] (**4**) is in monoclinic space group $P2_1$ ($\beta = 91.38^\circ$). While the a - and b -axes are similar, the c -axis value in Anavar[®] (9.512 Å) is approximately half of that in **43** (17.764 Å) (Table 2).

*Table 2. Lattice parameters of **43** in $P2_12_12_1$ and Anavar[®] in $P2_1$ space group.*

	a -axis (Å)	b -axis (Å)	c -axis (Å)
43	9.3361	9.6261	17.764
4	9.146	9.591	9.512

The molecules in the crystal structure of Anavar[®] pack in chains from head-to-tail connected by O17-H...O3 hydrogen bonds, similar to that found in lactone **43**. In **43**, the chains are interconnected by O-H...O hydrogen bonds between O6-H and O17 but in Anavar[®] (**4**) they are connected by weak C6-H...O17 hydrogen bonds. Similar layers are formed parallel to (110) in both the structures (Figure 21).

The (110) layer in the crystal structure of **34** is similar to layers found in **43** and Anavar[®] (**4**). Despite differences in molecular structure and conformation (r.m.s deviation of 0.2406 Å, $\Pi = 0.0137$), there is similarity within the layers, that is two-dimensional isostructurality. Although the molecular length in **34** appears to be longer because of the dioxolane ring, the tetracyclic skeleton is bent

on the α -face and the dioxolane E-ring accordingly adjusts to keep the distance between the two edges of the molecule (11.128 Å) similar to that in **43** (10.554 Å). A weak C22-H...O3 hydrogen bonded chain packs the translation related molecules in a head-to-tail fashion. These chains in turn are interconnected by C12-H...O6 hydrogen bonds (Table 5).

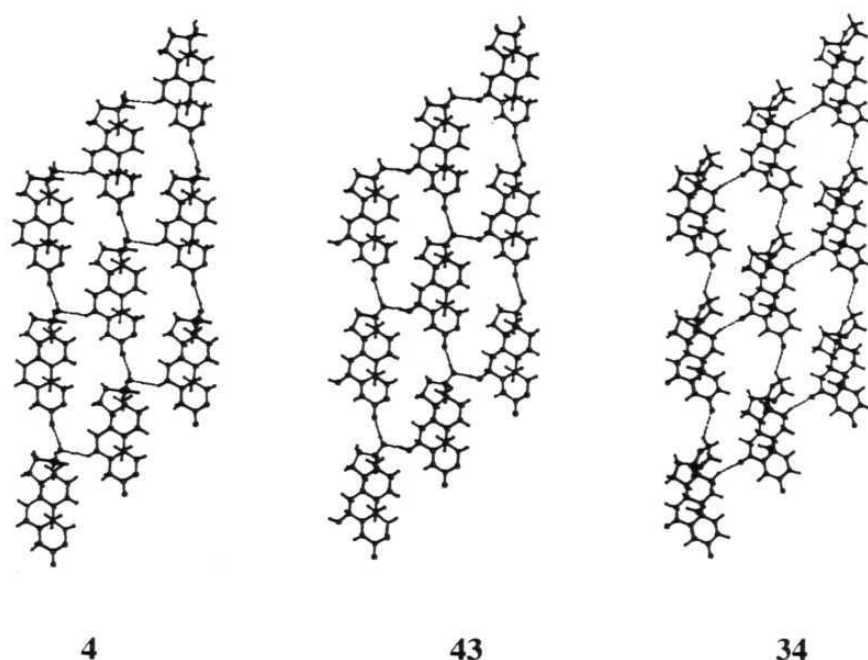
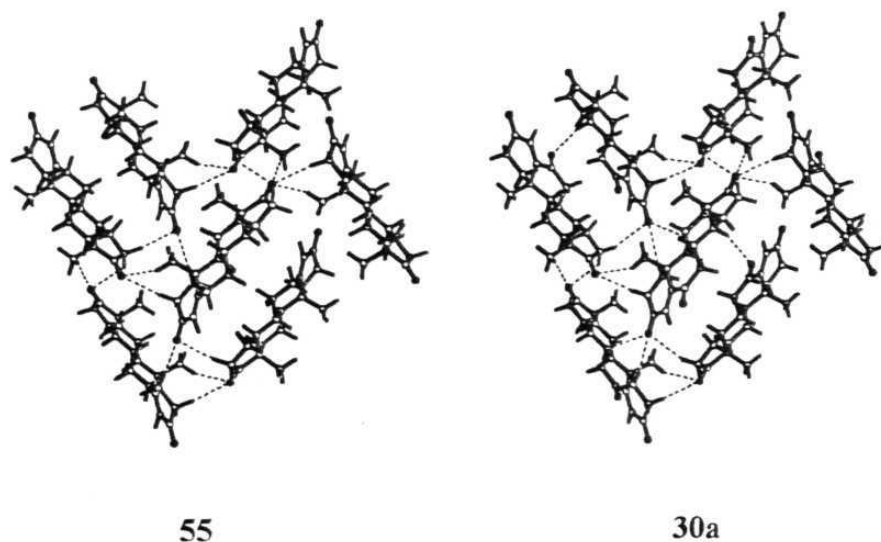


Figure 21. Crystal structures of **4**, **43** and **34** showing similar packing within the layers.

2.4.4 Three-Dimensional Isostructurality

Androst-4-ene-3,17-dione (**55**)²¹ is a natural substrate of aromatase and androst-4-ene-3,6,17-trione (**30a**) is a suicide inhibitor. Both these steroids compete for the same active site and hence it is appropriate to compare the geometry of these compounds. An overlay plot of the two steroids has low overall r.m.s deviation (0.0896 Å) though the deviation at C3 (0.104 Å) and C6 (0.279 Å) atoms is larger.

Isostructurality of the two structures is ascertained by Kalman's similarity index ($\Pi = 0.0015$) and isostructurality criteria ($I_D^{17} = 93.2\%$) (Table 3). Analysis of these crystal structures reveals that they have similar packing motifs and intermolecular interactions. Figure 22 shows the packing of **30a** (right) and androstenedione **55** (left) and the intermolecular C-H...O interactions are listed in Table 7. An inspection of Tables 5 and 7 suggests that there is a good correspondence in the interaction patterns and strengths of hydrogen bonds in the two structures. As one progresses from dione **55** to trione **30a**, the strength of hydrogen bonds formed by O3 decreases while those formed by O17 increases. The hydrogen bonds formed by O6 in **30a** should have minimal effect on the overall packing and so an exchange of few molecules in **30a** by molecules of **55** should not significantly alter the packing arrangement, suggesting that the two steroids could form a binary solid solution. Finally, it is noted that the C-H...O hydrogen bonds formed by O3 and O17 extend in three dimensions.



*Figure 22. The crystal packing of **55** and **30a**. Note the similarity in packing and intermolecular C-H...O hydrogen bonding pattern. The three dimensional approach of different C-H atoms to the three carbonyl groups in **30a** was shown in Figure 12.*

Table 3. Lattice parameters of 30a and 55 in $P2_12_12_1$

	<i>a</i> -axis (Å)	<i>b</i> -axis (Å)	<i>c</i> -axis (Å)
30a	7.2843	13.450	16.503
55	12.9780	16.9490	7.3650

In summary, three types of isostructural sets have been identified. A set of four steroids show one-dimensional isostructurality, three steroids have two-dimensional isostructurality, and two steroids show isostructurality in three dimensions, that is the entire crystal structure. As the dimensionality of isostructurality increases, the isostructurality index $I_i(n)$ also increases (except for **34**). In the one-dimensional case a C-O-H is replaced by a C-H bond, in the two-dimensional case the replacement is of a mixed interaction type, and in the 3D case a methylene is replaced by ketone functional group. Thus, isostructurality is observed at varying levels of dimensionality and functional group exchange.

2.5 EXPERIMENTAL

Synthesis of all the steroids studied in this chapter is delineated in Chapter 2. All the 2-oxasteroids (except for 6,17-dihydroxy steroid **41** which was yellow) were obtained as colourless cube-shaped crystals by slow evaporation of a mixture of EtOAc/hexane. Crystals of variable colour from light yellow to brown were obtained for the 6-ketosteroids. Space group and unit cell determination as well as all intensity measurements were carried out on a KM-4 diffractometer [KUMA] using graphite-monochromated CuK α or MoK α radiation in the Department of Crystallography, A. Mickiewicz University, Poznan, Poland. The reflection intensities were measured using a variable θ - 2θ scan by the background-peak-background method. The structures were solved using SHELXS-86 and all the non H-atoms were refined anisotropically using SHELXL-93 and SHELXL-97. The relevant crystallographic information is given at the end of this chapter.

2.6 TABLES

2.6.1 Intermolecular Interactions

Table 4. Geometry of *O*-H...*O* and *C*-H...*O* interactions in 2-oxasteroids.^a

Steroid	Interaction	H...O (Å)	O/C...O (Å)	O/C-H...O (°)
60	C(4)-H...O(3)	2.90	3.7344(3)	134
	C(1)-H...O(17)	2.54	3.2946(2)	126
	C(6)-H...O(3)	2.38	3.3873(2)	154
	C(6)-H...O(3)	2.67	3.6908(2)	157
	C(11)-H...O(17)	2.81	3.5657(3)	127
	C(11)-H...O(17)	2.58	3.4092(2)	133
	C(15)-H...O(2)	2.77	3.5441(3)	129
	C(16)-H...O(2)	2.63	3.4459(3)	132
58	C(1)-H...O(3)	2.39	3.279(3)	138
	C(1)-H...O(3)	2.70	3.716(3)	156
	C(4)-H...O(3)	2.81	3.518(3)	122
	C(6)-H...O(3)	2.66	3.576(3)	142
	C(15)-H...O(17)	2.62	3.624(4)	153
	C(16)-H...O(17)	2.80	3.638(4)	134
	C(18)-H...O(17)	2.50	3.346(3)	134
61	O(17)-H...O(3)	1.97(3)	2.853(3)	171(3)
	C(6)-H...O(17)	2.55	3.354(3)	131
	C(11)-H...O(17)	2.60	3.565(3)	149
	C(12)-H...O(3)	2.77	3.604(3)	134
	C(15)-H...O(2)	2.77	3.454(3)	121
	C(19)-H...O(17)	2.73	3.804(3)	174
	C(19)-H...O(3)	2.86	3.561(3)	123
41	O(6)-H...O(3)	1.90(5)	2.831(4)	171(4)
	C(1)-H...O(17)	2.31	3.376(4)	168
	C(6)-H...O(3)	2.38	3.409(4)	158
	C(8)-H...O(3)	2.87	3.752(4)	139
	C(9)-H...O(17)	2.79	3.706(3)	142
	C(11)-H...O(17)	2.62	3.339(4)	123
	C(15)-H...O(6)	2.83	3.797(4)	148
	C(15)-H...O(6)	2.76	3.686(4)	144
	C(16)-H...O(2)	2.71	3.625(4)	142
	C(18)-H...O(6)	2.69	3.757(4)	167
	C(19)-H...O(3)	2.63	3.693(4)	168
	C(19)-H...O(17)	2.55	3.609(4)	165

Table 2.6.1 continued

43	O(6)-H...O(17)	1.70(5)	2.760(2)	166
	O(17)-H...O(3)	1.91(3)	2.792(2)	167
	C(1)-H...O(6)	2.67	3.698(3)	157
	C(14)-H...O(3)	2.72	3.687(3)	149
	C(19)-H...O(17)	2.64	3.631(3)	152
	C(19)-H...O(3)	2.58	3.508(3)	143
42	O(6)-H...O(3)	1.99(7)	2.843(5)	164(6)
	C(1)-H...O(6)	2.37	3.196(5)	132
	C(7)-H...O(3)	2.55	3.538(6)	150
	C(14)-H...O(3)	2.77	3.552(5)	129
	C(15)-H...O(17)	2.78	3.837(6)	166
	C(16)-H...O(17)	2.37	3.305(6)	143

Table 5. Geometry of C-H...O interactions in 6-ketosteroids 30, 30a and 34.^a

30	C(1)-H...O(6)	2.64	3.341(4)	121
	C(2)-H...O(3)	2.64	3.685(5)	161
	C(4)-H...O(20)	2.41	3.472(4)	167
	C(15)-H...O(3)	2.97	3.745(4)	129
	C(16)-H...O(3)	2.80	3.681(5)	139
	C(16)-H...O(3)	2.70	3.602(5)	140
	C(19)-H...O(3)	2.78	3.607(4)	133
	C(21)-H...O(23)	2.70	3.457(4)	126
	C(21)-H...O(3)	2.70	3.556(5)	136
	C(22)-H...O(6)	2.72	3.549(4)	133
30a	C(1)-H...O(3)	2.83	3.897(4)	169
	C(1)-H...O(6)	2.62	3.337(4)	123
	C(2)-H...O(17)	2.39	3.461(4)	172
	C(2)-H...O(6)	2.68	3.409(4)	125
	C(14)-H...O(6)	2.76	3.791(3)	160
	C(16)-H...O(17)	2.60	3.438(4)	134
	C(16)-H...O(3)	2.52	3.523(4)	153
	C(18)-H...O(17)	2.50	3.516(4)	155
	C(19)-H...O(17)	2.62	3.513(4)	139
34	C(7)-H...O(3)	2.66	3.377(6)	156
	C(11)-H...O(3)	2.72	3.729(6)	155
	C(12)-H...O(6)	2.60	3.522(5)	143
	C(14)-H...O(20)	2.75	3.788(5)	160
	C(14)-H...O(3)	2.68	3.671(5)	152
	C(19)-H...O(23)	2.61	3.493(5)	137
	C(22)-H...O(3)	2.92	3.598(8)	121

Table 6. Geometry of *C-H...O* interactions in 5 β -androsterane-3,17-dione **56**.^a

56	C(4)-H...O(17)	2.59	3.535(3)	145
	C(5)-H...O(3)	2.64	3.622(4)	151
	C(6)-H...O(3)	2.90	3.551(3)	119
	C(7)-H...O(3)	2.62	3.394(3)	128
	C(9)-H...O(17)	2.53	3.583(3)	165
	C(15)-H...O(17)	2.83	2.583(4)	126
	C(19)-H...O(3)	2.60	3.539(4)	145

Table 7. Geometry of *C-H...O* interactions in **55**.^a

55	C(1)-H...O(3)	2.68	3.76	173
	C(2)-H...O(17)	2.51	3.59	171
	C(16)-H...O(17)	2.70	3.49	128
	C(16)-H...O(3)	2.38	3.44	167
	C(18)-H...O(17)	2.54	3.56	156
	C(19)-H...O(17)	2.51	3.48	150

^a All C-H bond distances are normalised to standard neutron distance (1.083 Å) and O-H bonds are refined from the difference density map.

2.6.2 Crystallographic Details.

	58	60	61	41	42
Empirical formula	$C_{18}H_{26}O_3$	$C_{18}H_{24}O_3$	$C_{18}H_{26}O_3$	$C_{18}H_{24}O_4$	$C_{18}H_{26}O_4$
Formula wt.	290.39	288.37	290.39	304.37	306.39
Crystal system	orthorhombic	monoclinic	orthorhombic	monoclinic	orthorhombic
Space group	$P2_12_12_1$	$P2_1$	$P2_12_12_1$	$P2_1$	$P2_12_12_1$
a (Å)	6.3180(4)	6.2321(3)	14.241(2)	6.2214(7)	6.335(10)
b (Å)	6.4489(5)	9.9264(6)	9.4401(9)	12.050(1)	9.4824(8)
c (Å)	38.41(3)	12.8120(18)	11.648(2)	10.888(1)	27.245(6)
α (°)	90	90	90	90	90
β (°)	90	97.079(5)	90	103.7(1)	90
γ (°)	90	90	90	90	90
Z	4	2	4	2	4
V (Å ³)	1582.5(2)	786.54(8)	1566.0(3)	795.1(1)	1636.7(5)
D_{calc} (Mg/m ³)	1.219	1.218	1.232	1.271	1.244
$F(000)$	632	312	632	328	664
2θ range	14-51	19-51	18-63	25-50	16-42
Index ranges	$0 \leq h \leq 7$ $0 \leq k \leq 7$ $0 \leq l \leq 44$	$0 \leq h \leq 7$ $0 \leq k \leq 12$ $-15 \leq l \leq 15$	$0 \leq h \leq 17$ $0 \leq k \leq 11$ $0 \leq l \leq 14$	$-7 \leq h \leq 2$ $-14 \leq k \leq 14$ $-13 \leq l \leq 13$	$0 \leq h \leq 7$ $0 \leq k \leq 10$ $0 \leq l \leq 32$
$m p$ (°C)	160-162	185-186	200-202	244-246	227-230
R_1	0.0307	0.0342	0.0305	0.0359	0.0344
wR_2	0.0891	0.0923	0.0964	0.1033	0.1042
Gof	1.05	1.073	1.074	1.073	0.982
N-total ^a	1733	1593	1722	1512	1610
N-observed ^b	1566	1435	1592	1458	913
Variables	219	216	222	228	231
$C_k^* c$	0.70	0.69	0.68	0.70	0.67

2.6.2 continued

43	81	30a	30	34	56
$C_{18}H_{26}O_4$	$(C_{18}H_{24}O_3)_{0.2}$ + $(C_{18}H_{24}O_4)_{0.7}$	$C_{19}H_{24}O_3$	$C_{21}H_{28}O_4$	$C_{21}H_{26}O_4$	$C_{19}H_{28}O_2$
306.39	299.89	300.38	344.43	342.42	288.41
orthorhombic	monoclinic	orthorhombic	orthorhombic	orthorhombic	orthorhombic
$P2_12_12_1$	$P2_1$	$P2_12_12_1$	$P2_12_12_1$	$P2_12_12_1$	$P2_12_12_1$
9.3361(7)	6.2246(7)	7.2842(6)	8.162(2)	9.854(2)	7.9475(5)
9.6261(7)	12.014(1)	13.4500(10)	9.919(2)	10.860(2)	8.3767(7)
17.764(2)	10.915(1)	16.503(2)	22.021(4)	16.524(3)	25.019(2)
90	90	90	90	90	90
90	103.09(1)	90	90	90	90
90	90	90	90	90	90
4	2	4	4	4	4
1596.5(3)	795.04(14)	1616.8(3)	1782.8(7)	1768.3(6)	1665.6(2)
1.275	1.252	1.234	1.283	1.286	1.150
664	328	648	744	736	632
13-72	14.7-17.3	16-84	7.5-22.9	7.5-21.5	15-76
$0 \leq h \leq 11$	$0 \leq h \leq 7$	$0 \leq h \leq 8$	$0 \leq h \leq 9$	$0 \leq h \leq 11$	$0 \leq h \leq 9$
$0 \leq k \leq 11$	$0 \leq k \leq 14$	$0 \leq k \leq 16$	$0 \leq k \leq 12$	$0 \leq k \leq 12$	$0 \leq k \leq 10$
$0 \leq l \leq 21$	$-13 \leq l \leq 12$	$0 \leq l \leq 19$	$0 \leq l \leq 26$	$0 \leq l \leq 19$	$0 \leq l \leq 30$
235-238	244-245	220-222	162-164	207-209	128-130
0.0305	0.0321	0.0350	0.0320	0.0371	0.0314
0.0890	0.0862	0.1005	0.0956	0.1140	0.0911
1.058	1.039	1.010	1.060	1.048	1.071
1741	1542	1603	1929	1810	1835
1631	1497	1436	1466	1097	1608
234	202	200	256	254	221
0.68	0.69	0.68	0.68	0.70	0.69

^a N-total is the total number of reflections collected.

^b N-observed is the number of reflections observed based on the criteria $F_o > 4\sigma(F_o)$.

^c C_k is the packing fraction calculated from program PLATON.

2.7 REFERENCES

1. Gavezzotti, A. *Cryst. Rev.*, **1998**, 7, 5.
2. Nangia, A., Biradha, K., Desiraju, G.R. *J. Chem. Soc. Perkin Trans. 2*, **1996**, 943.
3. Pascard, C. *Acta Crystallogr.*, **1995**, D51, 407.
4. Rosenfeld, R.E., Parthasarathy, R., Dunitz, J.D. *J. Am. Chem. Soc.*, **1977**, 99, 4860.
5. Murray-Rust, P., Glusker, J.P. *J. Am. Chem. Soc.*, **1984**, 106, 1018.
6. Klebe, G. *J. Mol. Biol.*, **1994**, 237, 212.
7. Jeffrey, G.A., Saenger, W. *Hydrogen Bonding in Biological Structures*, **1993**, Springer-Verlag, Berlin.
8. (a) Desiraju, G.R. *Acc. Chem. Res.*, **1996**, 29, 441. (b) Steiner, T. *Cryst. Rev.*, **1996**, 6, 1.
9. Sutor, D.J. *Nature*, **1962**, 68, 195.
10. Derewenda, Z.S., Lee, L., Derewenda, U. *J. Mol. Biol.*, **1995**, 252, 248.
11. Steiner, T., Saenger, W. *J. Am. Chem. Soc.*, **1992**, 114, 10146.
12. Wahl, M. C., Sundaralingam, M. *Trends Biochem. Sci.*, **1997**, 22, 97.
13. Duax, W.L., Weeks, C.M., Rhorer, D.C. In *Topics in Stereochemistry*, Eliel, E. L., Allinger, N. L. (Eds.), Wiley-Interscience, New York, **1976**, 271-383.
15. (a) Allen, F.H., Davies, J.E., Galloy, J.J., Johnson, O., Kennard, C.F., Macrae, C.F., Mitchell, E.M., Mitchell, G.F., Smith, J.M., Watson, D.G. *J. Chem. Inf. Comput. Sci.*, **1991**, 31, 187. (b) Kennard, O., Allen, F.H. *Chem. Des. Automat. News*, **1993**, 8, 1.
16. Brian, P.W., Curtis, P.J., Hemming, H.G., Norris, G.L.F. *Trans. Brit. Mycological Soc.*, **1957**, 40, 366.

17. Powis, G., Bonjouklian, R., Berggren, M.M., Gallegos, A., Abraham, R., Ashendel, C., Zalkow, L., Matter, W.F., Dodge, J., Grindey, G., Vlahos, C.J. *Cancer Res.*, **1994**, 54, 2419.
18. MacMillan, J., Simpson, T.J., Yeboah, S.K. *J. Chem. Soc., Chem. Commun.*, **1972**, 1063.
19. Trevor, J.P., Weber, H.-P., Kis, Z. *J. Chem. Soc., Chem. Commun.*, **1972**, 1061.
20. Norman, H.N., Shih, C., Toth, J.E., Ray, J.E., Dodge, J.A., Johnson, D.W., Rutherford, P.G., Schultz, R.M., Worzalla, J.F., Vlahos, C. J. *J. Med. Chem.*, **1996**, 39, 1106.
21. Haeusler, G., Schmitt, K., Blumel, P., Plochl, E., Waldhor, Th., Frish, H. *Acta Paediatr.*, **1996**, 85, 1408.
22. Rendle, D.F., Trotter, J. *J. Chem. Soc., Perkin II*, **1975**, 1361.
23. Pauling, L. in *The Nature of the Chemical Bond*, **1960**, 3rd edn., Cornell University Press, Ithaca, New York.
24. Briansó, J.L., Briansó, M.C., Piniella, J.F. *Cryst. Struct. Commun.*, **1982**, 11, 95.
25. Hrycko, S., Morand, P., Lee, F.L., Gabe, E.J. *J. Org. Chem.*, **1988**, 53, 1515.
26. Desiraju, G.R., Kashino, S., Coombs, M.M., Glusker, J.P. *Acta Crystallogr.*, **1993**, B49, 880.
27. Sarma, J.A.R.P., Desiraju, G.R. *Acc. Chem. Res.*, **1986**, 19, 222.
28. Zarges, W., Hall, J., Lehn, J.-M., Bohm, C. *Helv. Chim. Acta*, **1991**, 74, 1843.
29. (a) Desiraju, G.R. *J. Chem. Soc. Chem. Commun.*, **1990**, 454. (b) Pedireddi, V.R., Desiraju, G.R. *J. Chem. Soc., Chem. Commun.*, **1992**, 988.

30. (a) Steiner, T., Lutz, B., van der Maas, J., Schreurs, A.M.M., Kroon, J., Tamm, M. *Chem. Commun.*, 1998, 171. (b) Steiner, T., Desiraju, G.R. *Chem. Commun.*, 1998, 891.
31. Steiner, T. *Chem. Commun.*, 1994, 2341.
32. Duax, W.L., Griffin, J.F. Ghosh, D. In *Structure Correlation*, 1994, Volume 2, Bürgi, H.-B., Dunitz, J.D., (Eds.), VCH, New York, pp 605-633.
33. (a) Andrade, L.C.R., Paixao, J.A., de Almeida, M.J., Tavares da Silva, E.J., Sa e Melo, M.L., Campos Neves, A.S. *Acta Crystallogr.*, 1997, C53, 938. (b) Ramos Silva, M., Paixao, J.A., de Almeida, M.J., Tavares da Silva, E.J., Sa e Melo, M.L., Campos Neves, A. S. *Acta Crystallogr.*, 1996, C52, 2892.
34. (a) Duax, W.L., Norton, D.A. *Atlas of Steroid Structure*, 1975, Volume 1, Plenum, New York. (b) Griffin, J.F., Duax, W.L., Weeks, C. M. *Atlas of Steroid Structure*, 1984, Volume 2, Plenum, New York.
35. Busetta, B., Comberton, G., Courseille, C., Hospital, M. *Cryst. Struct. Commun.*, 1972, 1, 129.
36. (a) Smith, L.L. *Cholesterol Autooxidation*, 1981, Plenum, New York and the references therein. (b) Tichler, M., Ayer, S.W., Andersen, R.J., Mitchel, J.F., Clardy, F. *Can. J. Chem.*, 1988, 66, 1173.
37. Covey, D.F., Hood, W.F. *Endocrinology*, 1981, 108, 1597.
38. Numazawa, M., Tachibana, M. *Steroids*, 1994, 59, 579 and the references therein.
39. Swenson, D.C., Duax, W.L., Numazawa, M., Osawa, Y. *Am. Cryst. Assoc.*, 1980, Ser. 2, 7, 12.
40. Guarna, A., Occhianti, E.G., Machetti, F. *J. Med. Chem.* 1997, 40, 3466.
41. Lawrence, W.D., Osawa, Y.M., Davis, P.J., Blas, S.D. *Endocrinology*, 1986, 119, 2803.

42. (a) Coiro, V.M., Giglio, E., Lucano, A., Puliti, R. *Acta Crystallogr.*, **1973**, B29, 1404. (b) Peck, D.N., Langs, D.A., Eger, C., Duax, W.L. *Cryst. Struct. Commun.*, **1974**, 3, 573.
43. Norton, D.A., Lu, C.T., Campbell, A.E. *Acta Crystallogr.*, **1962**, 15, 1189.
44. (a) Kitaigorodskii, A.I. *Organic Chemical Crystallography*, **1961**, Consultant's Bureau, New York. (b) Kitaigorodskii, A.I. *Molecular Crystals and Molecules*, **1973**, Academic Press, New York.
45. (a) Kalman, A., Parkanyi, L., Argay, G. *Acta Crystallogr.*, **1993**, B49, 1039. (b) Kalman, A., Parkanyi, L. *Advances in Molecular Structure Research*, **1997**, 3, 189.
46. (a) Berkovitch-Yellin, Z., Leiserowitz, L. *Acta Crystallogr.*, **1984**, B40, 159. (b) Shimon, L.J.W., Vaida, M., Addadi, L., Lahav, M., Leiserowitz, L. **1990**, 112, 6215.
47. Steiner, T., Koellner, G., Gessler, K., Saenger, W. *J. Chem. Soc., Chem. Commun.*, **1995**, 511.
48. Duax, W.L., Strong, P.D. *Steroids*, **1980**, 34, 501.
49. Duax, W.L., Strong, P.D. *Cryst. Struct. Commun.*, **1979**, 8, 655.

CHAPTER 3

MODEL RECEPTOR SURFACE AND QSAR EVALUATION OF 2-OXASTEROIDS

Contents

3.1 INTRODUCTION

3.1.1 Aromatase Inhibitors and Drug Design Strategies

3.1.2 Model Receptor Surfaces

3.1.3 Comparative Molecular Field Analysis (CoMFA) or 3D QSAR

3.2 MOLECULAR MODELING

3.3 RESULTS AND DISCUSSION

3.3.1 Model Receptor Surfaces

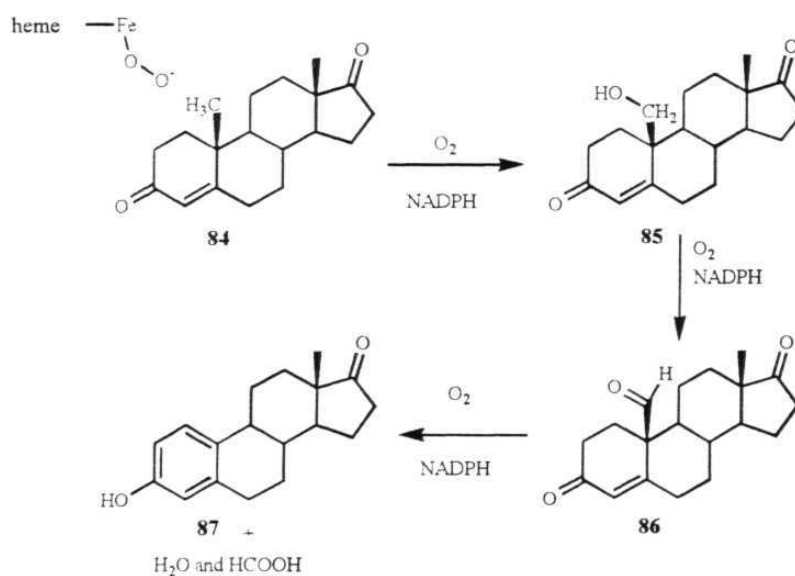
3.3.2 3D QSAR

3.4 REFERENCES

3.1 INTRODUCTION

3.1.1 Aromatase Inhibitors and Drug Design Strategies

Estrogens (**87**) are biosynthesised from androgens (**84**) with the removal of C19-methyl group and subsequent aromatisation of the A-ring.¹ Aromatase is the enzyme that catalyses the conversion of androgens and estrogens in three sequential steps in the presence of molar equivalents of NADPH and O₂ (Scheme 1).² Estrogen production via the aromatase pathway is important for growth, reproduction and development but is also known to cause malignant tumors, like breast cancer.³



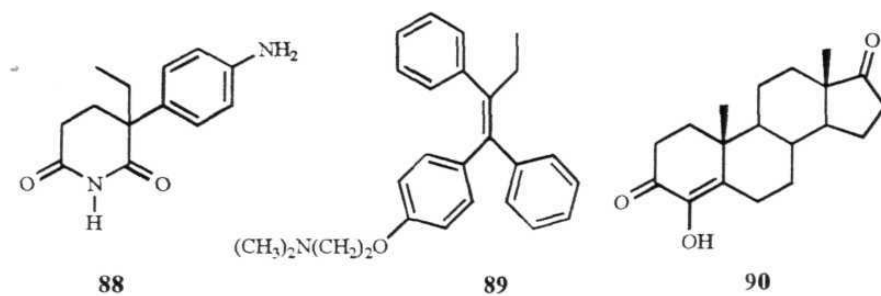
Scheme 1. Mechanism for conversion of androstenedione to estrone.

Aromatase inhibitors constitute a logical approach in the therapy of estrogen-dependent malignancies, since they block endogenous estrogen formation.⁴ Both steroidal and nonsteroidal compounds have been developed as aromatase inhibitors. Aminoglutethimide **88** is one of the early and important non-steroidal aromatase inhibitors developed as a drug against metastatic breast and prostate

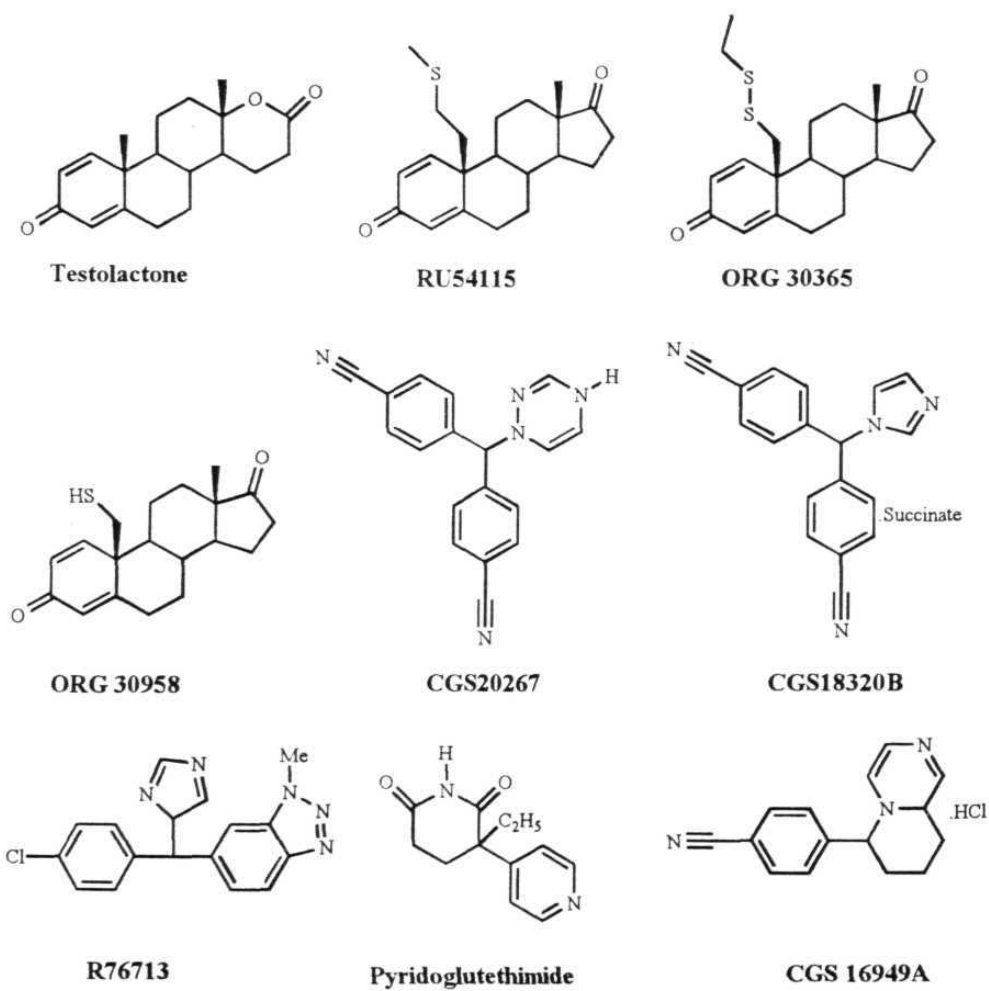
cancer.⁵ Tamoxifen **89**, a stilbene derivative is an antiestrogen to combat breast cancer. In clinical trials, 4-hydroxyandrost-4-ene-3,17-dione (**90**) is shown to be effective against tumors which are resistant to tamoxifen **89**.³ Some important steroidal and non-steroidal aromatase inhibitors which are in clinical trials⁶ are shown in Scheme 3.

Aromatase is a membrane-bound cytochrome P450 protein which requires detergent treatment for solubilisation. Crystallisation of aromatase is difficult and its three dimensional crystal structure has so far not been determined. The crystal structure of cytochrome P450_{cam} (camphor hydroxylase), a soluble bacterial protein isolated from *Pseudomonas putida*, has been determined to a high resolution (1.63 Å) and shows some similarity in the amino acid sequence with aromatase, the P450 enzyme.⁷ Based on the P450_{cam} crystal structure, models for aromatase were proposed⁸ but they failed⁹ to correctly identify the residues in the binding site. Since the exact structure of aromatase binding site is not fully understood, present-day synthetic efforts are based on trial and error methods.

The contemporary drug-design strategy involves different methods of mapping the 3D structure of the binding site.¹⁰ In the absence of crystallographic data or a model active site developed from related structures, the 3D crystallographic data of the ligands that are known to bind to the receptor can be used to map the receptor surface. The binding affinities of a series of ligands to a particular receptor protein are known for a number of ligand-receptor complexes and such relationships can be used to develop QSAR (quantitative structure-activity relationship) equations. QSAR studies have been reported for steroidal as well as non-steroidal aromatase inhibitors.^{9,11} A hypothetical model of the receptor site can be built by using a combination of QSAR data and ligand characteristics.



Scheme 2. Early-used inhibitors of aromatase.



Scheme 3. Aromatase inhibitors in clinical trials.

3.1.2 Model Receptor Surface

A Model Receptor Surface (MRS) provides a framework for representing the receptor active site in a nonatomistic fashion based on the principle of steric and electrostatic complementarity between the shape and properties of the receptor and the ligands that bind to it.¹² The surface is represented as a set of points organised in a triangular mesh which stores the information about different properties. Receptor surface models represent essential features of the active site while the pharmacophore models are generated by finding the chemically important functional groups that are common to the ligands.

A set of chemically homogeneous, active molecules are selected, aligned and the steric surface generated that encloses all the molecules. There are many techniques of aligning molecules and an error in the alignment step can lead to a bad model. The shape mapped by the active molecules is assumed to be complementary to the shape of the receptor. There are many functions which can be used to create a shape field around the aligned molecules, the common ones being van der Waals field function and Wyvill field function. In the former, the atom position of the aligned molecules are clearly defined and the surface so generated is considered to be tight and non flexible. In the Wyvill field method, the surface is smoother and contours of individual atoms are smoothened out. While generating the receptor, the charge complementarity between the molecules and the receptor can also be varied as electrostatic charge or potential charge. The generated receptor surface contains the molecular surface and chemical properties which include partial charge, electrostatic potential, hydrogen bonding propensity and hydrophobicity.¹² The scalar property for each of these can be calculated, stored and visualised by different colours. The intensity of the colour on the surface corresponds to the magnitude of the property. Once the receptor surface is generated, several energetics can be computed that are based on the nonbonded

interactions between ligand and the receptor model. Four important energy descriptors are: $E_{\text{interaction}}$, E_{inside} , E_{relax} and E_{strain} . The first term indicates the sum of the van der Waals and electrostatic energies. The second descriptor is the strain energy (enthalpy) of the ligand (molecule) inside the model receptor surface. E_{relaxed} is the energy of the molecule after minimising in the receptor site. Since the minimised molecules are close to the energy minima relative to the receptor bound conformation, E_{relaxed} is always less than or equal to E_{inside} . The final descriptor, E_{strain} is the difference between E_{inside} and E_{relaxed} . These descriptors represent the energy components of binding of ligands in the putative receptor site and can be used for QSAR modeling in cases where the activity is correlated with binding energies.

3.1.3 Comparative Molecular Field Analysis (CoMFA) or 3D QSAR

QSAR calculates the 2D and 3D spatial, electronic, fragment, topological, thermodynamic, conformational, and shape properties, and statistically analyses relationships between molecular structures and the descriptors to provide correlations for predicting biological activity.¹³ Statistical methods are an essential component of QSAR to build models, estimate their predictive ability, and find relationships and correlations among variables and activities. Comparative molecular field analysis (CoMFA) is a 3D QSAR approach that computes the steric and electrostatic interactions of a series of molecules with a receptor surface. The statistical techniques in CoMFA studies are partial least squares (PLS), principle component analysis (PCA) and genetic function approximation (GFA). Many of these regression techniques generate a single model or relatively small number of models, but GFA produces a large population of models. This is carried out by repeatedly performing the genetic crossover operation to combine the terms of the better performing models. The validity of QSAR equations generated can be

tested by a cross validation term (r^2) which is defined in terms of original activity versus predicted activity. The goodness of the model is estimated by the value of r^2 being closer to unity.

$$r^2 = 1 - \frac{PRESS}{SD}$$

$$\text{where } PRESS = \sum_i^N (Yp - Ya)^2 \text{ and } SD = \sum_i^N (Ya - Ym)^2$$

In the above equation, *PRESS* is the sum of squared deviations between the predicted (*Yp*) and measured (actual, *Ya*) biological activity values for all *N* molecules in the set, and *SD* is the sum of squared deviations between measured biological activity values of the training set and the mean (*Ym*) activity values for all *N* molecules.

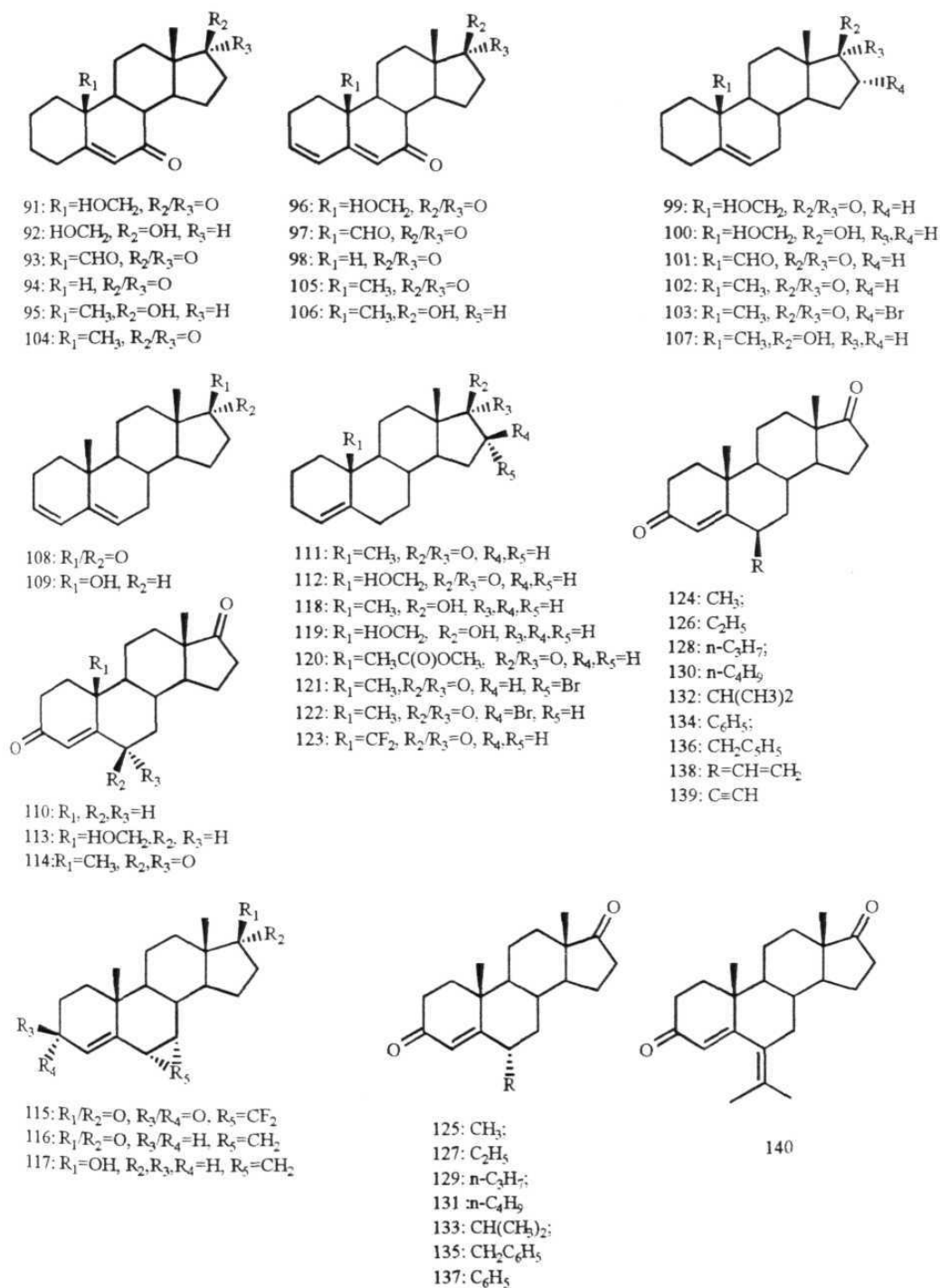
Numazawa *et al.*¹⁴ have characterised analogues of androstenedione as reversible and irreversible inhibitors of human aromatase. Oprea and Garcia⁹ developed a 3D QSAR model using the androstenedione derivatives of Numazawa *et al.*¹⁴ The 2-oxasteroids synthesised (Chapter 1) and described in this thesis are analogues of androstenedione with C2 being replaced by an O-atom, that is the A-ring functionality is a lactone instead of a ketone. In our computational studies, the parameters and molecules of Oprea and Garcia⁹ were used to generate the model receptor surface and to evaluate the interaction energy with 2-oxasteroids. The final interaction energies of the 2-oxasteroids with the putative receptor should provide information about the influence of chemical and conformational changes on ligand-receptor binding. Using the interaction energies obtained for the *training set* (a set of molecules used to generate the model) as 3D descriptors along with

other molecular descriptors, the 3D QSAR equation was generated to evaluate the activity of the heterosteroids.

3.2 MOLECULAR MODELING

All computations were performed on a Silicon Graphics Indigo/R4400 workstation running under the IRIX 6.2 operating system. The relevant modules were accessed from Version 3.7 of the *Cerius*² program. The set of 50 compounds used in this study as competitive inhibitors of aromatase are shown in Scheme 4.

Molecular geometries were determined starting from closely related crystal structures derived from the CSD or from our own structures described in Chapter 2. Each steroid structure was optimised with the MOPAC 6.0 program (MNDO Hamiltonian, using eigenvector following Minimiser). Alkyl and aryl chains were modeled in the all-*trans* extended conformation. Since the side chains are modeled in the all-*trans* conformation, there is little variation during minimisation. The conformational flexibility of the tetracyclic steroid skeleton is minimal.¹³ Therefore, an exhaustive conformational search of the molecules was not carried out prior to alignment. The rules followed for alignment was the rigid-body, least-squares fitting of all the common heavy atoms (carbons, oxygens) in the tetracyclic steroid skeleton (17-atom model) or the B-, C-, D-ring system (13-atom model) of each molecule to those in 3-deoxy- Δ^4 -androstene-17-one (steroid 111 in Scheme 4). Although, the 17-atom model is reported to be better,⁹ we used both the methods. All the 50 prealigned molecules were used to build the model (Figure 1). Different model receptor surfaces were generated for the 17-atom as well as the 13-atom models, using van der Waals surface or Wyvill soft surface criteria in combination with electrostatic or partial charge complementarity. So a total of eight models were developed for the two sets of prealigned molecules (Table 1).



Scheme 4. 50 training set steroid structures used in this study.

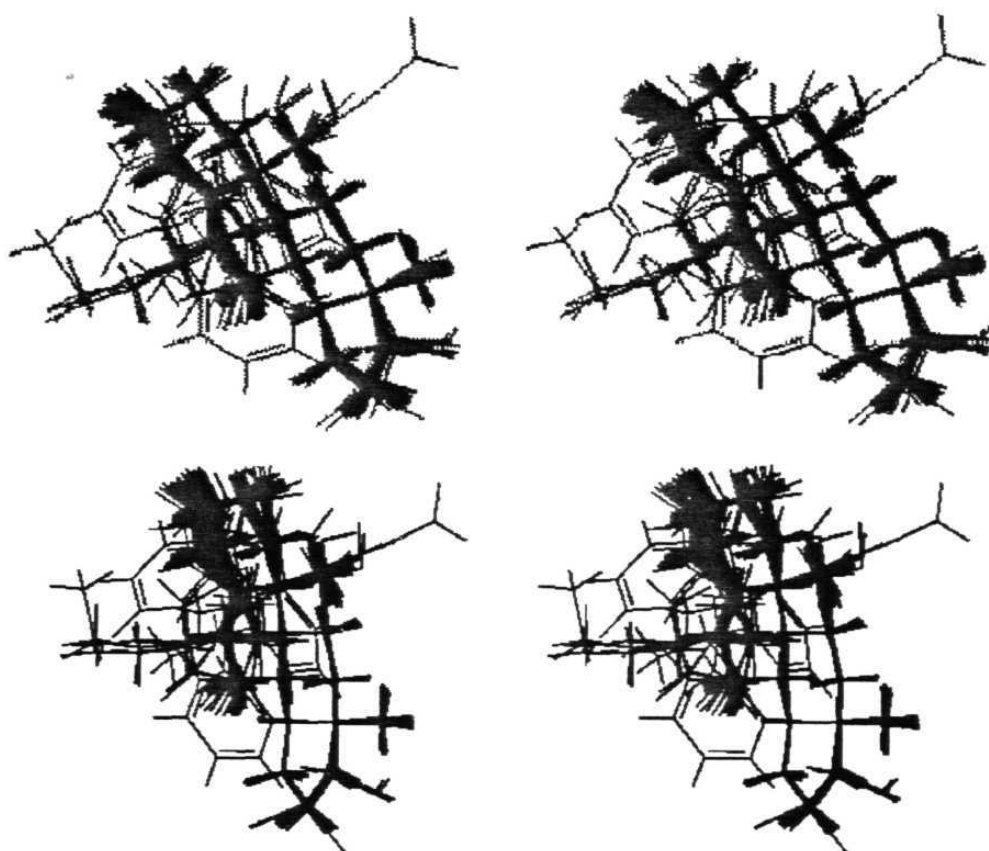
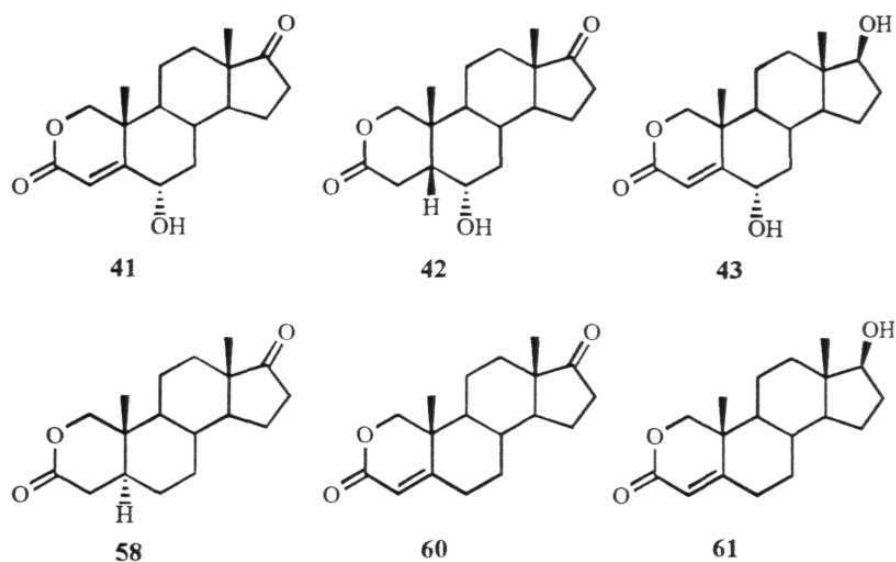


Figure 1. Stereoview of the overlay plots of 50 molecules with 17-atom (above) and 13-atom (below) models. The spatial distribution of the A-ring atoms in the latter case is spread out.

The method of minimisation and alignment followed for the six 2-oxasteroids (Scheme 5), whose crystal structures were discussed in Chapter 2, is the same as that for the training set molecules. The six 2-oxasteroids prealigned by the 17-atom and 13-atom methods are shown in the Figure 2 and their energy of interaction with different model receptor surfaces is shown in Table 1.



Scheme 5. 2-Oxasteroids evaluated for the Model Receptor Surface.

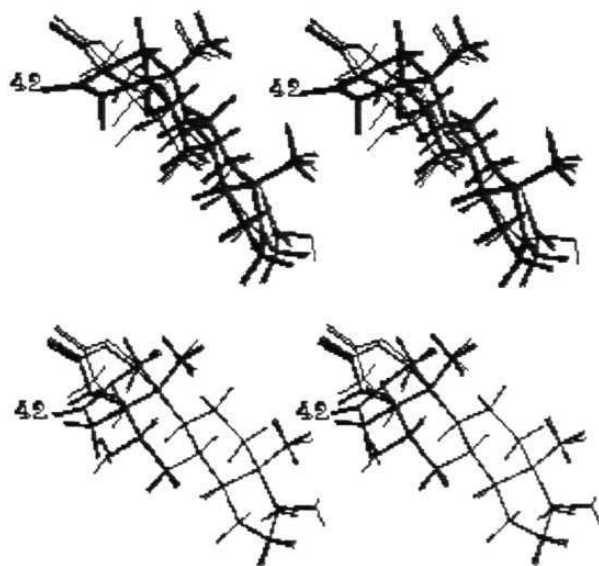


Figure 2. Overlay plot of 2-oxasteroids with 17-atom (upper stereopair) and 13-atom model (bottom stereopair). Note the relative position of the 3-keto and 6-hydroxy groups in the 5 β -steroid 42 (marked in the figure). In the 13-atom model, the B-, C- and D-rings are tightly bunched compared to the 17-atom model.

Table 1. Energy of interaction, E_{interact} of 2-oxasteroids with different model receptor surfaces generated with 50 molecules.

s t e r o i d	17 atom model				13 atom model			
	van der Waals surface		Wyvill surface		van der Waals surface		Wyvill surface	
	Pc	Ec	Pc	Ec	Pc	Ec	Pc	Ec
41	-5.11	-6.98	-6.18	-3.97	-5.99	-3.93	-3.40	-2.59
42	147.76	150.77	-2.33	-0.86	41.04	42.81	41.05	42.81
43	-7.62	-5.17	-3.49	-2.63	-3.39	-2.59	-6.03	-3.94
58	-7.57	-6.86	-6.21	-4.02	-5.75	-3.88	-5.76	-3.88
60	-5.40	-6.95	-6.19	-3.98	-6.03	-3.94	-3.70	-2.69
61	-7.60	-5.31	-3.74	-2.70	-3.70	-2.69	-5.99	-3.94

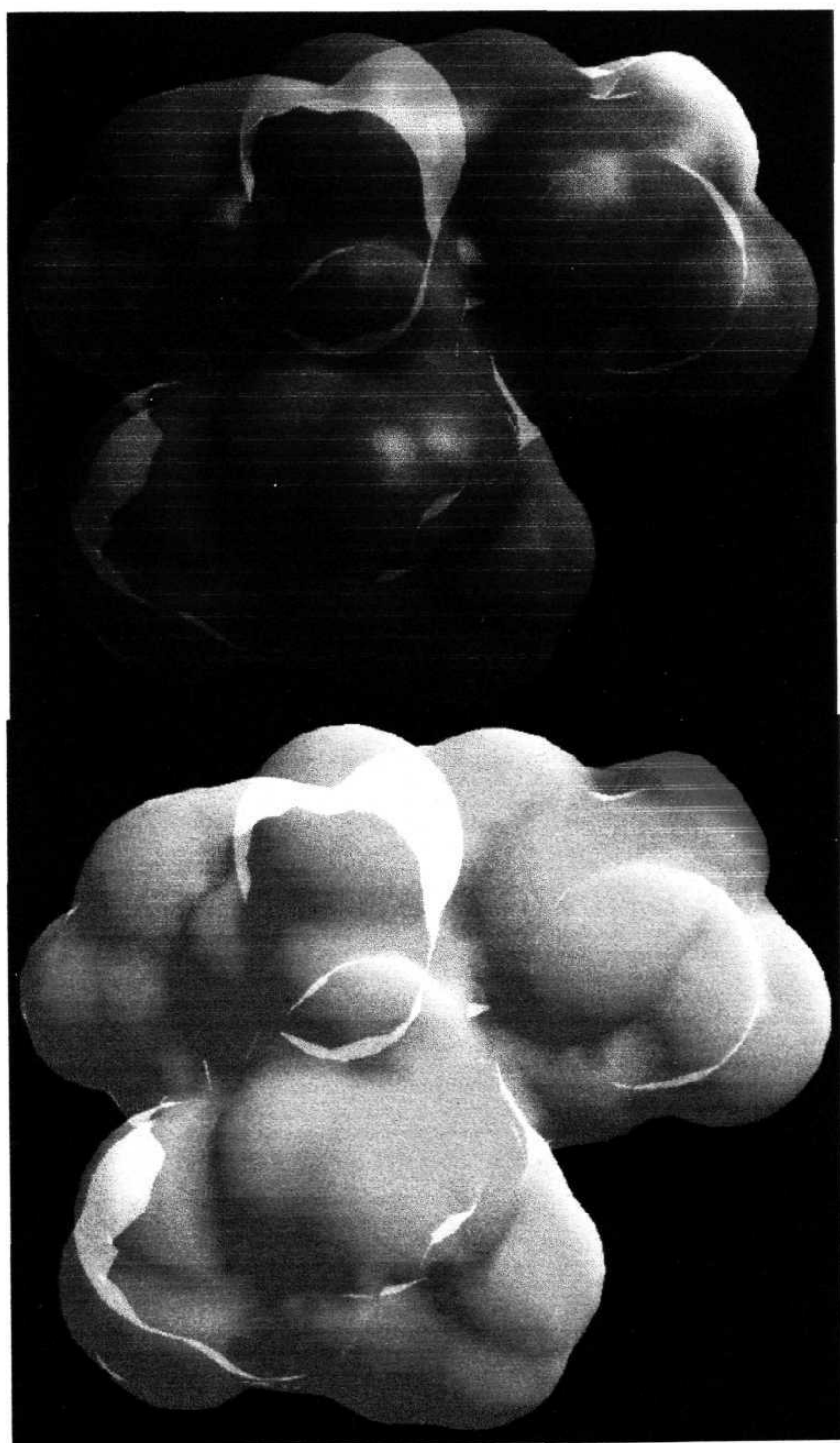
Pc: Partial charge complementarity; Ec: Electrostatic charge complementarity.

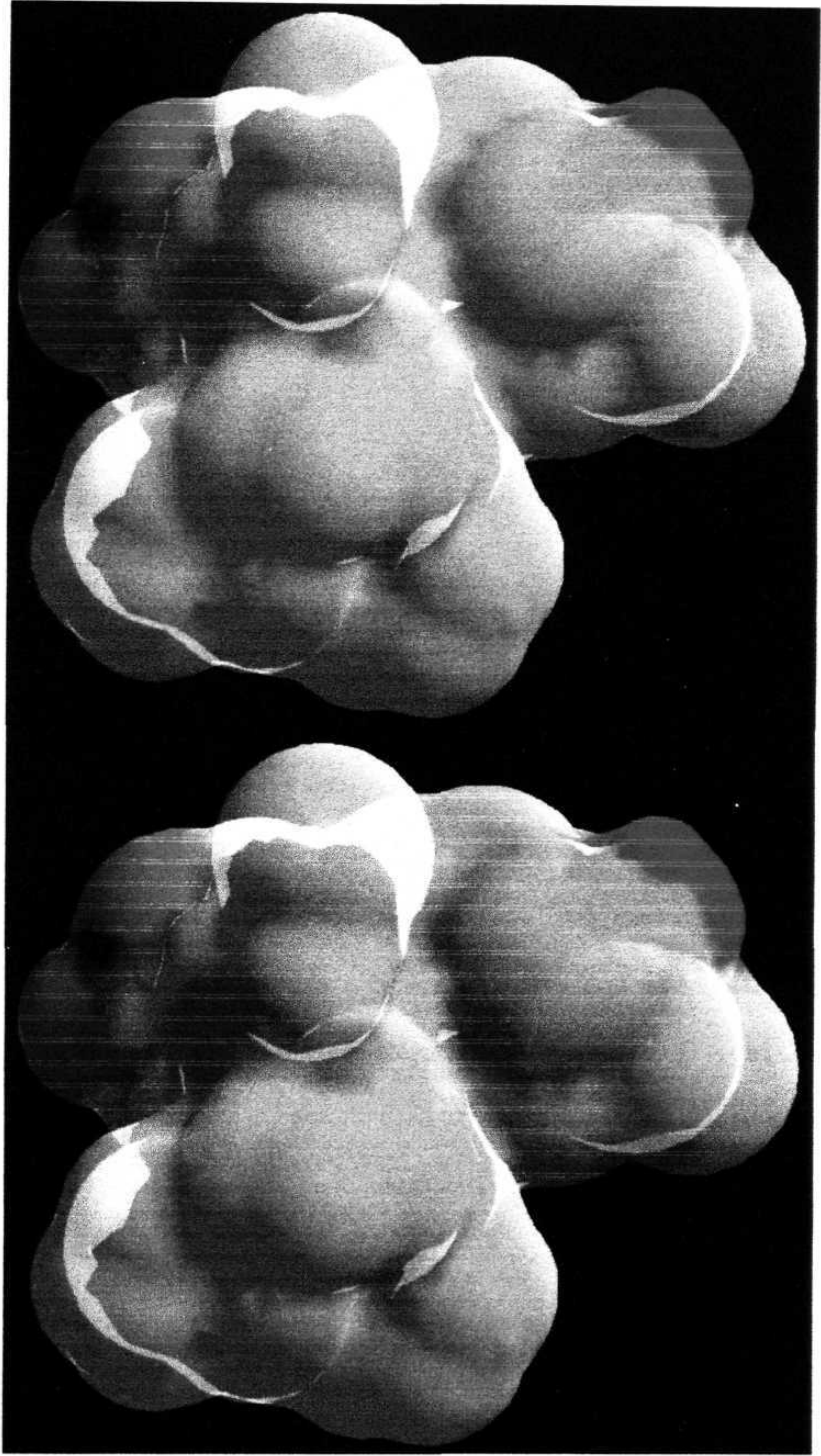
3.3 RESULTS AND DISCUSSION

3.3.1 Model Receptor Surfaces

All the receptor surfaces generated for the training set steroids have large hydrophobic areas, indicated by brown colour (Figure 3a), and electrostatic interactions in the region of O3 and O17, shown in magenta for attractive and green for repulsive (Figure 3b). The E_{interact} for the training set molecules varies between -5.5 to -8.0 Kcal/mmol with the receptor surface generated using 17-atom model and van der Waals surface with partial charge complementarity. The E_{interact} for the six 2-oxasteroids with different model receptors is summarised in Table 1. Examination of the receptor surface with 2-oxasteroid ligands for E_{interact} is green the vicinity of O2 (Figure 4a) indicating that the newly introduced O-heteroatom has an unfavourable interaction with the receptor surface. However, if the total interaction energy (electrostatic + hydrophobic) between ligand and receptor is considered, large parts of the surface that were featureless (grey in Figure 4a) are now attractive, as indicated by large patches of magenta colour

(Figure 4b). Table 1 shows that the interaction energies are comparable to the natural steroids except for the 6 α -hydroxy-5 β -lactone **42**. The fact that the interaction energies for oxasteroids are in the range observed for the training set molecules suggests that the chemical change of C2 methylene to an O-atom has little effect on the overall binding. The interaction of 2-oxasteroids with the receptor using Wyvill force field is similar (Figure 5a) though the surface is more smooth compared to that in Figure 3a. The Wyvill surface of the receptor evaluated with the six oxasteroid ligands, shown in Figure 5b, is a visual representation of the E_{interact} values in the Table 1. Because of the β -configuration at C5, the A-ring is bent by an angle of 81.7° with respect to the B/C/D ring mean plane (discussed in Chapter 2, section 2.2.3) towards the α -face of the steroid (Figure 2). Such a bend at the A/B-ring junction creates a large repulsive contact for the 5 β compound with the receptor surface and hence the E_{interact} term is large for this molecule compared to the other five ligands (Table 1, steroid **42**). The surfaces generated by the 13-atom model have a large diffused volume in the A-ring region and therefore the energy of interaction for the 5 β -steroid **42** is less repulsive compared to that observed in the 17-atom model case (Table 1). The energy difference for the other molecules is too small to attribute to a specific chemical or structural effect.





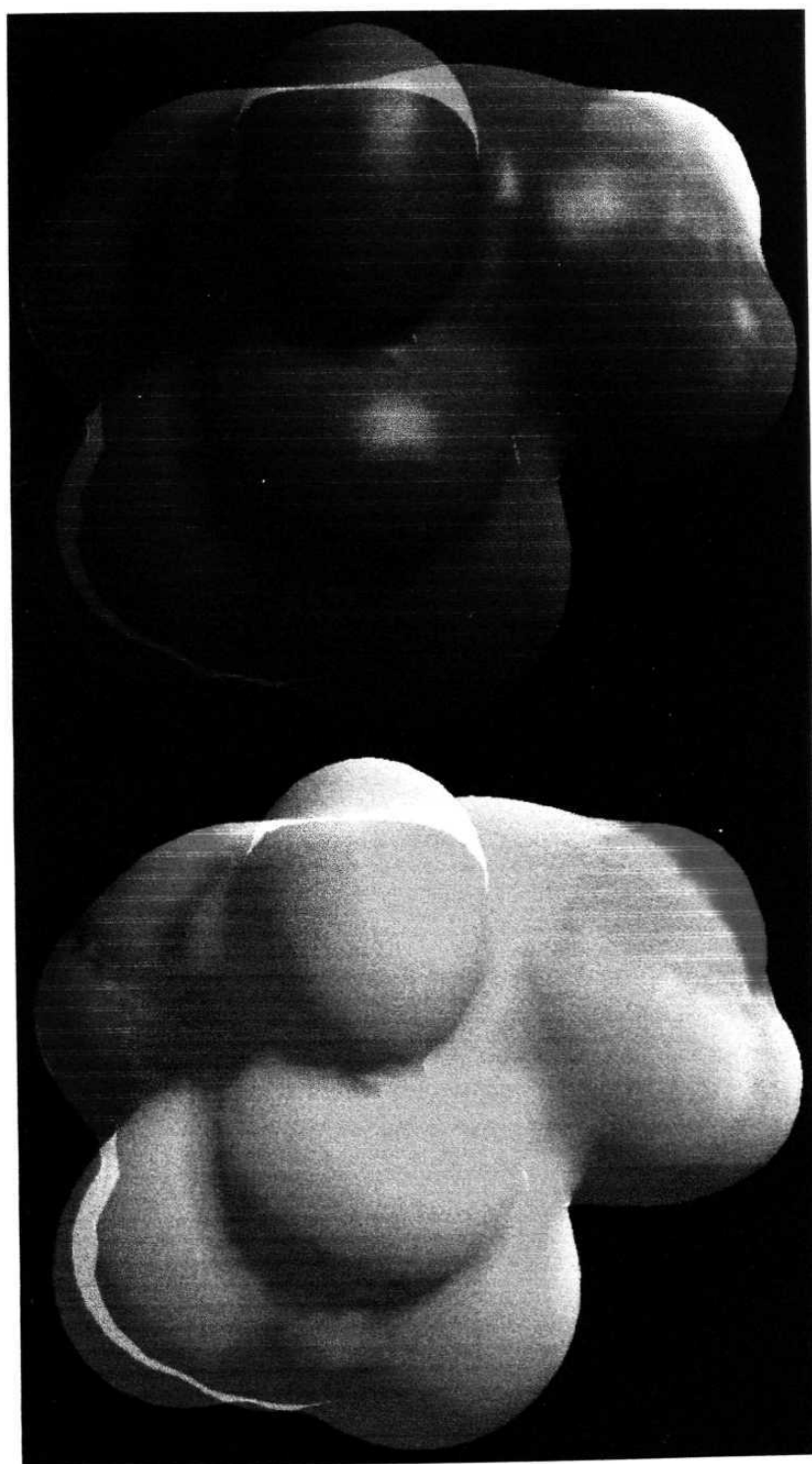


Figure 3. Receptor surfaces generated with the 17-atom model using van der Waals force function and electrostatic complementarity criteria. Note the well-defined shapes around functional groups. The top figure shows the hydrophobic property of the surface and the bottom figure shows the electrostatic interaction of the 50 training set molecules with the receptor surface.

Figure 4. Receptor surfaces generated with the 17-atom model using van der Waals function and electrostatic complementarity criteria showing the coloured representation of the energy of interaction (top) and total binding energy (bottom) with the six 2-oxasteroids.

Figure 5. Receptor surfaces generated with the 17-atom model using Wyvill function and electrostatic complementarity criteria. Notice that the surfaces in this case are smoother compared to those in Figures 3 and 4. The brown contour displays the hydrophobic property of the surface (top) and the bottom contour shows the energy of interaction of the six 2-oxasteroid ligands with the receptor.

The structure-activity relationship studies of Numazawa *et al.*¹⁵ suggest that substitution of a hydrophobic group at C6 enhances biological activity (Scheme 4). Due to C6 substituents, present in about half of the training set molecules, the resulting receptor surface has a large volume in the region of C6 (Figures 3 and 4). When the 2-oxasteroid ligands are evaluated, the electrostatic and hydrogen bonding OH group at C6 is too small compared to the groups present in the training set molecules and hence it is unable to find complementary groups on the receptor surface within bonding distance. Consequently, analysis of the oxasteroid ligands by the 17-atom and 13-atom models is unable to identify a relationship between the chemical nature of the steroid and binding energy with the receptor. In order to overcome this shortcoming in the present model, steroids with substitutions at C6 were excluded from the training set and a subset of 27 steroids in Scheme 4 (91, 92, 95-114, 118, 119, 121, 122 and 123) used to generate the 17-atom and 13-atom model surfaces. These receptors were evaluated against the six 2-oxasteroids and the results are summarised in Table 2.

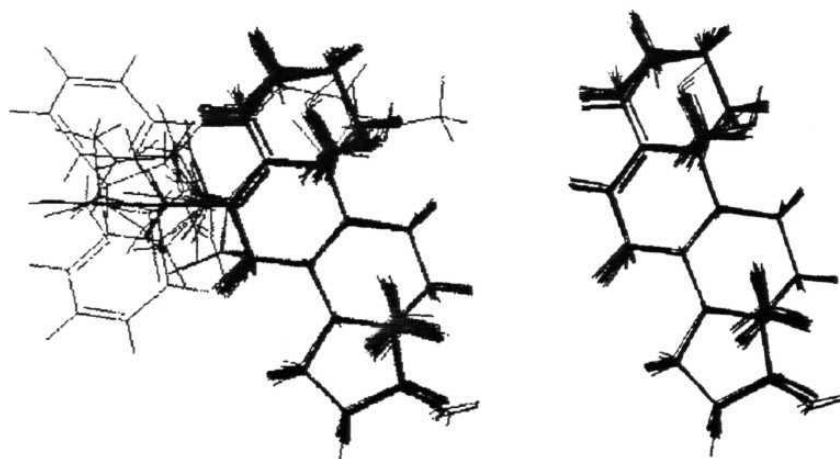


Figure 6. Overlay plots of the molecules in the training set of 50 (left) and 27 (right) molecules. Notice the large substitutions at C6 in the former case.

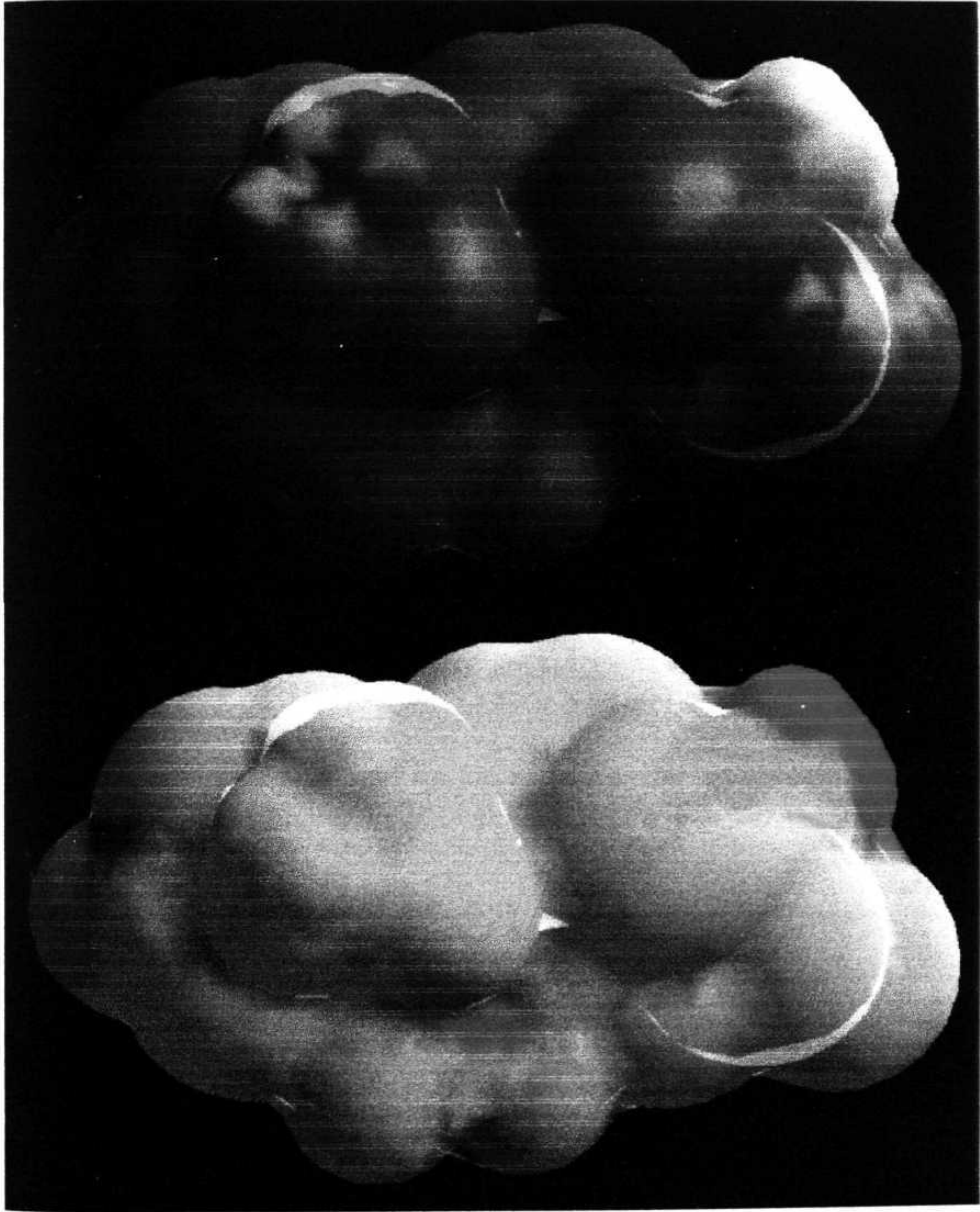


Figure 7. Receptor surfaces generated with the 17-atom model using 27 training set molecules (devoid of C6-substituent), van der Waals force function and electrostatic complementarity criteria. The top figure shows the hydrophobic property of the surface and the bottom contour shows the electrostatic interaction of the six 2-oxasteroids with the receptor surface. Notice that the region in the vicinity of C6 is somewhat repulsive (green) compared to that in Figure 4a.

Table 2. Energy of interaction, E_{interact} of the 2-oxasteroids with model receptor surfaces generated using 27 training set molecules.

s t r o i d	17 atom model				13 atom model			
	van der Waals surface		Wyvill surface		van der Waals surface		Wyvill surface	
	Pc	Ec	Pc	Ec	Pc	Ec	Pc	Ec
41	4663656.12	466419.62	357.63	359.41	42474.40	42424.71	155.84	157.67
42	757.14	758.90	8.74	10.08	3413.49	3413.47	-0.33	0.27
43	29057.14	29594.51	4.60	5.19	5123.47	5123.44	--- ^a	--- ^a
58	-8.25	-5.36	-5.92	-4.03	-3.82	-3.83	-5.86	-4.02
60	-8.25	-7.26	-5.73	-3.89	-8.27	-8.27	-6.85	-3.97
61	-6.50	-5.81	-3.69	-2.77	-6.30	-6.28	-3.70	-2.80

Pc: Partial charge complementarity, Ec: Electrostatic charge complementarity.

a: The repulsive energy value is too large for the program to handle.

The 27-molecule model receptors show that the 6-hydroxy oxasteroids **41-43** have large positive E_{interact} values indicating that the interaction with these ligands is repulsive, presumably due to the C6-substituent (Table 2). The variation in E_{interact} for the 6-hydroxy steroids (**41-43**) can be attributed to differences in conformation and intermolecular interactions in the remaining structure. The data in Table 2 suggests that the 6-hydroxy group forms a repulsive contact with the receptor but the 17-hydroxy functional group in these steroids stabilises binding with the receptor. This is revealed by the presence of repulsive contacts in the

vicinity of C6 (Figure 7b) which are absent in the model generated with 50 training set molecules (Figure 4a). Thus, the receptor is over-constrained for the diverse oxasteroid ligands to be evaluated when generated with selected 27-molecules training set.

3.3.2 3D QSAR

Two sets of 3D QSAR equations were derived, one with 50 training set molecules and the other with 27 molecules that are devoid of C6 hydrophobic groups. Since the free energy of binding, ΔG is proportional to the binding affinity, $-\log K$ ($\Delta G \approx 1.4$ pK, in Kcal/mol) and QSAR analyses are based on the formalism of linear free-energy relationships, the biological activities of the 50 steroids expressed in μM were converted to $\log_{10}(1/K_i)$ scale (Table 3). 3D QSAR equations were generated using the original activity as the dependent variable and the model receptor energy and other molecular descriptors as independent variables. The equations generated by genetic function approximation (GFA) statistical method were found to be better, and so these equations are discussed further. It was also noted that equations generated using the receptor energy descriptors from Wyvill force field have better predictive power.

Of the two sets of equations generated using 17-atom model receptor energies on 50 and 27-molecule training sets, the 27-molecule model was found to have a better correlation based on the r^2 criteria (0.710 and 0.767). The original and predicted activity for the above two QSAR equations derived using the van der Waals and Wyvill force fields are displayed in Figures 8 and 9. Table 4 shows the predicted activity for the 2-oxasteroids using the two 3D QSAR equations. These values are comparable to the training set molecules displayed in Table 3. With the

limited data, it is difficult to correlate predicted activity with chemical or molecular features of the 2-oxasteroid molecules.

Table 3. Activities of the 50 training set molecules used in QSAR equation generation.

Compound	pKi	Compound	pKi	Compound	pKi
91	-1.0414	108	1.2366	125	2.2518
92	-1.6532	109	-0.3010	126	2.8539
93	-1.1139	110	0.8539	127	2.3279
94	-0.3802	111	1.8861	128	2.3372
95	-0.7404	112	1.9031	129	2.1739
96	-1.1761	113	0.5961	130	2.0555
97	-0.2553	114	1.5870	131	1.9208
98	-0.4771	115	1.3010	132	1.6576
99	0.0000	116	2.3010	133	1.5086
100	-0.9912	117	0.9209	134	1.4318
101	-0.1461	118	0.0809	135	1.6778
102	0.9208	119	0.7696	136	1.2007
103	-1.0414	120	0.5391	137	2.0000
104	0.6021	121	0.6421	138	2.2924
105	0.6576	122	0.3420	139	1.2076
106	-0.7243	123	0.3536	140	2.3098
107	-0.4771	124	1.9586		

Table 4. Predicted activities of the 2-oxasteroids.

Compound	50 molecule training set	27 molecule training set
41	0.210	2.325
42	1.271	3.650
43	2.520	2.594
58	2.654	2.635
60	0.722	1.317
61	0.937	2.006

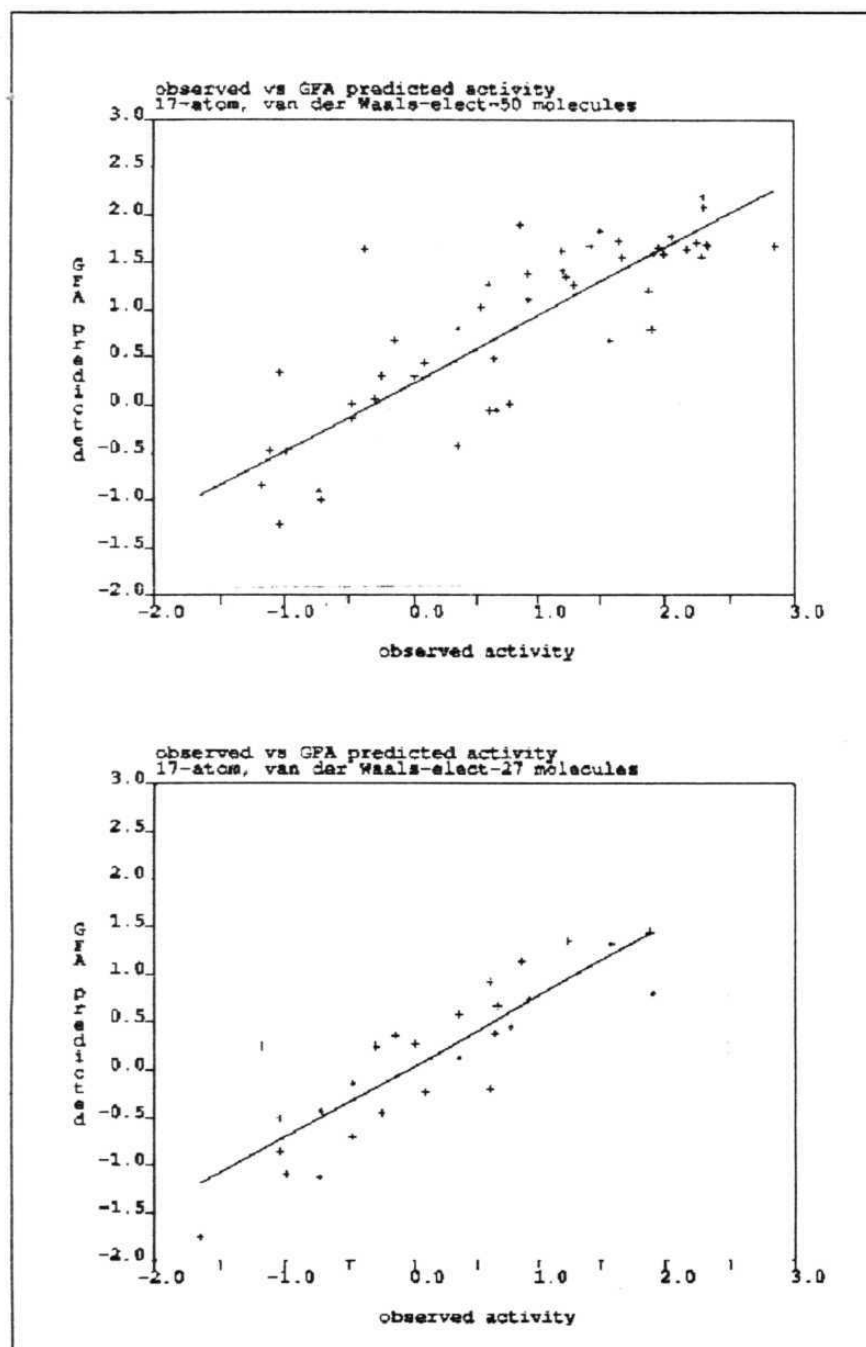


Figure 8. Plots of observed vs GFA predicted activities 50 (top) and 27 (bottom) molecule training sets with van der Waals force field and electrostatic potentials. The slope indicates the goodness of fit of each equation.

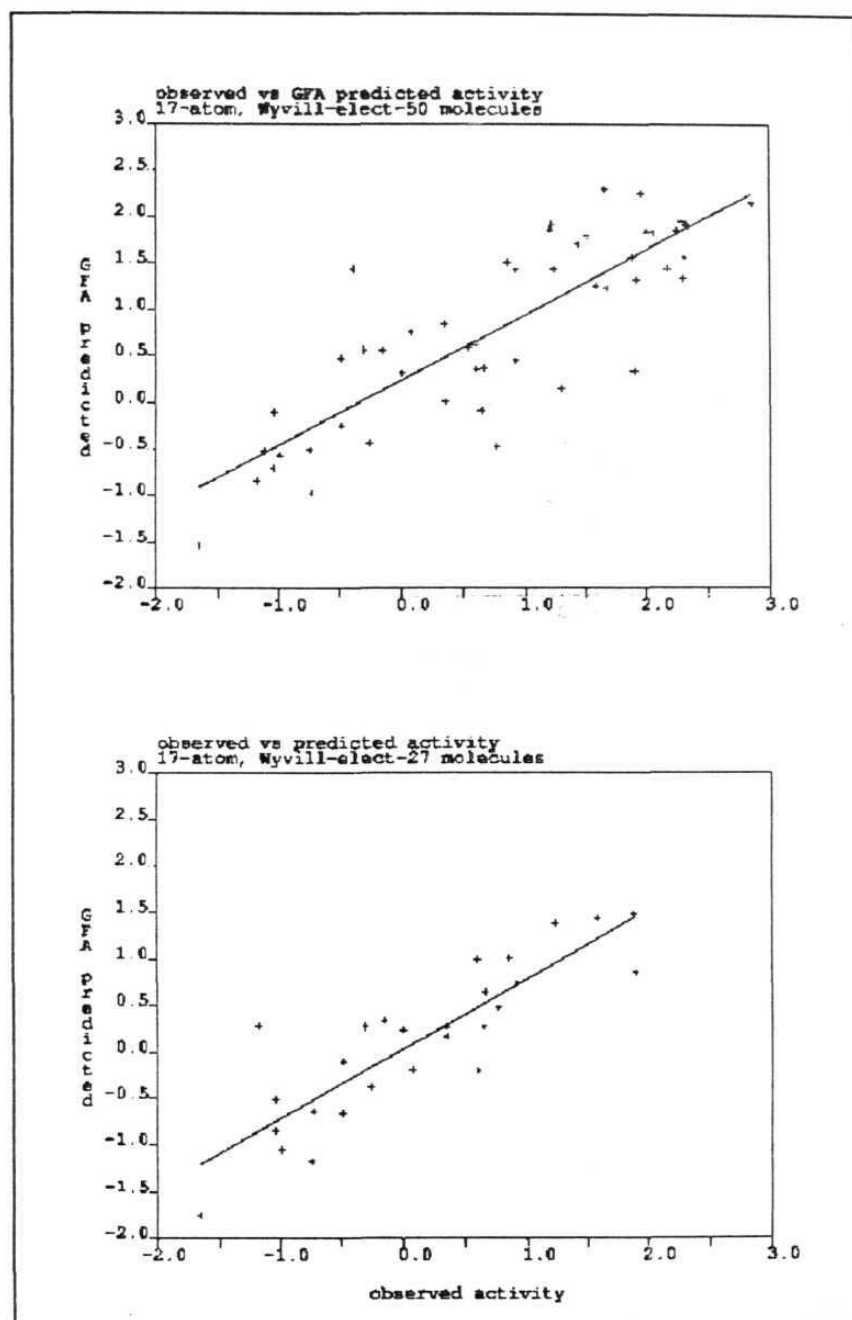


Figure 9. Plots of observed vs GFA predicted activities 50 (top) and 27 (bottom) molecule training sets with Wyvill force field and electrostatic potentials. The slope indicates the goodness of fit of each equation.

3.4 REFERENCES

1. Ganong, W.F. *Review of Medical Physiology*, 1993, Edition 16, Appleton and Lange, Morwalk, CT, 780.
2. Killis, J.J., Vikery, L.E. *J. Mol. Biol.*, 1987, 262, 4413.
3. Brodie, A.M.H. *J. Steroid Biochem. Mol. Biol.*, 1994, 45, 281.
4. Hervey, H.A., Lipton, A., Santen, R.J. *Cancer Res. (Suppl.)*, 1982, 42, 3261.
5. Strobl, J.S., *Modern Pharmacology*, 1994, Edition 4, Craig, C.R., Stitzel, R.E. (Eds.), Little Brown and Co., Boston, MA, 747.
6. Ibrahim, K.N., Buzdar, A.U. *Am. J. Clin. Oncol.*, 1995, 18, 407.
7. Poulos, T.L., Finzel, B.C., Howard, A.J. *J. Mol. Biol.*, 1987, 195, 687.
8. (a) Laughton, C.A., Zvelebil, M.J.J.M., Neidle, S. *J. Steroid Biochem. Mol. Biol.*, 1993, 44, 399. (b). Zhou, D., Cam, L., Laughton, C.A., Korzekwa, K.R., Chen, S. *J. Biol. Chem.*, 1994, 269, 19501. (c). Graham-Lorence, S., Amarneh, B., White, R. E., Peterson, J.A., Simpson, E.R. *Protein Science*, 1995, 4, 1065.
9. Oprea, T.I., Garcia, A.E. *J. Computer-Aided Mol. Des.*, 1996, 10, 186.
10. (a) Greer, J., Erickson, J.W., Baldwin, J.J., Varney, M.D. *J. Med. Chem.*, 1994, 37, 1035. (b) Bohm, H.-J., Klebe, G. *Angew. Chem. Int. Ed. Engl.*, 1996, 35, 2589. (c) Bevan, P., Hamish, R., Shaw, I. *Trends Biotech.*, 1995, 13, 115. (d) Sowdhamini, R., Burke, D.F., Deane, C., Huang, J.-F., Mizuguchi, K., Nagararam, H.A., Overington, J.P., Srinivasan, N., Steward, R.E., Blundell, T.L. *Acta Crysalllogr.*, 1998, D54, 1168.
11. (a) Nagy, P.I., Tokarski, J., Hopfinger, A.J. *J. Chem. Inf. Comput. Sci.*, 1994, 43, 1190. (b) Recanatini, M. *J. Computer-Aided Mol. Des.*, 1996, 10, 74.
12. Hahn, M. *J. Med. Chem.*, 1995, 38, 2080.

13. (a) Cramer, R.D. III, Patterson, D.E., Bunce, J.D. *J. Am. Chem. Soc.*, **1988**, 110, 5959. (b) Hahn, M., Rogers, D. *J. Med. Chem.*, **1995**, 38, 2091.
14. Numazawa, M., Mutsumi, A., Tachibana, M., Hoshi, K. *J. Med. Chem.*, **1994**, 37, 2198 and the references therein.
15. Numzawa, M., Oshibe, M. *J. Med. Chem.*, **1994**, 37, 1312.

CONCLUSIONS

Chapter 1. The synthetic route for B-ring functionalised 2-oxasteroids developed in this thesis is quite general, efficient, and should be serviceable for the synthesis of different analogues. Some novel synthetic methodologies were developed relevant to the synthesis of oxasteroids. The single-pot PCC oxidation of homoallylic alcohols to conjugated diketones provides the requisite starting materials for the oxasteroid synthesis. Interestingly, the protocol is mild enough that the C17-ketal protecting group survives most of the chemical transformations. Some novel and advanced B-ring functionalised steroid precursors were elaborated to complex oxa-analogues. Studies towards 2-thiasteroids were initiated but were terminated prematurely because of problems in A-ring annulation.

Chapter 2. The crystal structures of some 2-oxasteroids and related androgens were analysed. It was observed that in the presence of hydroxy functionality, the C-H...O hydrogen bonds are accommodated within the overall scheme of the stronger O-H...O hydrogen bonds. In the absence of strong donors, the C-H...O hydrogen bonds stabilise the crystal structure. In these donor-rich molecules, the acceptor oxygen atoms are multiply hydrogen bonded. In addition to the acidity of C-H atoms, their geometrical accessibility is also important in forming C-H...O hydrogen bonds. The conformation in 2-oxasteroids is largely similar to the natural analogues though the A-ring shows some variability. The A-ring conjugated oxasteroids adopt the generally observed $1\alpha,2\beta$ -half chair conformation. Isostructurality within the family of 2-oxasteroids and of some natural steroids is discussed at three levels of similarity: one dimensional, two

dimensional and three dimensional isostructurality. The greater the similarity between the two molecules, the higher is the dimensionality of isostructurality.

Chapter 3. Different model receptor surfaces and QSAR equations were developed by using DDW and other related modules in *Cerius²* platform. A set of 50 molecules (training set) active against aromatase enzyme were used to generate the hypothetical receptor surface. Based on the computed model, the interaction energies and structure-activity data suggest that 2-oxasteroids have binding affinities similar to the natural androgens. The C17 β -hydroxy group appears to favour binding to the receptor while the 6 α -hydroxy or 5 β -configuration are not favourable for binding.

In conclusion, the steroid category of biomolecules are studied using a combination of synthesis, small-molecule crystallography and drug design tools. This approach should be useful in finding new leads, particularly in cases where the enzyme or ligand-enzyme 3D structure is not known.

APPENDIX

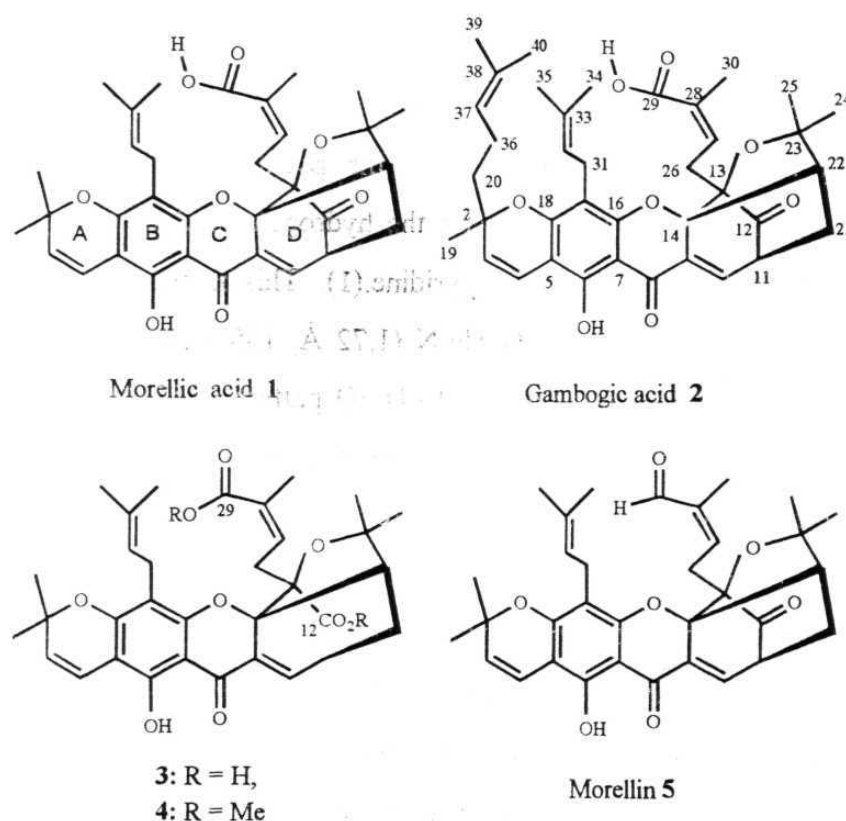
CRYSTAL STRUCTURES OF PIGMENTS FROM *GARCINIA HANBURI*

INTRODUCTION

The gamboge pigments are found in the latex of various *Garcinia* species. Morellic acid¹ **1** and gambogic acid² **2** are the principal acidic components of the pigment gamboge which is extensively found in India and South-East Asia.³ The fused ring xanthone structure of these compounds is peculiar to natural products obtained from this group. It was reported that these acids do not crystallise in native form but can be crystallised as solvates from pyridine, dimethylformamide (dmf), dimethylsulfoxide (dmso) and tetrahydrofuran. In 1962, Gupta *et al.*⁴ recorded the unit cell parameters of the pyridine solvate crystals of β -guttiferin **3** and α -gambogic acid **2** to determine the molecular formula⁵ through the cell volume. In 1963, Kartha *et al.*⁶ determined the X-ray crystal structure of *para*-bromobenzenesulfonate ester of morellin **5** and correctly established the skeletal backbone of the compound; no coordinates were reported. Over the years, many new derivatives of these natural products were isolated, structural and conformational studies were carried out by NMR and mass spectroscopic analysis.⁷

In this study, we have analysed the crystal structures of some of the natural products shown in Scheme 1 as solvates of pyridine, dmf and dmso. Attempted crystallisation of these carboxylic acids with a second organic acid component like formic acid, acetic acid or benzoic acid resulted in gummy material. The crystal structures of four complexes pyridine.(**1**), pyridine.(**2**), dmf.(**2**), dmso.(**3**) and the diester **4** are discussed. Acids **1**, **2** and **3** were isolated from the resinous exudation of *G. morella* by literature procedures.⁸ To obtain crystals of the respective complexes, the pyridine solvates of the acids were dissolved in the appropriate

solvent and a few drops of water added till a slight turbidity persisted. The solutions yielded excellent crystals upon standing. Crystals of **4** were obtained from methanol. Salient crystallographic details of the crystal structures discussed in the appendix are provided at the end.



Scheme 1. Pigments from *Garcinia Hanburyi* with fused rings.

CRYSTAL STRUCTURE ANALYSIS

Morellic, Gambogic and Guttiferic acids

In the crystal structure of pyridine(1), shown in Figure 1a, the pyridine molecule is not protonated by acid but is hydrogen bonded to the carboxylic group forming a hetero dimer with a strong O-H...N (1.65 Å, 172°) and a weak C-H...O (2.82 Å, 120°) hydrogen bond. However, it is also associated with a neighbouring acid molecule via an elaborate system of C-H...O bonds (2.58-2.80 Å, 120-131°)

as shown in I. There are other C-H...O interactions between the acid molecules which play a supportive role (Table 1). The small and rigid pyridine molecule is of key importance. It acts as a template in organising the conformationally flexible morellic acid molecules in the crystal because of its multiple hydrogen bonding capability. Interestingly, it is for the first time that an acid-pyridine hetero dimer is noted in the case of pyridine solvate without the protonation.

Figure 1b shows the structure of the pyridine.(2) solvate. The extra isoprenyl group does not interfere with the hydrogen bonding scheme which is virtually identical to that found in pyridine.(1). This is true not only for the carboxyl-pyridine motif with its O-H...N (1.72 Å, 155°) and C-H...O (2.71 Å, 122°) bonds but also the more diffuse C-H...O pattern (2.52-2.69 Å, 117-123°) between the pyridine and the neighbouring acid molecules (Table 1). The role of pyridine in assembling this structure is appreciated when one examines the crystal structure of the dmf.(2). The dmf molecule mimics the pyridine in its hydrogen bonding donor and acceptor abilities and a comparison of synthons I and II show that the carbonyl O-atom, the formyl H-atom and the methyl H-atom in dmf respectively substitute for the heterocyclic N-atom, the H_α atom and the H_β atom in pyridine. Like the pyridine molecules in the earlier structures, the dmf is the agent here that binds the gambogic acid molecules together via a complex system of O-H...O and C-H...O hydrogen bonds (Table 1). None of the C-H...O hydrogen bonds in these structures is particularly strong.⁹ Yet they are numerous and occur in widely separated parts of these flexible molecules. Inspection of Figures 1(a)-(c) show that they are effectively able to pin down the conformations of the long and floppy side chains in 1 and 2 to give networks that are ordered, intricate and beautiful.

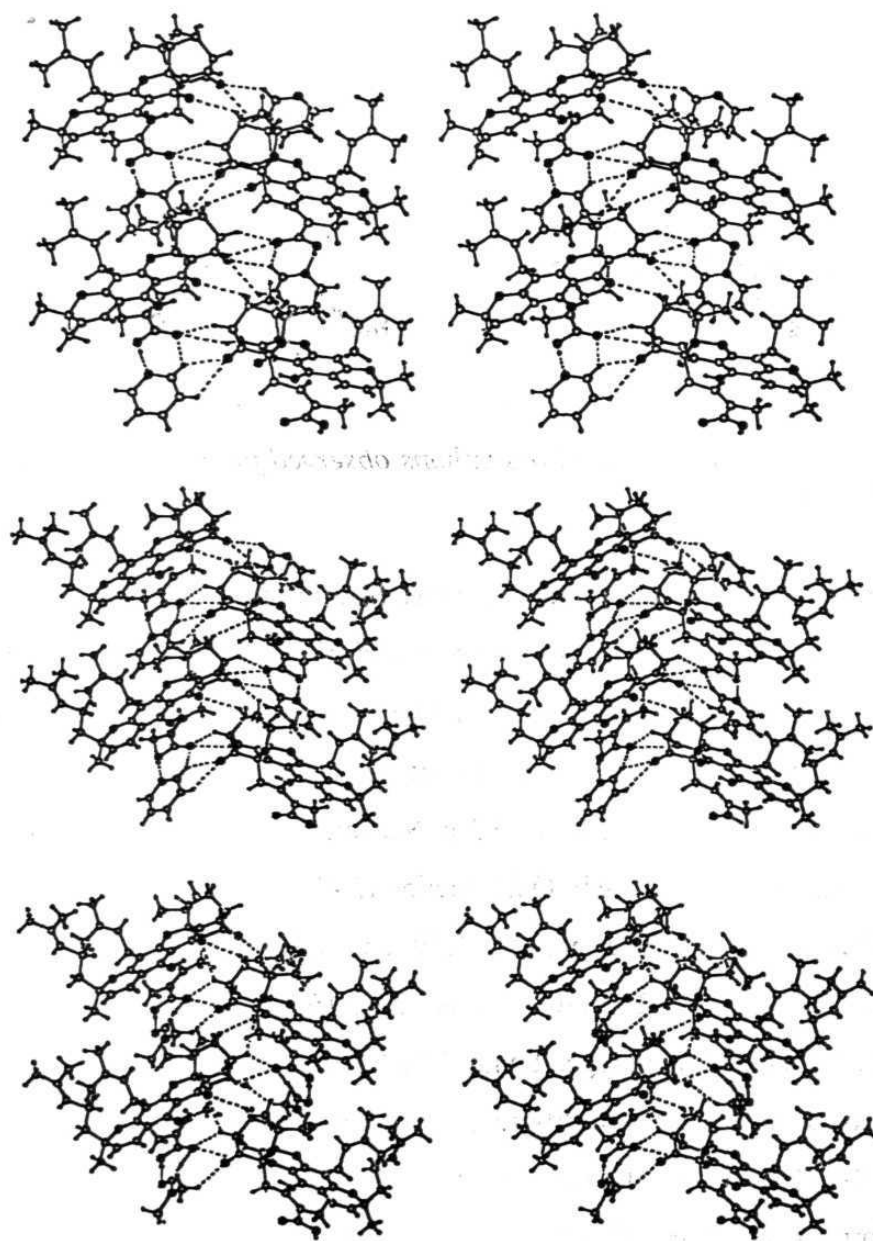
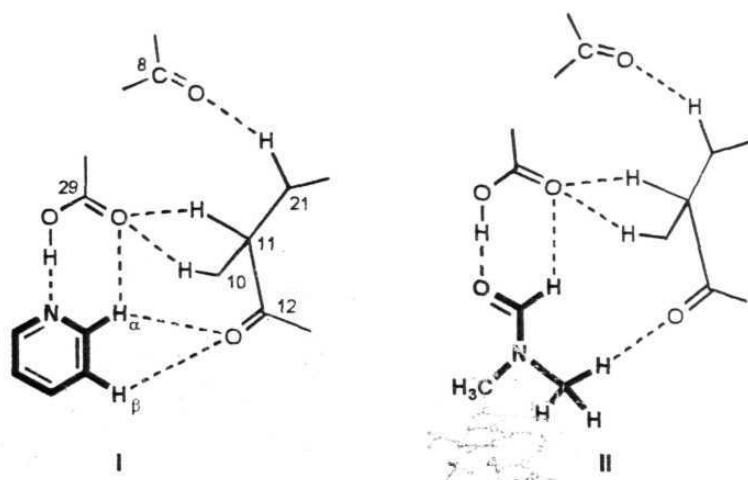


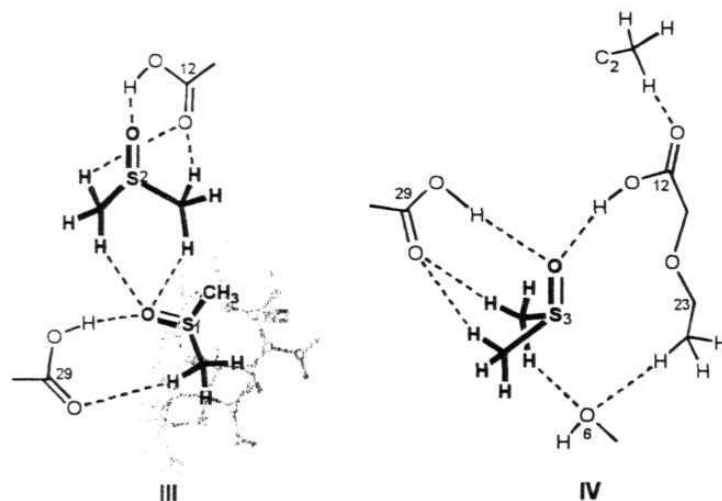
Figure 1. Stereoview of the pyridine and dmf solvates of morellic and gambogic acids: (a) pyridine.(1); (b) pyridine.(2); (c) dmf.(2). Notice the striking similarity between the three structures.



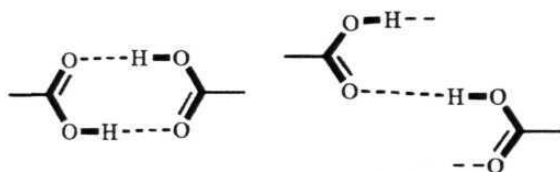
Scheme 2. Similar supramolecular synthons observed for pyridine and dmf with large acid molecules.

The role of solvent in promoting crystallisation is even more evident in the structure of $(\text{dmso})_3 \cdot (3)_2$ solvate formed by the dibasic guttiferic acid. The packing is shown in Figure 2. The recognition features are depicted schematically in synthons **III** and **IV**. The three dmso molecules are symmetry-independent. Two of them (identified by atoms S1 and S2 in Scheme 3 and Figure 2) are hydrogen bonded to each other via a $\text{C-H}\cdots\text{O}$ interaction (2.43 \AA , 160°) and in turn seek out two distinct carboxylic acid groups (C29 and C12) from screw-related acid molecules to form $\text{O-H}\cdots\text{O}$ (1.70 , 1.59 \AA ; 158 , 168°) and $\text{C-H}\cdots\text{O}$ (2.68 , 2.57 , 2.31 \AA ; 130 , 141 , 149°) hydrogen bonds. The O-atom of the third (S3 in Figure 2) is linked to carboxyl groups of different molecules via $\text{O-H}\cdots\text{O}$ bonds (1.71 , 1.84 \AA ; 167 , 144°) with one of them having *anti* (C12) conformation. The methyl groups form several $\text{C-H}\cdots\text{O}$ bonds with adjacent carbonyl O-atoms belonging to acid molecules that are in themselves linked with additional $\text{C-H}\cdots\text{O}$ bonds (Table 1). The entire structure is so abstruse that it has necessitated the use of two stereodrawings but the role of the dmso is clear — by forming strong and weak

hydrogen bonds with itself and with guttiferic acid, it is able to draw together molecules that by themselves are unable to properly self-assemble into a crystal.



Scheme 3. Synthons formed by three symmetry independent dmso molecules with diacid (3).



Scheme 4. Robust dimer and catemer type synthons generally observed for carboxylic acids.

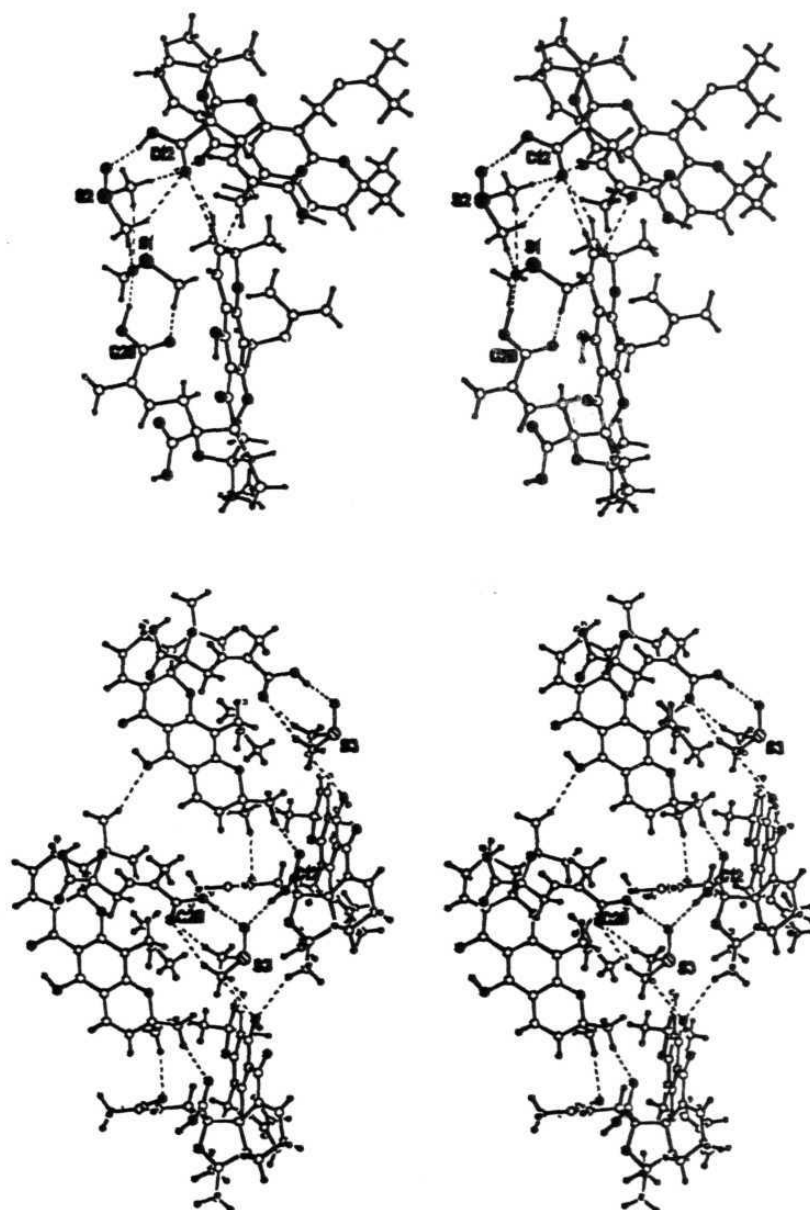


Figure 2. Two of the three molecules of dmsu in the asymmetric unit form hydrogen bonded dimers with one of the two symmetry independent molecules of 3 (above). The third dmsu molecule connects the other symmetry independent acid molecule utilising the carboxylic group in the syn (C29) and anti (C12) conformation (below).

Most carboxylic acids crystallise as dimers or catemers, in other words after some kind of carboxyl-carboxyl recognition has taken place. In the present instance, the formation of dimers or catemers (Scheme 4) may just not be sufficient enough to ensure crystallisation because of the entropic penalty that has to be paid upon the loss of conformational freedom that would necessarily accompany crystallisation of these highly flexible molecules. Solvents like pyridine, dmf and dmsO are then hydrogen bond nucleators that can immobilise distant portions of the acid molecules to an extent that is critically sufficient to induce crystallisation.¹⁰ Accordingly, the formation of solvent-free crystals would appear unlikely while solvents like formic and acetic acids that have been traditionally used for these pigments are unable to link the large acid molecules through multi-point recognition patterns.

Dimethyl guttiferic acid

This diester crystallises without solvent in the crystal in space group $R\bar{3}$. There are free O-H groups to form strong hydrogen bonds. C-H...O hydrogen bonds stabilise the structure (Table 1). The carbonyl oxygen of C12 carboxylate forms hydrogen bond (2.57 Å, 157°) with methyl hydrogen of the C17 side chain (Figure 3). These two molecules are related by 3-fold axis along [001]. The translation related molecules are connected by C22-H...O6 hydrogen bonds along [001] (2.44 Å, 143°). The carbonyl oxygen atom of C29 carboxylic group forms a hydrogen bond (2.64 Å, 142°) with the 3_1 -related molecule. From an analysis of the crystal structure it is not clear why this molecule adopts the high symmetry $R\bar{3}$ space group. Further studies in this direction are ongoing.

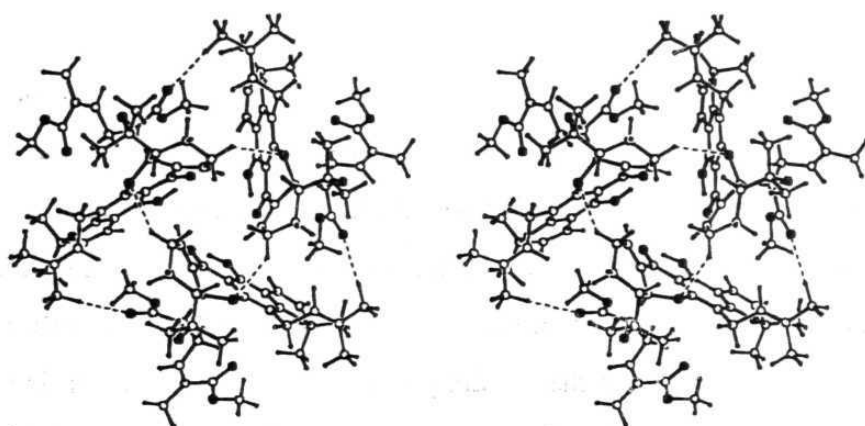


Figure 3. Crystal structure of **4**. Molecules related by 3-fold axis are connected by C-H...O hydrogen bonds.

EXPERIMENTAL

The data were collected on a Siemens P4 diffractometer at 228 (2) K for pyridine (**2**) and **4** or a Bruker SMART diffractometer at 158 (2) K for the others, using Mo-K α X-rays in the ω -2 θ scan mode. Structure solution and refinement was carried with SHELX-97.

Table 1: Geometry of *O-H...O* and *C-H...O* interactions.

Compd. No.	Interactions	H...O (Å)	O/C...O (Å)	/C-H...O (°)
pyridine.(1)	O(292)-H...N(41)	1.73	2.65	155
	C(3)-H...O(13)	2.37	3.36	151
	C(11)-H...O(8)	2.76	3.45	121
	C(11)-H...O(291)	2.67	3.37	122
	C(21)-H...O(8)	2.63	3.35	123
	C(22)-H...O(292)	2.73	3.73	153
	C(25)-H...O(292)	3.01	3.94	144
	C(30)-H...O(6)	2.96	3.81	135
	C(39)-H...O(8)	2.69	3.42	125
	C(45)-H...O(12)	2.65	3.30	118
	C(46)-H...O(291)	2.71	3.41	122
	C(46)-H...O(12)	2.52	3.26	124
pyridine.(2)	O(292)-H...N(41)	1.65	2.62	172
	C(10)-H...O(291)	2.80	3.46	120
	C(11)-H...O(8)	2.92	3.59	121
	C(11)-H...O(291)	2.68	3.48	131
	C(43)-H...O(12)	2.64	3.32	120
	C(42)-H...O(291)	2.82	3.48	120
	C(42)-H...O(12)	2.58	3.30	123
	C(21)-H...O(8)	2.71	3.49	128
	C(35)-H...O(8)	2.82	3.71	139
dmf.(2)	O(291)-H...O(43)	1.60	2.58	176
	C(3)-H...O(13)	2.55	3.55	154
	C(11)-H...O(292)	2.65	3.34	121
	C(21)-H...O(8)	2.56	3.35	129
	C(22)-H...O(43)	2.52	3.54	156
	C(22)-H...O(291)	2.83	3.77	145
	C(22)-H...O(292)	3.05	3.67	117
	C(25)-H...O(291)	2.87	3.78	142
	C(39)-H...O(8)	2.50	3.51	154
	C(43)-H...O(12)	2.94	3.63	122
dmso.(3)	O(124)-H...O(2)	1.60	2.56	165
	O(122)-H...O(3)	1.84	2.70	144
	O(294)-H...S(1)	2.86	3.58	131
	O(294)-H...O(1)	1.70	2.61	152
	O(292)-H...O(3)	1.73	2.67	160

Table 1. Continued

	C(3B)-H...O(123)	2.76	3.65	140
	C(45)-H...O(291)	2.55	3.54	152
	C(45)-H...O(6A)	2.74	3.49	126
	C(44)-H...O(2)	2.56	3.30	125
	C(44)-H...O(291)	2.71	3.67	146
	C(43)-H...O(3)	2.64	3.38	125
	C(43)-H...O(1)	2.76	3.71	147
	C(43)-H...O(8B)	2.63	3.35	123
	C(43)-H...O(123)	2.32	3.30	149
	C(41)-H...O(121)	2.55	3.62	169
	C(41)-H...O(124)	2.66	3.60	145
	C(42)-H...O(123)	2.56	3.48	141
	C(42)-H...O(1)	2.43	3.47	160
	C(40)-H...O(13B)	2.30	3.37	170
	C(11A)-H...O(294)	2.46	3.21	125
	C(11A)-H...O(6B)	2.58	3.58	153
	C(40)-H...O(293)	2.68	3.48	130
	C(40)-H...O(294)	3.01	3.73	124
	C(19B)-H...O(123)	2.50	3.42	142
	C(19A)-H...O(291)	2.78	3.70	142
	C(20A)-H...O(121)	2.37	3.29	141
	C(24A)-H...O(6A)	2.56	3.53	149
	C(24A)-H...O(15B)	2.82	3.85	158
	C(34A)-H...O(292)	2.76	3.72	147
	C(35B)-H...O(2)	2.69	3.63	145
diester 4	C(11)-H...O(15)	2.89	3.69	131
	C(22)-H...O(6)	2.44	3.37	143
	C(44)-H...O(292)	2.86	3.61	126
	C(34)-H...O(121)	2.57	3.59	157
	C(24)-H...O(122)	2.81	3.70	139
	C(25)-H...O(292)	2.93	3.94	154
	C(30)-H...O(291)	2.64	3.56	142

Crystallographic Details

	pyridine.(1)	pyridine.(2)	dmf.(2)	dmso.(3)	4
Emp. formula	C ₅ H ₅ N. C ₃₈ H ₄₄ O ₈	C ₅ H ₅ N. C ₃₃ H ₃₅ O ₈	C ₃ H ₇ NO. C ₃₈ H ₄₄ O ₈	3x(C ₂ H ₆ OS). C ₃₅ H ₄₂ O ₉ 2x(C ₃₃ H ₃₇ O ₉)	
Formula wt.	707.83	638.73	690.79	695.32	667.79
Crystal system	orthorhombic	orthorhombic	orthorhombic	monoclinic	rhombohedral
Space group	<i>P</i> 2 ₁ 2 ₁ 2 ₁	<i>P</i> 2 ₁ 2 ₁ 2 ₁	<i>P</i> 2 ₁ 2 ₁ 2 ₁	<i>P</i> 2 ₁	<i>R</i> 3
<i>a</i> (Å)	9.515(1)	9.9048 (7)	9.576 (2)	11.9627 (19)	30.8517 (16)
<i>b</i> (Å)	18.158(7)	17.2116 (12)	18.567 (5)	12.787 (2)	30.8517 (16)
<i>c</i> (Å)	33.179(1)	20.1845(15)	21.800 (6)	23.492 (4)	8.8132 (6)
α (°)	90	90	90	90	90
β (°)	90	90	90	90.214 (2)	90
γ (°)	90	90	90	90	120
<i>Z</i>	4	4	4	10	9
<i>V</i> (Å ³)	3832.1 (9)	3441.0 (4)	3875.9 (17)	3593.6 (10)	7264.8 (7)
<i>D</i> _{calc} (Mg/m ³)	1.090	1.237	1.077	1.182	1.248
<i>F</i> (000)	1512	1356	1508	1482	2916
Index ranges	-11 ≤ <i>h</i> ≤ 4 -22 ≤ <i>k</i> ≤ 22 -26 ≤ <i>l</i> ≤ 27	-9 ≤ <i>h</i> ≤ 12 -21 ≤ <i>k</i> ≤ 21 -25 ≤ <i>l</i> ≤ 25	-4 ≤ <i>h</i> ≤ 11 -23 ≤ <i>k</i> ≤ 11 22 ≤ <i>l</i> ≤ 21	-12 ≤ <i>h</i> ≤ 14 -15 ≤ <i>k</i> ≤ 13 -29 ≤ <i>l</i> ≤ 29	-37 ≤ <i>h</i> ≤ 38 -38 ≤ <i>k</i> ≤ 37 -10 ≤ <i>l</i> ≤ 10
mp (°C)	147-148	119-120	99-101	104-106	156-157
<i>R</i> ₁	0.0407	0.0828	0.057	0.0479	0.0983
<i>wR</i> ₂	0.0838	0.2035	0.1439	0.1090	0.2435
Gof	0.753	1.215	0.761	0.497	2.021
N-total ^a	7500	6710	7208	12839	6060
N-observed ^b	3859	2887	3211	4511	3935
Variables	473	424	468	884	400

^a N-total is the total number of reflections collected.^b N-observed is the number of reflections observed based on the criteria $F_o > 4\sigma(F_o)$.

REFERENCES

1. Furrer, M. *Dissertation*, Basle, 1934.
2. Karanjgaonkar, C.G., Nair, P.M., Venkataraman, K. *Tetrahedron Lett.* **1966**, 687.
3. K. Venkataraman, *Pigments of Garcinia Species*, Indian National Science Academy, New Delhi, 1973.
4. Guptha, V.S., Narasimha Rao, P.L., Vaidya, S. N., Ramaseshan, S. *Chemistry and Industry*, **1962**, 1499.
5. Gavezzotti, A. *Cryst. Rev.*, **1998**, 7, 5.
6. Kartha, G., Ramachandran, G.N., Bhat, B.H., Nair, P.M., Raghavan, V.K.V., Venkataraman, K. *Tetrahedron Lett.*, **1963**, 459.
7. (a) Ahmad, S.A., Rigby, W., Taylor, R.B. *J. Chem. Soc. (C)*, **1966**, 772. (b) Lin, L-J., Lin, L-Z., Pezzuto, J.M., Cordell, G.A. *Magnetic Resonance in Chemistry* **1993**, 31, 340. (c) Ito, C., Miyamoto, Y., Sunder Rao, K., Furukawa, H. *Chem. Pharm. Bull.* **1996**, 44, 441. (d) Asano, J., Chiba, K., Tada, M., Yoshii, T. *Phytochemistry* **1996**, 41, 815.
8. Rao, D.R. A. A. I. Sci. Thesis, **1955**, Indian Institute of Science, Bangalore.
9. Desiraju, G.R., *Acc. Chem. Res.*, **1996**, 29, 441.
10. Wijaya, K., Moers, O., Blaschette, A., Jones, P.G. *Acta Crystallogr.*, **1998**, C54, 1707.

ABOUT THE AUTHOR

Addlagatta Anthony, son of Balaiah and Mariamma, was born on 1 June 1971 in Kammaguda in the outskirts of Hyderabad. After obtaining his elementary and primary school education at Government Primary School, Raithunagar and Vijaya Mary Convent, Bodhan in Nizamabad District of Andhra Pradesh, he joined St. Mary's High School, Secunderabad. Completed Intermediate and B.Sc. degrees from St. Mary's Centenary Junior College, Secunderabad and A.V. College, Osmania University, Hyderabad. He joined the School of Chemistry, University of Hyderabad for M.Sc. in 1991 and continued for his Ph.D. degree in 1993.

LIST OF PUBLICATIONS

1. A mild protocol for lactone to thiolactone transform.
Nangia, A., Anthony, A., Prasuna, G. *Ind. J. Chem.*, 1996, 35B, 52.
2. Facile synthesis of steroidal Δ^4 -3,6-diones from Δ^5 -3-ols using pyridinium chlorochromate.
Nangia, A., Anthony, A. *Synth. Commun.* 1996, 26, 225.
3. Expeditious synthetic route to B-ring functionalised 2-oxa steroids: Synthesis of 17-Ethylenedioxy-6 α -hydroxy-2-oxa-4-androsten-3-one as key synthon.
Nangia, A., Anthony, A. *Ind. J. Chem.* 1997, 35B, 1113.
4. Crystal Engineering: Some Further Strategies.
Anthony, A., Desiraju, G.R., Jetty, R.K.R., Kuduva, S.S., Madhavi, N.N.L., Nangia, A., Thaimattam, R., Thalladi, V.R. *Crystal Engineering, Mat. Res. Bull.*, 1998, 1, 1.
5. Isostructurality in crystalline oxa-androgens. A case of C-O-H...O and C-H...O interaction mimicry and solid solution formation.
Anthony, A., Jaskolski, M., Nangia, A., Desiraju, G.R. *Chem. Commun.*, 1998, 2537.
6. 17-Ethylenedioxyandrost-4-ene-3,6-dione and 17-Ethylenedioxyandrost-1,4-diene-3,6-dione.
Anthony, A., Jaskolski, M., Nangia, A., Desiraju, G.R. *Acta Crystallogr.*, 1998, C54, 1894.
7. 5 β -Androstan-3,17-dione.
Anthony, A., Jaskolski, M., Nangia, A., Desiraju, G.R. *Acta Crystallogr.*, 1998, C54, 1898.
8. Androst-4-ene-3,6,17-trione.
Anthony, A., Jaskolski, M., Nangia, A. (communicated)

- 9 Pseudopolymorphism. 3. Crystallisation of pyridine, dimethylformamide and dimethylsulfoxide solvates of gamboge pigments.
Anthony, A., Rao, D.R., Desiraju, G.R. (communicated)
10. Synthesis of 2-thiaandrosterone and its derivatives.
(manuscript in preparation)
11. Molecular shape, conformation and crystalline packing motifs of some 2-oxaandrogens.
(manuscript in preparation)
12. QSAR and Model Receptor studies of 2-oxa and related steroids.
(manuscript in preparation)